NONLINEAR DYNAMICS AND SYSTEMS THEORY

An International Journal of Research and Surveys

Volume 20   Number 3   2020

CONTENTS

NONLINEAR DYNAMICS & SYSTEMS THEORY

Volume 20, No. 3, 2020

Nonlinear Dynamics and Systems Theory

An International Journal of Research and Surveys

InforMath Publishing Group
http://www.e-ndst.kiev.ua

INSTRUCTIONS FOR CONTRIBUTORS

(1) General. Nonlinear Dynamics and Systems Theory (ND&ST) is an international journal devoted to publishing peer-refereed, high quality, original papers, brief notes and review articles focusing on nonlinear dynamics and systems theory and their practical applications in engineering, physical and life sciences. Submission of a manuscript is a representation that the submission has been approved by all of the authors and by the institution where the work was carried out. It also represents that the manuscript has not been previously published, has not been copyrighted, is not being submitted for publication elsewhere, and that the authors have agreed that the copyright in the article shall be assigned exclusively to InforMath Publishing Group by signing a transfer of copyright form. Before submission, the authors should visit the website:

http://www.e-ndst.kiev.ua

for information on the preparation of accepted manuscripts. Please download the archive Sample_NDST.zip containing example of article file (you can edit only the file Samplefilename.tex).

(2) Manuscript and Correspondence. Manuscripts should be in English and must meet common standards of usage and grammar. To submit a paper, send by e-mail a file in PDF format directly to

Professor A.A. Martynyuk, Institute of Mechanics,
Nesterov str.3, 03057, MSP 680, Kiev-57, Ukraine
e-mail: journalndst@gmail.com

or to one of the Regional Editors or to a member of the Editorial Board. Final version of the manuscript must typeset using LaTex program which is prepared in accordance with the style file of the Journal. Manuscript texts should contain the title of the article, name(s) of the author(s) and complete affiliations. Each article requires an abstract not exceeding 150 words. Formulas and citations should not be included in the abstract. AMS subject classifications and key words must be included in all accepted papers. Each article requires a running head (abbreviated form of the title) of no more than 30 characters. The sizes for regular papers, survey articles, brief notes, letters to editors and book reviews are: (i) 10-14 pages for regular papers, (ii) up to 24 pages for survey articles, and (iii) 2-3 pages for brief notes, letters to the editor and book reviews.

(3) Tables, Graphs and Illustrations. Each figure must be of a quality suitable for direct reproduction and must include a caption. Drawings should include all relevant details and should be drawn professionally in black ink on plain white drawing paper. In addition to a hard copy of the artwork, it is necessary to attach the electronic file of the artwork (preferably in PCX format).

(4) References. Each entry must be cited in the text by author(s) and number or by number alone. All references should be listed in their alphabetic order. Use please the following style:

Journal: [1] H. Poincare, Title of the article. *Title of the Journal* **volume**
(issue) (year) pages. [Language]

Book: [2] A.M. Lyapunov, *Title of the Book.* Name of the Publishers, Town, year.

Proceeding: [3] R. Bellman, Title of the article. In: *Title of the Book.* (Eds.).
Name of the Publishers, Town, year, pages. [Language]

(5) Proofs and Sample Copy. Proofs sent to authors should be returned to the Editorial Office with corrections within three days after receipt. The corresponding author will receive a sample copy of the issue of the Journal for which his/her paper is published.

(6) Editorial Policy. Every submission will undergo a stringent peer review process. An editor will be assigned to handle the review process of the paper. He/she will secure at least two reviewers' reports. The decision on acceptance, rejection or acceptance subject to revision will be made based on these reviewers' reports and the editor's own reading of the paper.

CONTENTS

NONLINEAR DYNAMICS AND SYSTEMS THEORY

An International Journal of Research and Surveys

Nonlinear Dynamics and Systems Theory (ISSN 1562–8353 (Print), ISSN 1813–7385 (Online)) is an international journal published under the auspices of the S.P. Timoshenko Institute of Mechanics of National Academy of Sciences of Ukraine and Curtin University of Technology (Perth, Australia). It aims to publish high quality original scientific papers and surveys in areas of nonlinear dynamics and systems theory and their real world applications.

AIMS AND SCOPE

Nonlinear Dynamics and Systems Theory is a multidisciplinary journal. It publishes papers focusing on proofs of important theorems as well as papers presenting new ideas and new theory, conjectures, numerical algorithms and physical experiments in areas related to nonlinear dynamics and systems theory. Papers that deal with theoretical aspects of nonlinear dynamics and/or systems theory should contain significant mathematical results with an indication of their possible applications. Papers that emphasize applications should contain new mathematical models of real world phenomena and/or description of engineering problems. They should include rigorous analysis of data used and results obtained. Papers that integrate and interrelate ideas and methods of nonlinear dynamics and systems theory will be particularly welcomed. This journal and the individual contributions published therein are protected under the copyright by International InforMath Publishing Group.

PUBLICATION AND SUBSCRIPTION INFORMATION

Nonlinear Dynamics and Systems Theory will have 4 issues in 2020, printed in hard copy (ISSN 1562–8353) and available online (ISSN 1813–7385), by InforMath Publishing Group, Nesterov str., 3, Institute of Mechanics, Kiev, MSP 680, Ukraine, 03057. Subscription prices are available upon request from the Publisher, EBSCO Information Services (`mailto:journals@ebsco.com`), or website of the Journal: `http://e-ndst.kiev.ua`. Subscriptions are accepted on a calendar year basis. Issues are sent by airmail to all countries of the world. Claims for missing issues should be made within six months of the date of dispatch.

ABSTRACTING AND INDEXING SERVICES

Papers published in this journal are indexed or abstracted in: Mathematical Reviews / MathSciNet, Zentralblatt MATH / Mathematics Abstracts, PASCAL database (INIST–CNRS) and SCOPUS.

Existence of Weak Solutions for Nonlinear p-Elliptic Problem by Topological Degree

A. Abbassi, C. Allalou * and A. Kassidi

Laboratory LMACS, FST of Beni Mellal, Sultan Moulay Slimane University, Morocco

Abstract: In this work, we establish the existence results on weak solutions via the recent Berkovits topological degree for the following nonlinear p-elliptic problems :

$$-div(|\nabla u|^{p-2}\nabla u) = \lambda |u|^{q-2}u + f(x,\ u,\ \nabla u)$$

in a bounded set $\Omega \in \mathbb{R}^N$, where the vector field f is a Carathéodory function.

Keywords: *weighted Sobolev spaces; Hardy inequality; topological degree; Berkovits topological degree; p-elliptic problems.*

Mathematics Subject Classification (2010): 35J60, 46E35, 47J05, 47H11.

1 Introduction

Let Ω be a bounded open set of $\mathbb{R}^N$ $(N \geq 1)$ with a Lipschitz boundary if $N \geq 2$, and let p, q be real numbers such that $2 < q < p < \infty$, and $w = \{w_i(x),\ 0 \leq i \leq N\}$ be a vector of weight functions on Ω, i.e., each $w_i(x)$ is measurable a.e. positive on Ω. Let $W_0^{1,p}(\Omega, w)$ be the weighted Sobolev space associated with the vector w. Our objective is to prove the existence of weak solutions to the following nonlinear p-elliptic problem :

$$\begin{cases} -div(a(x, \nabla u)) = \lambda |u|^{q-2}u + f(x, u, \nabla u) & \text{in} \quad \Omega, \\ u = 0 & \text{on} \quad \partial\Omega, \end{cases} \tag{1}$$

where $a(x, \nabla u) = |\nabla u|^{p-2}\nabla u$. We shall suppose that the following degenerate ellipticity condition is satisfied for all $\xi \in \mathbb{R}^N$ and almost every $x \in \Omega$:

$$a(x, \xi) \cdot \xi \geq \gamma \sum_{i=1}^{N} w_i |\xi_i|^p, \tag{2}$$

---

* Corresponding author: mailto:chakir.allalou@yahoo.fr

such that γ is a positive constant, and λ is a real parameter. The function $f : \Omega \times \mathbb{R} \times \mathbb{R}^N \to \mathbb{R}$ is a Carathéodory function which satisfies only the growth condition, for a.e $x \in \Omega$ and all $(\eta, \zeta) \in \mathbb{R} \times \mathbb{R}^N$,

$$|f(x, \ \mu, \ \xi)| \leq \beta(M(x) + \sigma^{\frac{1}{p'}}|\mu|^{\frac{q}{p'}} + \sum_{j=1}^{N} w_j^{\frac{1}{p'}}|\xi_j|^{p-1}), \qquad (3)$$

where β is a positive constant, $M \in L^{p'}(\Omega), M(x) \geq 0$ and q is a real number such that $2 < q < p$.

We use, in this paper, the framework of the recent Berkovits topological degree. This notion was introduced by J. Berkovits [7] in the study of the solvability of abstract Hammerstein type equations and variational inequalities. The topological degree theory was introduced for the first time by Leray and Schauder [17] in their study of the nonlinear equations for compact perturbations of the identity in infinite-dimensional Banach spaces. Browder [8] constructed a topological degree for the operators of class (S_+) in reflexive Banach spaces with the Galerkin method, see also [20, 22, 23]. This notion was then extented by Berkovits [7] to the classical Leray-Schauder degree for the operators of generalized monotone type. Roughly speaking, the class of operators for the extended degree is essentially obtained by replacing the compact perturbation by a composition of operators of monotone type. We refer to [10, 24] for more details.

For $f \equiv 0$ and $p = q$, Melián et. al. (in [19]) study the eigenvalues of the problem, and there the differentiability with respect to the domain of the first Dirichlet eigenvalue of the minus $p-$Laplacian is shown for the first time. S. Liu [18], by using the Morse theory, has established the existence of weak solutions to the equation $\triangle_p u = f(x, u)$ with the Dirichlet boundary conditions. It should be mentioned that the results in this paper are generalised to the case of the p-Laplacian results obtained in [14] for the strongly nonlinear case using the Berkovits topological degree. One of the motivations for studying (1) comes from the applications to such models of fluid mechaincs (see [5,6,11]), nonlinear diffusion(see [21]) and nonlinear elasticity (see [4]). We note that the case $1 < p < 2$ relates to the elastic-plastic models.

This paper is divided into four sections. In the next section, we give some preliminaries and the definition of weighted Sobolev spaces and we recall some classes of mappings of generalized (S_+) type and the recent Berkovits degree. In the third section, we discuss the p-Laplace operator. Finally, we give some existence results for weak solutions of problem (1).

2   Preliminaries

In order to discuss problem (1), we need some theories on topological degree and on spaces $W^{1,p}(\Omega, w)$ which we call the weighted Lebesgue–Sobolev spaces. Firstly, we state some classes of mappings and topological degree, secondly, we give basic properties of spaces $W^{1,p}(\Omega, w)$ which will be used later.

2.1   Classes of mappings and topological degree

Let X be a real separable reflexive Banach space with dual X^* and with continuous dual pairing $\langle \, \cdot \, , \, \cdot \, \rangle$ between X^* and X in this order, and for a nonempty subset Ω of X, let $\overline{\Omega}$ and $\partial\Omega$ denote the closure and the boundary of Ω in X, respectively. The symbol $\to (\rightharpoonup)$ stands for strong (weak) convergence.

Definition 2.1 Let Y be another real Banach space. An operator $F : \Omega \subset X \to Y$ is said to be

1. bounded if it takes any bounded set into a bounded set.

2. demicontinuous if for any $(u_n) \subset \Omega$, $u_n \to u$ implies $F(u_n) \rightharpoonup F(u)$.

3. compact if it is continuous and the image of any bounded set is relatively compact.

Definition 2.2 A mapping $F : \Omega \subset X \to X^*$ is said to be

1. of class (S_+) if for any $(u_n) \subset \Omega$ with $u_n \rightharpoonup u$ and $\limsup\limits_{n \to \infty} \langle Fu_n, u_n - u \rangle \leq 0$, we have $u_n \to u$.

2. quasimonotone if for any $(u_n) \subset \Omega$ with $u_n \rightharpoonup u$, we have $\limsup\limits_{n \to \infty} \langle Fu_n, u_n - u \rangle \geq 0$.

Definition 2.3 Let $T : \Omega_1 \subset X \to X^*$ be a bounded operator such that $\Omega \subset \Omega_1$. For any operator $F : \Omega \subset X \to X$, we say that

1. F satisfies condition $(S_+)_T$ if for any $(u_n) \subset \Omega$ with $u_n \rightharpoonup u$, $y_n := Tu_n \rightharpoonup y$ and $\limsup\limits_{n \to \infty} \langle Fu_n, y_n - y \rangle \leq 0$, we have $u_n \to u$.

2. F has the property $(QM)_T$ if for any $(u_n) \subset \Omega$ with $u_n \rightharpoonup u$, $y_n := Tu_n \rightharpoonup y$, we have $\limsup\limits_{n \to \infty} \langle Fu_n, y - y_n \rangle \geq 0$.

Let $\mathcal{O}$ be the collection of all bounded open sets in X. For any $\Omega \subset X$, we consider the following classes of operators:

$\mathcal{F}_1(\Omega) := \{F : \Omega \to X^* | F \text{ is bounded, demicontinuous and satifies condition} (S_+)\}$,

$\mathcal{F}_{T,B}(\Omega) := \{F : \Omega \to X | F \text{ is bounded, demicontinuous and satifies condition} (S_+)_T\}$,

$\mathcal{F}_T(\Omega) := \{F : \Omega \to X | F \text{ is demicontinuous and satifies condition} (S_+)_T\}$,

$\mathcal{F}_B(X) := \{F \in \mathcal{F}_{T,B}(\overline{G}) | G \in \mathcal{O}, \ \mathrm{T} \in \mathcal{F}_1(\overline{\mathrm{G}})\}$.

Throughout the paper $T \in \mathcal{F}_1(\overline{G})$ is called an essential inner map to F.

Lemma 2.1 (*[7], Lemmas 2.2 and 2.4) Let $T \in \mathcal{F}_1(\overline{G})$ be continuous and $S : D_S \subset X^* \to X$ be demicontinuous such that $T(\overline{G}) \subset D_s$, where G is a bounded open set in a real reflexive Banach space X. Then the following statements are true :*

1. *If S is quasimonotone, then $I + SoT \in \mathcal{F}_T(\overline{G})$, where I denotes the identity operator.*

2. *If S is of class (S_+), then $SoT \in \mathcal{F}_T(\overline{G})$.*

Definition 2.4 Suppose that G is a bounded open subset of a real reflexive Banach space X, $T \in \mathcal{F}_1(\overline{G})$ be continuous and let $F, S \in \mathcal{F}_T(\overline{G})$. The affine homotopy $H : [0,1] \times \overline{G} \to X$ defined by

$$H(t, \ u) := (1-t)Fu + tSu \qquad \text{for} \qquad (t, \ u) \in [0,1] \times \overline{G}$$

is called an admissible affine homotopy with the common continuous essential inner map T.

Remark 2.1 *[7] The above affine homotopy satisfies the condition $(S_+)_T$.*

Now, we introduce the Berkovits topological degree for the class $\mathcal{F}_B(X)$, for more details see [7].

Theorem 2.1 *There exists a unique degree function*

$$d : \{(F, \ G, \ h)|G \in \mathcal{O}, \ T \in \mathcal{F}_1(\overline{G}), \ F \in \mathcal{F}_{T,B}(\overline{G}), \ h \notin F(\partial G)\} \longrightarrow \mathbb{Z}$$

that satisfies the following properties:

1. *(Normalization) For any $h \in G$, we have $d(I, \ G, \ h) = 1$.*

2. *(Additivity) Let $F \in \mathcal{F}_{T,B}(\overline{G})$. If G_1 and G_2 are two disjoint open subsets of G such that $h \notin F(\overline{G} \backslash (G_1 \cup G_2))$, then we have*

   $$d(F, G, h) = d(F, G_1, h) + d(F, G_2, h).$$

3. *(Homotopy invariance) If $H : [0,1] \times \overline{G} \to X$ is a bounded admissible affine homotopy with a common continuous essential inner map and $h: [0,1] \to X$ is a continuous path in X such that $h(t) \notin H(t, \ \partial G)$ for all $t \in [0,1]$, then the value of $d(H(t,\cdot), \ G, \ h(t))$ is constant for all $t \in [0,1]$.*

4. *(Existence) If $d(F,G,h) \neq 0$, then the equation $Fu = h$ has a solution in G.*

2.2   The weighted Sobolev space

Let Ω be a bounded open set of $\mathbb{R}^N$ ($N \geq 1$), p be a real number such that $1 < p < \infty$, and $\omega = \{\omega_i(x), \ 0 \leq i \leq N\}$ be a vector of weight functions, i.e., every component $\omega_i(x)$ is a measurable function which is positive a.e. in Ω. Further, we suppose for any $0 \leq i \leq N$ in all our considerations that

$$w_i \in L^1_{\text{loc}}(\Omega), \tag{4}$$

$$w_i^{\frac{-1}{p-1}} \in L^1_{\text{loc}}(\Omega). \tag{5}$$

We denote $\partial_i = \dfrac{\partial}{\partial x_i}$. The weighted Sobolev space, denoted by $W^{1,p}(\Omega, w)$, is defined as follows :

$$W^{1,p}(\Omega, w) = \left\{ u \in L^p(\Omega, w_0) \quad \text{and} \quad \partial_i u \in L^p(\Omega, w_i), \quad i = 1, ..., N \right\}.$$

Note that the derivatives $\dfrac{\partial u}{\partial x_i}$ are understood in the sense of distributions. This set of functions forms a Banach space under the norm

$$\|u\|_{1,p,w} = \left[\int_\Omega |u(x)|^p w_0(x)\, dx + \sum_{i=1}^N \int_\Omega |\partial_i u(x)|^p w_i(x)\, dx \right]^{1/p}. \tag{6}$$

The condition (4) implies that $C_0^\infty(\Omega)$ is a subspace of $W^{1,p}(\Omega, w)$ and, consequently, we can introduce the subspace

$$X = W_0^{1,p}(\Omega, w)$$

of $W^{1,p}(\Omega, w)$ as the closure of $C_0^\infty(\Omega)$ with respect to the norm (6). Moreover, condition (5) implies that $W^{1,p}(\Omega, w)$ as well as $W_0^{1,p}(\Omega, w)$ are the reflexive Banach spaces.

We recall that the dual space of weighted Sobolev spaces $W_0^{1,p}(\Omega, w)$ is equivalent to $W^{-1,p'}(\Omega, w^*)$, where $w^* = \{w_i^* = w_i^{1-p'}, i = 0, \dots, N\}$ and where p' is the conjugate of p; i.e., $p' = \frac{p}{p-1}$ (for more details we refer to [1–3]).

Let us define the norm on X equivalent to the norm (6) by

$$\|\|u\|\|_X = \Big(\sum_{i=1}^N \int_\Omega |\partial_i u(x)|^p \, w_i(x) \, dx \Big)^{1/p}. \tag{7}$$

We can find a weight function σ on Ω and a parameter q, $1 < q < \infty$, such that

$$\sigma^{1-q'} \in L^1(\Omega) \quad \text{and} \quad \sigma^{-p/(q-p)} \in L^1(\Omega) \tag{8}$$

with $q' = \frac{q}{q-1}$. Then the Hardy inequality,

$$\Big(\int_\Omega |u(x)|^q \sigma \, dx \Big)^{1/q} \le c \Big(\sum_{i=1}^N \int_\Omega |\partial_i u(x)|^p w_i(x) \, dx \Big)^{1/p}, \tag{9}$$

holds for every $u \in X$ with a constant $c > 0$ independent of u, otherwise the imbedding

$$X \hookrightarrow\hookrightarrow L^q(\Omega, \sigma), \tag{10}$$

expressed by the inequality (9), is compact. Note that $(X, \|\|.\|\|_X)$ is a uniformly convex (and thus, reflexive) Banach space.

Remark 2.2 If we suppose that $w_0(x) \equiv 1$, the integrability condition holds : there exists $\nu \in]\frac{N}{p}, +\infty[\cap]\frac{1}{p-1}, +\infty[$ such that

$$w_i^{-\nu} \in L^1(\Omega), \text{ for all } i = 1.....N, \tag{11}$$

and note that the assumption *(11) is stronger than (5), then*

$$\|\|u\|\| = \Big(\sum_{i=1}^N \int_\Omega |\partial_i u|^p \, w_i(x) \, dx \Big)^{1/p} \tag{12}$$

is a norm defined on $W_0^{1,p}(\Omega, w)$ and equivalent to *(6), and also, the imbedding*

$$W_0^{1,p}(\Omega, w) \hookrightarrow L^q(\Omega) \tag{13}$$

is compact for all $1 \le q \le p_1^*$ if $p\nu < N(\nu + 1)$, and for all $q \ge 1$ if $p\nu \ge N(\nu + 1)$, where $p_1 = p\nu/\nu + 1$ and p_1^* is the Sobolev conjugate of p_1 (see [12], pp.30-31).

3 Notions of Solutions and Properties of p-Laplace Operator

In this section, we give the definition of a weak solution for problem (1), and we discuss the p-Laplace operator $\triangle_p u := div(|\nabla u|^{p-2}\nabla u)$.

Definition 3.1 A point $u \in W_0^{1,p}(\Omega, w)$ is said to be a weak solution of (1) if

$$\int_\Omega |\nabla u|^{p-2} \nabla u \nabla v \, dx = \int_\Omega (\lambda |u|^{q-2} u + f(x, \ u, \ \nabla u)) v \, dx, \quad \forall v \in W_0^{1,p}(\Omega, w).$$

Let us consider the following functional :

$$K u = \int_\Omega \frac{1}{p} |\nabla u|^p \, dx, \qquad u \in X := W_0^{1,p}(\Omega, w) \ .$$

In view of [9], we have $K \in C^1(X, \mathbb{R})$, and the p-Laplace operator is the derivative operator of K in the weak sense. We denote $L = K' : X \to X^*$, then

$$\langle Lu, \ v \rangle = \int_\Omega |\nabla u|^{p-2} \nabla u \nabla v \, dx \qquad \forall v, \ u \in X.$$

Lemma 3.1 $i)$ $L : X \to X^*$ *is a continuous, bounded and strictly monotone operator;*

$ii)$ L *is a mapping of type* (S_+);

$iii)$ $L : X \to X^*$ *is a homeomorphism.*

Proof. i) It is obvious that L is continuous and bounded. For all $\xi, \eta \in \mathbb{R}^N$, we obtain the following inequalities (see [15]), from which we can get the strict monotonicity of L :

$$(|\xi|^{p-2}\xi - |\eta|^{p-2}\eta)(\xi - \eta) \geq (\frac{1}{2})^p |\xi - \eta|^p, \qquad p \geq 2. \tag{14}$$

ii) From (i), if $u_n \rightharpoonup u$ and $\limsup\limits_{n \to \infty} \langle L u_n - L u, \ u_n - u \rangle \leq 0$, then

$$\lim_{n \to \infty} \langle L u_n, u_n - u \rangle = \lim_{n \to \infty} \langle L u_n - L u, u_n - u \rangle = 0.$$

In view of (14), ∇u_n converges in measure to ∇u in Ω, so we get a subsequence denoted again by ∇u_n satisfying $\nabla u_n(x) \to \nabla u(x)$, a.e. $x \in \Omega$.

Since $u_n \rightharpoonup u$ in $X = W_0^{1,p}(\Omega, w)$, one has $(u_n)_n$ is bounded. Therefore, the sequence $(|\nabla u_n|^{p-2} \nabla u_n)_n$ is bounded in $\prod\limits_{i=1}^{N} L^{p'}(\Omega, \ w_i^*)$ and $|\nabla u_n|^{p-2} \nabla u_n \to |\nabla u|^{p-2} \nabla u$ a.e. in Ω, according to Lemma 2.1 in [2] we have

$$|\nabla u_n|^{p-2} \nabla u_n \rightharpoonup |\nabla u|^{p-2} \nabla u \quad \text{in} \ \prod_{i=1}^{N} L^{p'}(\Omega, \ w_i^*) \quad \text{and a.e. in} \ \Omega.$$

We set $\overline{y}_n = |\nabla u_n|^p$ and $\overline{y} = |\nabla u|^p$. As in [13] (Lemma 5) we can write

$$\overline{y}_n \to \overline{y} \quad \text{in} \ L^1.$$

By (2) we have

$$\gamma \sum_{i=1}^{N} w_i |\partial_i u_n|^p \leq |\nabla u_n|^p.$$

Let $z_n = \sum_{i=1}^{N} w_i |\partial_i u_n|^p$, $z = \sum_{i=1}^{N} w_i |\partial_i u|^p$, $y_n = \dfrac{\overline{y}_n}{\gamma}$ and $y = \dfrac{\overline{y}}{\gamma}$. Then, by Fatou's theorem, we obtain

$$\int_\Omega 2y dx \leq \liminf_{n\to\infty} \int_\Omega y + y_n - |z_n - z| dx,$$

i.e., $0 \leq -\limsup\limits_{n\to\infty} \int_\Omega |z_n - z| dx$. Then

$$0 \leq \liminf_{n\to\infty} \int_\Omega |z_n - z| dx \leq \limsup_{n\to\infty} \int_\Omega |z_n - z| dx \leq 0.$$

This implies

$$\nabla u_n \to \nabla u \quad \text{in} \quad \prod_{i=1}^{N} L^p(\Omega, \ w_i).$$

Hence $u_n \to u$ in $W_0^{1,p}(\Omega, w)$, i.e., L is of type (S_+).

iii) By the strict monotonicity, L is an injection. Since

$$\lim_{\||u\||\to\infty} \frac{\langle L u_n, u_n - u\rangle}{\||u\||} = \lim_{\||u\||\to\infty} \frac{\int_\Omega |\nabla u|^p \, dx}{\||u\||} = \infty,$$

L is coercive, thus L is a surjection in view of the Minty−Browder theorem (see [24], Theorem 26A) Hence L has an inverse mapping $L^{-1} : X^* \to X$. Therefore, the continuity of L^{-1} is sufficient to ensure L to be a homeomorphism.

If $f_n, \ f \in X^*$, $f_n \to f$, let $u_n = L^{-1} f_n$, $u = L^{-1} f$, then $L u_n = f_n$, $L u = f$.

So $(u_n)_n$ is bounded in X. Without loss of generality, we can assume that $u_n \rightharpoonup u_0$. Since $f_n \to f$, we have

$$\lim_{n\to\infty} \langle Lu_n - Lu_0, \ u_n - u_0\rangle = \lim_{n\to\infty} \langle f_n, u_n - u_0\rangle = 0. \qquad (15)$$

Since L is of type (S_+), $u_n \to u_0$, we conclude that $u_n \to u$, so L^{-1} is continuous.

4 Existence of Solutions

In this section, we study the strongly nonlinear problem (1) based on the degree theory in Section 2.

Lemma 4.1 *Under assumption* (3), *the operator* $S : W_0^{1,p}(\Omega, w) \to W^{-1,p'}(\Omega, w^*)$ *set by*

$$\langle S u, \ v\rangle = -\int_\Omega (\lambda |u|^{q-2} u + f(x, \ u, \ \nabla u)) v dx, \qquad \forall u, \ v \in W_0^{1,p}(\Omega, w),$$

is compact.

Proof. Step 1. Let $\psi : W_0^{1,p}(\Omega, w) \to L^{p'}(\Omega)$ be the operator defined by

$$\psi u(x) := -\lambda |u(x)|^{q-2} u(x) \quad \text{for} \quad u \in W_0^{1,p}(\Omega, w) \quad \text{and} \quad x \in \Omega.$$

It is obvious that ψ is continuous. We prove that ψ is bounded.

We pose $\alpha = (q-1)p'$ with $1 < \alpha < p$. For each $u \in W_0^{1,p}(\Omega, w)$, by using the continuous embedding $L^p(\Omega) \hookrightarrow L^\alpha(\Omega)$ and the Hölder and the Hardy inequality, we have

$$
\begin{aligned}
\|\psi\,u\|_{p'}^{p'} &= \int_\Omega |-\lambda|u|^{q-2}u|^{p'} dx \\
&\leq \lambda^{p'} \int_\Omega |u|^{(q-1)p'} dx \\
&\leq C\,\lambda^{p'} \int_\Omega |u|^p dx \\
&\leq C\,\lambda^{p'} \int_\Omega |u|^p \sigma^{\frac{p}{q}}\, \sigma^{-\frac{p}{q}}\, dx \\
&\leq C\,\lambda^{p'} \left(\int_\Omega |u|^q \sigma dx \right)^{\frac{p}{q}} \left(\int_\Omega \sigma^{-\frac{p}{q-p}}\, dx \right)^{\frac{q-p}{q}} \\
&\leq c'\Big(\sum_{i=1}^N \int_\Omega |\partial_i u|^p\, w_i\, dx \Big)\left(\int_\Omega \sigma^{-\frac{p}{q-p}}\, dx \right)^{\frac{q-p}{q}} \\
&\leq C'\|\|u\|\|^p. \quad (\text{ Due to }(8))
\end{aligned}
$$

This implies that $\|\psi\,u\|_{p'} \leq C'\,\|\|u\|\|^{p-1}$. Finally, ψ is bounded on $W_0^{1,p}(\Omega, w)$.

Step 2. Let $\varphi : W_0^{1,p}(\Omega, w) \to L^{p'}(\Omega)$ be an operator defined by

$$
\varphi u(x) := -f(x,\, u,\, \nabla u) \quad \text{for} \quad u \in W_0^{1,p}(\Omega, w) \quad \text{and} \quad x \in \Omega.
$$

We show that φ is bounded and continuous. For any $u \in W_0^{1,p}(\Omega, w)$, we have by the growth condition (3) and the Hardy inequality (9) that

$$
\begin{aligned}
\|\varphi\,u\|_{p'} &\leq \left(\int_\Omega |f(x,\, u_n,\, \nabla u_n)|^{p'} dx \right)^{\frac{1}{p'}} \\
&\leq \beta \left(\int_\Omega \big(M(x) + \sigma^{\frac{1}{p'}}|u|^{\frac{q}{p'}} + \sum_{i=1}^N w_i^{\frac{1}{p'}}|\partial_i u|^{p-1}\big)^{p'} dx \right)^{\frac{1}{p'}} \\
&\leq C_1\beta \left(\int_\Omega (M(x))^{p'} dx + \int_\Omega |u|^q \sigma dx + \sum_{i=1}^N \int_\Omega |\partial_i u|^p w_i\, dx \right)^{\frac{1}{p'}} \\
&\leq C_1\beta \left(\int_\Omega (M(x))^{p'} dx \right)^{\frac{1}{p'}} + C_1\beta \left(\int_\Omega |u|^q \sigma dx + \sum_{i=1}^N \int_\Omega |\partial_i u|^p w_i\, dx \right)^{\frac{1}{p'}} \\
&\leq C_3 \left(\sum_{i=1}^N \int_\Omega |\partial_i u|^p w_i\, dx + \sum_{i=1}^N \int_\Omega |\partial_i u|^p w_i\, dx \right)^{\frac{1}{p'}} \\
&\leq C_4 \|\|u\|\|^{\frac{p}{p'}}.
\end{aligned}
\tag{16}
$$

This implies that φ is bounded on $W_0^{1,p}(\Omega, w)$.

Now, we prove that φ is continuous, let $u_n \to u$ in $W_0^{1,p}(\Omega, w)$. Then $u_n \to u$ in $L^p(\Omega, w_0)$ and $\nabla u_n \to \nabla u$ in $L^p(\Omega, w)$. Hence there exist a subsequence still denoted

by (u_n) and measurable functions h in $L^p(\Omega, w_0)$ and g in $\prod_{i=1}^{N} L^{p_i}(\Omega, w_i)$ such that

$$u_n(x) \to u(x) \quad \text{and} \quad \nabla u_n(x) \to \nabla u(x),$$

$$|u_n(x)| \leq h(x) \quad \text{and} \quad |\nabla u_n(x)| \leq |g(x)|$$

for a.e., $x \in \Omega$ and all $n \in \mathbb{N}$. Since f satisfies the Carathéodory condition, we obtain that

$$f(x, \ u_n(x), \ \nabla u_n(x)) \to f(x, \ u(x), \ \nabla u(x)) \quad \text{a.e. } x \in \Omega. \tag{17}$$

According to (3) we get

$$|f(x, \ u_n(x), \ \nabla u_n(x))| \leq \beta(M(x) + \sigma^{\frac{1}{p'}}|h(x)|^{\frac{q}{p'}} + \sum_{j=1}^{N} w_j^{\frac{1}{p'}}|g_j(x)|^{p-1})$$

for a.e. $x \in \Omega$ and for all $k \in \mathbb{N}$.

Since

$$M(x) + \sigma^{\frac{1}{p'}}|h(x)|^{\frac{q}{p'}} + \sum_{j=1}^{N} w_j^{\frac{1}{p'}}|g_j(x)|^{p-1} \in L^{p'}(\Omega),$$

and using (17), we have

$$\int_{\Omega} |f(x, \ u_k(x), \ \nabla u_k(x)) - f(x, \ u(x), \ \nabla u(x))|^{p'} dx \longrightarrow 0.$$

The dominated convergence theorem implies that

$$\varphi u_k \to \varphi u \quad \text{in} \quad L^{p'}(\Omega).$$

Thus, the entire sequence (φu_n) converges to φu in $L^{p'}(\Omega)$, and then φ is continuous.

Step 3. As the embedding $I : W_0^{1,p}(\Omega, w) \to L^{p'}(\Omega)$ is compact, it is known that the adjoint operator $I^* : L^{p'}(\Omega) \to W^{-1,p'}(\Omega, w^*)$ is also compact. Therefore, the compositions $I^* o\varphi$ and $I^* o\varphi : W_0^{1,p}(\Omega, w) \to W^{-1,p'}(\Omega, w^*)$ are compact. We conclude that $S = I^* o\varphi + I^* o\varphi$ is compact. This completes the present proof.

Theorem 4.1 *Assume that hypothesis* (3) *is satisfied. Then problem* (1) *has a weak solution* u *in* $W_0^{1,p}(\Omega, w)$.

Proof. Let $S : W_0^{1,p}(\Omega, w) \to W^{-1,p'}(\Omega, w^*)$ be as defined in Lemma 4.1 and $L : W_0^{1,p}(\Omega, w) \to W^{-1,p'}(\Omega, w^*)$, set by

$$\langle Lu, v \rangle = \int_{\Omega} |\nabla u|^{p-2} \nabla u \nabla v dx, \quad \text{for all} \quad u, v \in W_0^{1,p}(\Omega, w).$$

Then $u \in W_0^{1,p}(\Omega, w)$ is a weak solution of (1) if and only if

$$Lu = -Su. \tag{18}$$

By dint of the properties of the operator L given in Lemma 3.1 and in view of the Minty-Browder theorem (see [24], Theorem 26 A), the inverse operator $T := L^{-1} :$

$W^{-1,p'(x)}(\Omega) \to W_0^{1,p}(\Omega, w)$ is bounded, continuous and satisfies condition (S_+). Furthermore, note that by Lemma (4.1) the operator S is bounded, continuous and quasimonotone.

Consequently, equation (18) is equivalent to

$$u = Tv \quad \text{and} \quad v + SoTv = 0. \tag{19}$$

According to the terminology of [24], the equation $v + SoTv = 0$ is an abstract Hammerstein equation in the reflexive Banach space $W^{-1,p'}(\Omega, w^*)$.

To solve equations (19), we will apply the degree theory introduced in Section 2. To do this, we first show that the set

$$B := \left\{ v \in W^{-1,p'}(\Omega, w^*) \mid v + tSoTv = 0 \quad \text{for some} \quad t \in [0,1] \right\}$$

is bounded. Indeed, let $v \in B$. Set $u := Tv$.

According to (2), (8), (9) and (16), the Hölder inequality, the Young inequality and the continuous embedding $L^p(\Omega) \hookrightarrow L^q(\Omega)$, we get

$$\||Tv\||^p = \||u\||^p = \sum_{i=1}^{N} \int_{\Omega} |\partial_i u|^p w_i \, dx$$

$$\leq \frac{1}{\gamma} \sum_{i=1}^{N} \int_{\Omega} |\partial_i u|^p dx = \frac{1}{\gamma} \langle Lu, u \rangle = \frac{1}{\gamma} \langle v, Tv \rangle$$

$$\leq \frac{t}{\gamma} |\langle S \circ Tv, Tv \rangle|$$

$$\leq \frac{t\lambda}{\gamma} \int_{\Omega} |u|^q dx + \frac{t}{\gamma} \int_{\Omega} |f(x, u, \nabla u)| u \, dx$$

$$\leq C_1 \int_{\Omega} |u|^p dx + C_2 \Big(\int_{\Omega} |f(x, u, \nabla u)|^{p'} dx \Big)^{\frac{1}{p'}} + C_3 \Big(\int_{\Omega} |u|^p dx \Big)^{\frac{1}{p}}$$

$$\leq C_1 \int_{\Omega} |u|^p \sigma^{\frac{p}{q}} \sigma^{-\frac{p}{q}} dx + C_2 \Big(\int_{\Omega} |f(x, u, \nabla u)|^{p'} dx \Big)^{\frac{1}{p'}}$$

$$\quad + C_3 \Big(\int_{\Omega} |u|^p \sigma^{\frac{p}{q}} \sigma^{-\frac{p}{q}} dx \Big)^{\frac{1}{p}}$$

$$\leq C_1 \Big(\int_{\Omega} |u|^q \sigma dx \Big)^{\frac{p}{q}} \Big(\int_{\Omega} \sigma^{\frac{-p}{q-p}} dx \Big)^{\frac{q-p}{q}} + C_2 \|\varphi u\|_{p'}$$

$$\quad + C_3 \Big(\int_{\Omega} |u|^q \sigma dx \Big)^{\frac{1}{q}} \Big(\int_{\Omega} \sigma^{\frac{-p}{q-p}} dx \Big)^{\frac{q-p}{pq}}$$

$$\leq C_1' \sum_{i=1}^{N} \int_{\Omega} |\partial_i u|^p w_i dx + C_2' \||Tv\||^{\frac{p}{p'}} + C_3' \Big(\sum_{i=1}^{N} \int_{\Omega} |\partial_i u|^p w_i dx \Big)^{\frac{1}{p}}$$

$$\leq C_1' \||Tv\||^p + C_2' \||Tv\||^{\frac{p}{p'}} + C_3' \||Tv\||.$$

It follows that $\{Tv \mid v \in B\}$ is bounded.

Since the operator S is bounded, it is obvious from (19) that the set B is bounded in $W^{-1,p'}(\Omega, w^*)$. Consequently, we can now choose a positive constant R such that

$$\|v\|_{W^{-1,p'}(\Omega, w^*)} < R \quad \text{for all} \quad v \in B.$$

As a result

$$v + tSoTv \neq 0 \quad \text{for all} \quad v \in \partial B_R(0) \quad \text{and all} \quad t \in [0, 1].$$

Notice by Lemma 2.1 it follows that

$$I + SoT \in \mathcal{F}_T(\overline{B_R(0)}) \quad \text{and} \quad I = LoT \in \mathcal{F}_T(\overline{B_R(0)}).$$

Since the operators I, S and T are bounded, $I + SoT$ is also bounded. We conclude that

$$I + SoT \in \mathcal{F}_{T,B}(\overline{B_R(0)}) \quad \text{and} \quad I \in \mathcal{F}_{T,B}(\overline{B_R(0)}).$$

Consider an affine homotopy $H : [0, 1] \times \overline{B_R(0)} \to W^{-1,p'}(\Omega, w^*)$ given by

$$H(t, \ v) := v + tSoTv \quad \text{for} \quad (t, \ v) \in [0, 1] \times \overline{B_R(0)}.$$

From the homotopy invariance and normalization property of the degree d stated in Theorem 2.1, we have

$$d(I + SoT, B_R(0), 0) = d(I, B_R(0), 0) = 1,$$

then there exists a point $v \in B_R(0)$ such that

$$v + SoTv = 0.$$

Finally, we conclude that $u = Tv$ is a weak solution of (1). This completes the proof.

Example. Let us consider the following special case :

$$a(x, \nabla u) = |\nabla u|^{p-2} \nabla u \quad \text{and} \quad f(x, s, \xi) = \sum_{i=1}^{N} w_i |\xi_i|^{p-1} sign(\xi_i).$$

It is easy to show that the Carathéodory function $f(x, s, \xi)$ satisfies the growth condition (3). In particular, let us use a special weight function, w, expressed in terms of the distance to the bounded $\partial\Omega$. Denote $d(x) = dist(x, \partial\Omega)$ and set $w(x) = d^{\varrho(x)}, \sigma(x) = d^{\mu}(x)$. Finally, the hypotheses of Theorem 4.1 are satisfied. Therefore, the following problem:

$$\int_{\Omega} |\nabla u|^{p-2} \nabla u \nabla v \, dx = \int_{\Omega} (\lambda |u|^{q-2} u + f(x, u, \nabla u)) v \, dx, \quad \forall v \in W_0^{1,p}(\Omega, w),$$

has at least one weak solutions.

5   Conclusion

In this paper, the existence of weak solutions to the stated problem (1) is proved in the weighted Sobolev space, by using the Berkovits topological degree theory. All this, after transforming this Dirichlet boundary value problem related to the p-Laplacian with nonlinearity into a new one governed by a Hammerstein equation. We intend to apply the method for higher order and higher dimensional PDEs of physical interest.

Acknowledgment

References

[1] Y. Akdim and C. Allalou. Existence and uniqueness of renormalized solution of nonlinear degenerated elliptic problems. *Analysis in Theory and Applications* **30** (2014) 318–343.

[2] Y. Akdim, E. Azroul and A. Benkirane. Existence of solutions for quasilinear degenerate elliptic equations. *Electronic Journal of Differential Equations (EJDE)* **2001** (71) (2001) 1–19.

[3] L. Aharouch, E. Azroul, and A. Benkirane. Quasilinear degenerated equations with L^1 datum and without coercivity in perturbation terms. *Electronic Journal of Qualitative Theory* **19** (2006) 1–18.

[4] C. Atkinson and C. R. Champion. Some boundary value problems for the equation $\nabla.(|\nabla\phi|^N \nabla\phi) = 0$. *Quart. J. Mech. Appl. Math.* **37** (1984) 401–419.

[5] C. Atkinson and C. W. Jones. Similarity solutions in some non-linear diffusion problems and in boundary-layer flow of a pseudo plastic fluid. *Quart. J. Mech. Appl. Malh.* **27** (1974) 193–211.

[6] J. Baranger and K. Najib. Numerical analysis for quasi-Newtonian flow obeying the power Iaw or the Carreau law. *Numer. Math.* **58** (1990) 35–49.

[7] J . Berkovits. Extension of the Leray-Schauder degree for abstract Hammerstein type mappings. *Journal of Differential Equations* **234** (2007) 289–310.

[8] F. E. Browder. Fixed point theory and nonlinear problems. *Bull. Amer. Math. Soc. (N.S.)* **9** (1983) 1–39.

[9] K. C. Chang. *Critical Point Theory and Applications.* Shanghai Scientific and Technology Press, Shanghai, 1986.

[10] Y. J. Cho and Y. Q. Chen. *Topological Degree Theory and Applications. Chapman and Hall/CRC*, 2006.

[11] S. Chow. *Finite Element Error Estimates for Non-linear Elliptic Equations of Monotone Type.* Ph.D. Thesis, *Aust. Nat. Univ.*, Canberra, Australia, 1983.

[12] P. Drabek, A. Kufner and F. Nicolosi. *Non Linear Elliptic Equations, Singular and Degenerated Cases.* University of West Bohemia, 1996.

[13] P. Drabek, A. Kufner and V. Mustonen. Pseudo-monotonicity and degenerate or singular elliptic operators. *Bull. Austral. Math. Soc.* **58** (1998) 213–221.

[14] J. P. García Azorero and I. Peral Alonso. Existence and nonuniqueness for the p-Laplacian. *Communications in Partial Differential Equations* **12** (12) (1987) 126–202.

[15] S. Kichenassamy and L. Veron. Singular solutions of the p-Laplace equation. *Math. Ann.* **275** (1985) 599–615.

[16] B. Lahmi, K. El Haiti and A. Abbassi. Strongly Nonliear Degenerated Elliptic Equation Having Lower Order Term in Weighted OrliczSobolev Spaces and L^1 Data. *Journal of Nonlinear Evolution Equations and Applications* **3** (2016) 37–54.

[17] J. Leray and J. Schauder. Topologie et quations fonctionnelles. *Ann. Sci. Ec. Norm.* **51** (1934) 45–78.

[18] S. Liu. Existence of solutions to a superlinear p-Laplacian equation. *Electron. J. Differential Equations* **2001** (66) (2001) 1–6.

[19] J. G. Melián and J. Sabina de Lis. On the perturbation of eigenvalues for the p-Laplacian. *Comptes Rendus de l'Académie des Sciences-Series I-Mathematics* **332** (10) (2001) 893–898.

[20] R. P. Agarwal, M. Meehan and D. O'regan. *Fixed Point Theory and Applications*. Cambridge university press, **141** (2001).

[21] J. R. Philip. N-diffusion. *Aust. J. Phiys.* **14** (1961) 1–13.

[22] I. V. Skrypnik. *Methods for Analysis of Nonlinear Elliptic Boundary Value Problems*. Translated from the 1990 Russian original by Dan D. Pascali, Translations of Mathematical Monographs. American Mathematical Society, Providence, RI, 1994.

[23] I. V. Skrypnik. Nonlinear elliptic equations of higher order. *Gamoqeneb. Math. Inst. Sem. Mosen. Anotacie.* **7** (1973) 51–52.

[24] E. Zeider. *Nonlinear Functional Analysis and its Applications*, II\B: *Nonlinear Monotone Operators*. Springer, New York, 1990.

Unified Continuous and Discrete Lur'e Systems Stability Analysis Based on Augmented Model Description

A. Ayadi [1*], K. Dchich [2], B. Sfaihi [1] and M. Benrejeb [1]

[1] *Reseach Laboratory of Automatic Control (LA.R.A), University of Tunis El Manar, National Engineering School of Tunis, PO Box 37, 1002 Tunis Le Belvdre, Tunisia,*
[2] *Laborotory LISIER, University of Tunis, ENSIT, PO Box 56, 1008, Tunis, Tunisia*

Abstract: The proposed unified approach for stability analysis of nonlinear Lur'e continuous- and discrete-time systems is based on a unified Borne-Gentina practical stability criterion and augmented systems description. New Lur'e systems stability conditions are developed and compared with the original ones. An illustrative example is considered to show the efficiency of the proposed stability approaches.

Keywords: *Lur'e systems; augmented models; stability; vector norms; arrow form matrix.*

Mathematics Subject Classification (2010): 93C55, 93D09, 93D15.

1 Introduction

The presence of model nonlinearities in most control problems is still a big challenge for modern control theory [2, 6, 7] since there is no universal design procedure for nonlinear systems. Lur'e systems [3] represent an important and common class of nonlinear systems and refer to such systems that consist of a linear dynamical system and a nonlinear feedback loop satisfying certain sector conditions.

The stability of Lur'e systems is stated, first, as an absolute stability problem of the equilibrium point at the origin, then, as the asymptotic stability for any nonlinearity belonging to certain section conditions. Later, different stability criteria are derived via different forms of Lyapunov functions (LFs): the classical quadratic LF [16], non-quadratic Lur'e-type LF [3], the piecewise quadratic LF [1] and fuzzy LF [20].

---

* Corresponding author: `mailto:anis.ayadi@enit.utm.tn`

Despite these advances, most results of stability analysis of Lur'e systems are based on the Lyapunov approach and presented in continuous-time and discrete-time, separately. Moreover, to the best knowledge of the authors, there is no unified technique that develops stability conditions in the continuous- and discrete-time domain.

Among stability analysis techniques, the comparison principle is an efficient solution to the stability problem of dynamical systems [7, 9]. The method is powerful and efficient and has been applied successfully to continuous- and discrete-time systems. The comparison principle is based on defining an ordinary differential equation or functional differential equation, called the comparison system, whose stability properties imply the stability properties of the initial system. The idea is to approximate the available differential equation from above or below through relations that ensure guaranteed upper or lower solution estimates by operating with functions simpler than those in the original equation. Two main approaches have been used to construct the comparison system. The first approach is based on the construction of a Lyapunov function for the comparison system. Lyapunov theory is then used to synthesize system stability criteria [9, 16, 17]. However, this approach is generally conservative and is not systematic because of the chosen Lyapunov function. The second approach is to associate a second level comparison system to the original one. Stability criteria of the original system can be established based on the comparison system. The method is simpler and can be combined with other techniques (i.e., vector norms) leading to systematic stability approaches [9–12, 16].

Arrow form representations provide a straightforward method to describe linear and nonlinear systems, that show effective results when integrated in the systems analysis process. The arrow form state space matrices, i.e., the Benrejeb arrow form matrix, have been introduced by Benrejeb in the early seventies [13, 15]. Since then, combined with aggregation techniques [10, 15], it has become a systematic procedure for stability analysis and synthesis of large classes of nonlinear systems [10, 11, 15]. The arrow form matrix representations were successfully applied to the stability/stabilization study of important classes of nonlinear systems: fuzzy models [11, 20], singularly perturbed systems [4, 12], time-delay systems [19], interconnected systems [5] and choatic systems [18].

The main contribution of this paper is to develop a new technique to solve the stability analysis problem of Lur'e type systems in a unified and systematic manner for continuous- and discrete-time descriptions. In this context, based on the Borne-Gentina practical stability criteria [8, 9], an advanced and unified formulation for stability criteria of nonlinear systems is synthesized. The case of Lur'e systems is considered for investigations and new stability conditions are synthesized in a systematic manner by the definition of a unified augmented model description and the use of the comparison principle. Convenient further results are developed based on the arrow form matrix representation.

The paper is organized as follows. In Section 2, the Lur'e augmented model is developed and the stability problem is formally stated. In Section 3, a unified formulation of the Borne-Gentina practical stability criteria is introduced. In Section 4, new unified continuous and discrete Lur'e systems asymptotic stability conditions are provided. The case of diagonal characteristic matrix of the linearized system is considered. In Section 5, a second-order Lur'e system and the associated discretized model are considered to illustrate the efficiency of the proposed approaches. Concluding remarks are found in Section 6.

2   Problem Statement

Let us consider the continuous-time and discrete-time nonlinear systems described in a unified state space description as follows:

$$D[x(\tau)] = A(.)x(\tau). \tag{1}$$

$D[.]$ is the derivative operator $\frac{d}{dt}$ and Δ is the shift operator for the continuous-time and the discrete-time systems, respectively, $x(\tau) \in D \subset R^n$ is the state vector and $A(.) = \{a_{i,j}(.)\} \in R^{n \times n}$ is the instantaneous characteristic matrix.

When the study of system (1) turns out to be complex, the comparison principle gives a way of comparing system stability property with a simpler system one, for which it can be easier to establish algebraic stability conditions.

The aggregation technique using a regular vector norm $p(x)$ enables one to construct in a systematic way the corresponding comparison system defined as [16]

$$D\left[z(\tau)\right] = M(A(.))z(\tau), z_0 = p(x_0), \tag{2}$$

$M(A(.))$, called the overvaluing of the matrix $A(.)$, is such that

$$D\left[p(x(\tau))\right] \leq M(A(.))z(\tau). \tag{3}$$

When its off diagonal elements are non-negative and nonconstant elements are regrouped in one column or one row, the stability condition can be easily deduced from the application of the Borne-Gentina practical stability criterion based on the M-matrices technique [16].

A change of basis remained an abundant solution to bypass this structured condition problem on the matrix $A(.)$, and the transformation of the caracteristic matrix to an arrow form matrix appears to be a well-adapted model description to the use of this method, in particular, when the model $A(.)$ is in the companion or Frobenius form [10–15].

Let us consider both continuous- and discrete-time Lur'e system [3] described by

$$\begin{cases} D\left[x(\tau)\right] = Ax(\tau) + Bu(\tau), \\ u(\tau) = f\left(\varepsilon(\tau)\right)\varepsilon(\tau), \\ \varepsilon(\tau) = r(\tau) - C^T x(\tau), \end{cases} \tag{4}$$

$A \in R^{n \times n}$, $B \in R^{n \times 1}$ and $C \in R^{n \times 1}$ are constant matrices, $x(\tau) \in R^n$ is the state vector, $u(\tau) \in R$ is the control input, $r \in R$ is the reference input, $\varepsilon(\tau) \in R$ is the error of the closed-loop system, and $f(\varepsilon(\tau)) : R \to R$ is a nonlinear function.

Use the analytical relationship linking together the nonlinear equation description of the system (4) and its linearized model (5), for which the nonlinearity $f(\varepsilon(\tau))$ is considered constant and equal to f_l.

$$D[x(\tau)] = A_l x(\tau) \tag{5}$$

with

$$A_l = A - f_l BC^T. \tag{6}$$

Let us introduce an augmented model description for the autonomous Lur'e system (4) or (7) by choosing $\bar{X} \in R^{n+1}$ as the new state space vector such that $\bar{X} = \begin{bmatrix} x^T & \varepsilon \end{bmatrix}^T$.

$$\begin{cases} D[x(\tau)] = \left(A - f\left(\varepsilon(\tau)\right)BC^T\right)x(\tau), \\ D[\varepsilon(\tau)] = -C^T D[x(\tau)]. \end{cases} \tag{7}$$

Adding and removing $f_l BC^T$ in the first equation of (7), we obtain the following model:

$$\begin{cases} D[x(\tau)] = \left(A - f_l BC^T\right) x(\tau) - \left(f\left(\varepsilon(\tau)\right) - f_l\right) BC^T x(\tau), \\ D[\varepsilon(\tau)] = -C^T \left(A - f\left(\varepsilon(\tau)\right) BC^T\right) x(\tau), \end{cases} \tag{8}$$

which can be written, in a compact form, as

$$D[\bar{X}(\tau)] = A_a\left(.\right) \bar{X}(\tau) \tag{9}$$

with

$$A_a\left(.\right) = \left(\begin{array}{c|c} A_l & B(f\left(\varepsilon(\tau)\right) - f_l) \\ \hline -C^T A & -C^T B f\left(\varepsilon(\tau)\right) \end{array}\right). \tag{10}$$

The instantaneous characteristic matrix of the augmented system (9), $A_a(.) = \{a_{i,j}(.)\} \in R^{(n+1)\times(n+1)}$, highlights the characteristic matrix of the linearized system (5).

Now, the stability analysis of this system is synthesized, in Section 4, by using the Borne-Gentina stability criterion [8, 9], introduced in Section 3, and the arrow form matrices for system description.

3 Proposed Unified Formulation of the Borne-Gentina Practical Stability Criterion

Consider the dynamic systems (1) and introduce two parameters δ_1 and δ_2 and the matrix $M(A(.)) = \{m_{i,j}(.)\}$ defined such that
  for the continuous-time case

$$\delta_1 = 0, \;\; \delta_2 = -1, \tag{11}$$

and

$$M(A(.)) = M_1(A(.)) \tag{12}$$

with

$$M_1(A(.)) : \begin{cases} m_{i,i}(.) = a_{i,i}(.) & \forall i = 1, 2, \ldots, n, \\ m_{i,j}(.) = |a_{i,j}(.)| & \forall i \neq j, \forall i, j = 1, 2, \ldots, n, \end{cases} \tag{13}$$

  and for the discrete-time case

$$\delta_1 = \delta_2 = 1 \tag{14}$$

and

$$M(A(.)) = M_2(A(.)) \tag{15}$$

with

$$M_2(A(.)) : m_{i,j}(.) = |a_{i,j}(.)| \quad \forall i, j = 1, 2, \ldots, n. \tag{16}$$

The following theorem is proposed.

Theorem 3.1 *The nonlinear system (1) is asymptotically stable if the matrix*

$$M^*(.) = \delta_2\left(\delta_1 I_n - \delta_2 M(.)\right) \tag{17}$$

satisfies the following conditions:
  (i) the non-constant elements of $M^*(.)$ are isolated in only one row,
  (ii) the successive minors $\Delta_j(M^*(.))$ of $M^*(.)$ are positive, i.e.,

$$(\delta_2)^j \Delta_j(M^*(.)) > 0 \;\; \forall j = 1, ..., n \forall x \in D \subset R^n. \tag{18}$$

If $D = R^n$, the stability property is global.

Proof. Theorem 3.1 constitutes a direct application of the Borne-Gentina practical stability criterion [8,9], for which a unified formulation is proposed here. The choice of the vector norm

$$p\left(x(\tau)\right) = \left[|x_1(\tau)|, |x_2(\tau)|, \ldots, |x_n(\tau)|\right]^T, \ \forall x(\tau) = \left[x_1(\tau), x_2(\tau), \ldots, x_n(\tau)\right]^T, \qquad (19)$$

as a vector Lyapunov function, leads to the corresponding comparison system

$$D\left[z(\tau)\right] = M(A(.))z(\tau) \qquad (20)$$

characterized by the overvaluing matrix $M(A(.))$ defined previously.

If the nonlinear elements of that matrix are isolated in only one row, the stability conditions given by the application of the Borne-Gentina criterion are based on the verification of the positivity of n principal minors of the matrix $M^*(.)$, i.e.,

- $(-M_1(A(.)) \begin{pmatrix} 1 & 2 & \cdots & j \\ 1 & 2 & \cdots & j \end{pmatrix} > 0 \ \forall j = 1, 2, \ldots, n,$ (21)

for the continuous-time system case with

$$M^*(.) = -M_1(A(.)); \qquad (22)$$

- $(I - M_2(A(.)) \begin{pmatrix} 1 & 2 & \cdots & j \\ 1 & 2 & \cdots & j \end{pmatrix} \succ 0 \ \forall j = 1, 2, \ldots, n,$ (23)

for the discrete-time system case with

$$M^*(.) = I - M_2(A(.)). \qquad (24)$$

This completes the Theorem 3.1 proof.

4 New Unified Continuous- and Discrete-time Lur'e System Asymptotic Stability Conditions

Let us consider the augmented system described by ((9)-(10)) and the corresponding pseudo-overvaluing matrix $\bar{M}(.)$ obtained by the choice of the vector norm $p\left(\bar{X}\right) = \left[|\bar{X}_1|, |\bar{X}_2|, \ldots, |\bar{X}_n|, |\bar{X}_{n+1}|\right]^T$ such that

$$D\left[p(\bar{X})\right] \leq \bar{M}\left(A_a(.)\right)p(\bar{Z}). \qquad (25)$$

We have the following comparison system:

$$D\left[\bar{Z}\right] = \bar{M}(A_a(.))\bar{Z}, \bar{Z}_0 = p(\bar{X}_0), \qquad (26)$$

characterized by the matrix $\bar{M}(A_a(.)) = \{\bar{m}_{i,j}(.)\} \in R^{(n+1)\times(n+1)}$, such that
for the continuous-time system case

$$\begin{cases} \bar{m}_{i,i}(.) = a_{i,i}(.) \ \forall i = 1, 2, \ldots, n+1, \\ \bar{m}_{i,j}(.) = |a_{i,j}(.)| \ \forall i \neq j, \end{cases} \qquad (27)$$

and for the discrete-time system case

$$\bar{m}_{i,j}(.) = |a_{i,j}(.)| \ \forall i, j = 1, 2, \ldots, n+1. \qquad (28)$$

Theorem 4.1 *The continuous-time system, i.e., $\delta_1 = 0$, $\delta_2 = -1$, (resp. the discrete-time system, $\delta_1 = \delta_2 = 1$) defined by (1) is asymptotically stable if the following conditions are satisfied:*

1. The linearized system is stable, i.e., the first n successive principal minors of the matrix $(\delta_1 I_{n+1} - \delta_2 \bar{M}(.))$ are such that

$$\delta_2{}^j (\delta_1 I_{n+1} - \delta_2 \bar{M}(.)) \begin{pmatrix} 1 & 2 & \cdots & j \\ 1 & 2 & \cdots & j \end{pmatrix} \succ 0 \quad \forall j = 1, ..., n, \tag{29}$$

2. The nonlinearity $f(\varepsilon(\tau))$ satisfies the inequality

$$\delta_2{}^{n+1} \det(\delta_1 I_{n+1} - \delta_2 \bar{M}(.)) \succ 0 . \tag{30}$$

Proof. Since the nonlinearities of the comparison Lur'e system (26-28) are isolated in the last column of the matrix, stability conditions are obtained by the application of the BorneGentina stability criterion [8,9] based on the verification of the positivity definition of $n+1$ principal minors of the matrix $-\bar{M}(.)$ (for the continuous-time system case) and of $(I_{n+1} - \bar{M}(.))$ (for the discrete-time system case), the first n ones corresponding to the sufficient stability conditions of the linearized system characterized by the matrix A_l. This completes the Theorem 4.1 proof.

Let us consider, now, the stability conditions reformulation for A_l diagonalizable. When the eigenvalues $\rho_i \, \forall i = 1, 2, \ldots, n$ of the characteristic matrix of the linearized system A_l are

$$\begin{cases} \rho_i \in R \text{ and } \rho_i \neq 0 \ \forall i = 1, 2, \ldots, n, \\ \rho_i \neq \rho_j, \quad i \neq j \qquad \forall i = 1, 2, \ldots, n, \end{cases} \tag{31}$$

the matrix $P_d \in R^{n \times n}$ diagonalizing A_l, is such that

$$D = P_d^{-1} A_l P_d, \tag{32}$$

and the change of base (33) with $\tilde{X} = \left[\tilde{X}_1, \tilde{X}_2, \ldots, \tilde{X}_n, \tilde{X}_{n+1} \right]^T$, and the matrix $P \in R^{(n+1) \times (n+1)}$ is an invertible matrix such that

$$\tilde{X} = P\bar{X}, \ P = \begin{pmatrix} P_d & 0 \\ 0 & 1 \end{pmatrix}, \tag{33}$$

the system (9) can be characterized in the new state space by

$$D\left[\tilde{X} \right] = \tilde{A}_a(.)\tilde{X}, \tag{34}$$

such that the matrix $\tilde{A}_a(.)$ is in arrow form

$$\tilde{A}_a(.) = \quad P^{-1} A_a(.) P, \tag{35}$$

$$\tilde{A}_a(.) = \left(\begin{array}{c|c} D & P_d{}^{-1} B \left(f\left(\varepsilon \right) - f_l \right) \\ \hline -C^T A P_d & -C^T B f\left(\varepsilon \right) \end{array} \right) = \left\{ \tilde{a}_{ij} \left(. \right) \right\}, \tag{36}$$

$$\tilde{A}_a(.) = \left(\begin{array}{cccc|c} \tilde{a}_{1,1} & 0 & \cdots & 0 & \tilde{a}_{1,n+1}(.) \\ 0 & \tilde{a}_{2,2} & \ddots & \vdots & \tilde{a}_{2,n+1}(.) \\ \vdots & \ddots & \ddots & 0 & \vdots \\ 0 & \cdots & 0 & \tilde{a}_{n,n} & \tilde{a}_{n,n+1}(.) \\ \hline \tilde{a}_{n+1,j} & \tilde{a}_{n+1,2} & \cdots & \tilde{a}_{n+1,n} & \tilde{a}_{n+1,n+1}(.) \end{array} \right), \tag{37}$$

$$\tilde{a}_{i,i} = \rho_i \ \forall i = 1, 2, \ldots, n. \tag{38}$$

For the stability study of this system, when $p\left(\tilde{X}\right) = \left[\left|\tilde{X}_1\right|, \left|\tilde{X}_2\right|, \ldots, \left|\tilde{X}_n\right|, \left|\tilde{X}_{n+1}\right|\right]^T$ as a vector norm, we have the comparison system

$$D\left[\tilde{Z}\right] = \tilde{M}(\tilde{A}_a(.))\tilde{Z}, \ \tilde{Z}_0 = p(\tilde{X}_0), \tag{39}$$

where the elements $\tilde{m}_{i,j}(.)$ of the pseudo-overvaluing matrix $\tilde{M}(\tilde{A}_a(.))$

for the continuous-time system case, are such that

$$\begin{cases} \tilde{m}_{i,i}(.) = \tilde{a}_{i,i}(.) \ \forall i = 1, 2, \ldots, n+1, \\ \tilde{m}_{i,j}(.) = |\tilde{a}_{i,j}(.)| \ \ \forall i \neq j, \end{cases} \tag{40}$$

and for the discrete-time system case, are such that

$$\tilde{m}_{i,j}(.) = |\tilde{a}_{i,j}(.)| \ \ \forall i, j = 1, 2, \ldots, n+1. \tag{41}$$

Corollary 4.1 *The continuous nonlinear Lur'e system (4) ($\delta_1 = 0$, $\delta_2 = -1$), (the discrete system ($\delta_1 = \delta_2 = 1$)), is asymptotically stable if the following conditions are verified:*

1. The linearized system is stable, i.e., the first n successive principal minors of the matrix $(\delta_1 I_n - \delta_2 \tilde{M}(.))$ are such that

$$(\delta_2)^j \prod_{j=1}^{n} (\delta_1 - \delta_2 \tilde{m}_{j,j}) > 0 \ \forall j = 1, 2, \ldots, n, \tag{42}$$

2. The nonlinearity $f(\varepsilon(\tau))$ satisfies the inequality

$$(\delta_2)\left[(\delta_1 - \delta_2 \tilde{m}_{n+1,n+1}(.)) - \sum_{j=1}^{n} \left(\frac{(-\delta_2 \tilde{m}_{n+1,j})(-\delta_2 \tilde{m}_{j,n+1}(.))}{(\delta_1 - \delta_2 \tilde{m}_{j,j})}\right)\right] > 0. \tag{43}$$

Proof. By applying the Borne-Gentina stability criterion to the comparison system (39), we obtain the following stability conditions:

$$\delta_2{}^j(\delta_1 I_{n+1} - \delta_2 \tilde{M}(.)) \begin{pmatrix} 1 & 2 & \cdots & j \\ 1 & 2 & \cdots & j \end{pmatrix} \succ 0 \ \forall j = 1, \ldots, n+1, \tag{44}$$

with

$$(\delta_1 I_{n+1} - \delta_2 \tilde{M}(.)) =$$
$$\begin{pmatrix} \delta_1 - \delta_2 \tilde{m}_{1.1} & 0 & \cdots & 0 & -\delta_2 \tilde{m}_{1,n+1}(.) \\ 0 & \delta_1 - \delta_2 \tilde{m}_{2.2} & \ddots & \vdots & -\delta_2 \tilde{m}_{2,n+1}(.) \\ \vdots & \ddots & \ddots & 0 & \vdots \\ 0 & \cdots & 0 & \delta_1 - \delta_2 \tilde{m}_{n.n} & -\delta_2 \tilde{m}_{n,n+1}(.) \\ -\delta_2 \tilde{m}_{n+1,1} & -\delta_2 \tilde{m}_{n+1,2} & \cdots & -\delta_2 \tilde{m}_{n+1,n} & \delta_1 - \delta_2 \tilde{m}_{n+1,n+1}(.) \end{pmatrix}. \tag{45}$$

It is clear that, for $j = 1, ..., n$, the first n minors of (44) correspond to condition (42). For $j = n + 1$, the last condition is

$$(\delta_2)^{n+1} \left[\begin{array}{l} \left(\prod_{q=1}^{n} (\delta_1 - \delta_2 \tilde{m}_{q,q}) \right) (\delta_1 - \delta_2 \tilde{m}_{n+1,n+1} (.)) - \\ \sum_{i=1}^{n} \left((-\delta_2 \tilde{m}_{n+1,i}) (-\delta_2 \tilde{m}_{i,n+1} (.)) \left(\prod_{\substack{j=1 \\ j \neq q}}^{n} (\delta_1 - \delta_2 \tilde{m}_{j,j}) \right) \right) \end{array} \right] > 0 \quad (46)$$

which is equivalent to (43). This ends Corollary 4.1 proof.

5   Illustrative Example

Let consider the second order autonomous Lur'e system described in state space by

$$\begin{cases} D\left[x(\tau)\right] = Ax(\tau) + Bu(\tau), \\ u(\tau) = f\left(\varepsilon(\tau)\right)\varepsilon(\tau), \\ \varepsilon(\tau) = -C^T x(\tau). \end{cases} \quad (47)$$

The corresponding continuous-time system, shown in Figure 1, is such that

$$x(t) = \begin{pmatrix} x_1(t) \\ x_2(t) \end{pmatrix} = \begin{pmatrix} y(t) \\ \dot{y}(t) \end{pmatrix}, \quad A = A_c = \begin{pmatrix} 0 & 1 \\ -0.5 & -1.5 \end{pmatrix},$$

$$B = B_c = \begin{pmatrix} 0 \\ 0.5 \end{pmatrix}, \quad C = \begin{pmatrix} -0.5 \\ 5 \end{pmatrix}^T.$$

When using the sampler such that $T_e = 0.2s$ and the zero-order-holder characterised by
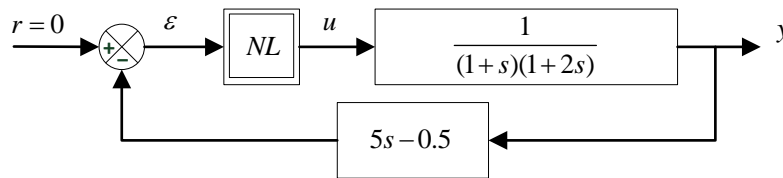
Figure 1:   The continuous-time Lur'e-Postnikov system.

$H(s) = s^{-1}(1 - e^{-T_e s})$, the state space description of the associate discrete-time system is such that

$$x(k) = \begin{pmatrix} x_1(k) \\ x_2(k) \end{pmatrix} = \begin{pmatrix} y(k) \\ \dot{y}(k) \end{pmatrix}, \quad A = A_d = \begin{pmatrix} 0.99 & 0.17 \\ -0.09 & 0.73 \end{pmatrix},$$

$$B = B_c = \begin{pmatrix} 0.01 \\ 0.04 \end{pmatrix}, \quad C = \begin{pmatrix} -0.5 \\ 5 \end{pmatrix}^T.$$

The closed-loop system descriptions of both continuous- and discrete-time are, respectively,

$$\begin{pmatrix} \dot{x}_1(t) \\ \dot{x}_2(t) \end{pmatrix} = \begin{pmatrix} 0 & 1 \\ 0.25f(\varepsilon(t)) - 0.5 & -2.5f(\varepsilon(t)) - 1.5 \end{pmatrix} \begin{pmatrix} x_1(t) \\ x_2(t) \end{pmatrix}$$

and

$$\begin{pmatrix} x_1(k+1) \\ x_2(k+1) \end{pmatrix} = \begin{pmatrix} 0.99 + 0.004f(\varepsilon(k)) & 0.17 - 0.045f(\varepsilon(k)) \\ -0.861 + 0.0431f(\varepsilon(k)) & 0.73 - 0.431f(\varepsilon(k)) \end{pmatrix} \begin{pmatrix} x_1(k) \\ x_2(k) \end{pmatrix}.$$

For $f(\varepsilon(\tau)) = f_l = 1$, the linearized continuous and discrete models are, respectively,

$$\begin{pmatrix} \dot{x}_1(t) \\ \dot{x}_2(t) \end{pmatrix} = \begin{pmatrix} 0 & 1 \\ -0.25 & -4 \end{pmatrix} \begin{pmatrix} x_1(t) \\ x_2(t) \end{pmatrix}$$

and

$$\begin{pmatrix} x_1(k+1) \\ x_2(k+1) \end{pmatrix} = \begin{pmatrix} 0.99 & 0.13 \\ -0.04 & 0.3 \end{pmatrix} \begin{pmatrix} x_1(k) \\ x_2(k) \end{pmatrix},$$

According to (9-10), the instantaneous characteristic matrix of the augmented system is

$$A_{ca}(.) = \left(\begin{array}{cc|c} 0 & 1 & 0 \\ -0.25 & -4 & 0.5(f(\varepsilon(t)) - 1) \\ \hline 2.5 & 8 & -2.5f(\varepsilon(t)) \end{array} \right),$$

$$A_{da}(.) = \left(\begin{array}{cc|c} 0.99 & 0.13 & 0.009(f(\varepsilon(k)) - 1) \\ -0.04 & 0.3 & 0.09(f(\varepsilon(k)) - 1) \\ \hline 0.92 & -3.57 & -0.43f(\varepsilon(k)) \end{array} \right).$$

Due to (35), with the change of base P_c for the continuous system (P_d for the discrete system)

$$P_c = \left(\begin{array}{cc|c} 1 & 1 & 0 \\ -0.06 & -3.93 & 0 \\ \hline 0 & 0 & 1 \end{array} \right), \quad P_d = \left(\begin{array}{cc|c} 1 & -0.18 & 0 \\ -0.06 & 0.98 & 0 \\ \hline 0 & 0 & 1 \end{array} \right),$$

the matrices $A_{ca}(.)$ and $A_{da}(.)$ become in a thin arrow form, i.e., only the diagonal elements and last row and last column elements can be non zero, such that

$$\tilde{A}_{ca}(.) = \left(\begin{array}{cc|c} -0.06 & 0 & 0.12(f(\varepsilon(t)) - 1) \\ 0 & -3.93 & -0.12(f(\varepsilon(t)) - 1) \\ \hline 1.99 & -29 & -2.5f(\varepsilon(t)) \end{array} \right)$$

and

$$\tilde{A}_{da}(.) = \left(\begin{array}{cc|c} 0.99 & 0 & 0.02(f(\varepsilon(k)) - 1) \\ 0 & 0.31 & 0.09(f(\varepsilon(k)) - 1) \\ \hline 1.15 & -3.69 & -0.43f(\varepsilon(k)) \end{array} \right).$$

For the regular vector norm $p(X) = [|x_1(\tau)| , |x_2(\tau)| , |\varepsilon(\tau)|]^T$, the corresponding characteristics matrices of the comparison system are

$$\tilde{M}(\tilde{A}_{ca}(.)) = \left(\begin{array}{cc|c} -0.06 & 0 & 0.12|(f(\varepsilon) - 1)| \\ 0 & -3.93 & 0.12|(f(\varepsilon) - 1)| \\ \hline 1.99 & 29 & -2.5f(\varepsilon) \end{array} \right)$$

and

$$\tilde{M}(\tilde{A}_{da}(.)) = \left(\begin{array}{cc|c} 0.99 & 0 & 0.02|(f(\varepsilon(k)) - 1)| \\ 0 & 0.31 & 0.09|(f(\varepsilon(k)) - 1)| \\ \hline 1.15 & 3.69 & 0.43|f(\varepsilon(k))| \end{array} \right).$$

By Corollary 4.1, the system under study is asymptotically stable if the nonlinearity function $f(\varepsilon(\tau))$ is within the domain given in Figure 2,

    – Stability domain for the continuous-time case: $0.67 < f(\varepsilon(t)) < 2$,

    – Stability domain for the discrete-time case: $0.76 < f(\varepsilon(k)) < 1.17$.
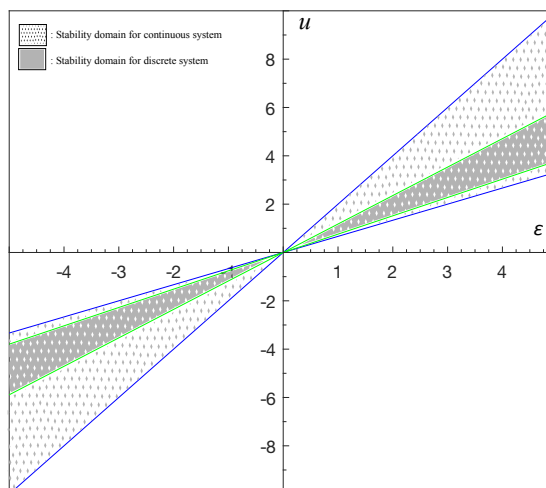
Figure 2: Continuous- and discrete-time stability domains.

6   Conclusion

In this work, a unified stability study of both continuous and discrete systems is presented. Based on the augmented model description and the Borne-Gentina stability criterion, new systematic systems stability conditions depending on the stability property of the linearized model and the nonlinearity are established. In the case of the diagonalizable characteristic matrix of linearised model, more convenient stabilty conditions are easily obtained with the use of arrow form characteristic matrices.

The studied example shows the simplicity of applying the proposed method to a unified stability study of the second order continuous Lur'e system and its associate discrete system.

It is expected that the approach will be extended to more general classes of nonlinear systems, in particular, interconnected nonlinear systems.

References

[1] A. Garulli, A. Masi, G. Valmorbida and L. Zaccarian. Global Stability and Finite L2-Gain of Saturated Uncertain Systems via Piecewise Polynomial Lyapunov Functions. *IEEE Trans. Automat. Contr.* **58** (1) (2013) 242–246.

[2] A. G. Mazko. Robust Output Feedback Stabilization and Optimization of Discrete-Time Control Systems. *Nonlinear Dyn. Syst. Theory* **18** (1) (2018) 92–106.

[3] A. I. Lure and V. N. Postnikov. On the theory of stability of control systems. *Appl. Math. Mech.* **8** (3) (1944) 246-248. [Russian]

[4] B. Sfaihi, M. Benrejeb and P. Borne. On stability conditions of singularly perturbed nonlinear Lur'e discrete-time systems. *Nonlinear Dyn. Syst. Theory* **13** (2) (2013) 203–216.

[5] B. Sfaihi, S. Fekih, and M. Benrejeb. New Approach for Stability Analysis of Interconnected Nonlinear Discrete-Time Systems Based on Vector Norms. *Circuits, Syst. Signal Process* **36** (10) (2017) 3983–4005.

[6] H. Ait Abbas, A. Seghiour, M. Belkheiri and M. Rahmani. Robust Output Feedback Stabilization and Boundedness of Highly Nonlinear Induction Motors Systems Using Single-Hidden-Layer Neural-Networks. *Nonlinear Dyn. Syst. Theory* **19** (3) (2019) 331–347.

[7] H. K. Khalil. *Nonlinear Systems, 3rd.* Prentice Hall, Upper Saddle River, New Jewsey, 2002.

[8] J. C. Gentina, P. Borne, C. Burgat, J. Bernussou and L. T. Grujic. Stability of large-scale systems-vector norms. *RAIRO-Automatique-Systems Anal. Control* **13** (1) (1979) 57–75.

[9] L. T. Gruyitch, J. P. Richard, P. Borne and J. C. Gentina. *Stability Domains.* CRC Press, Boca Raton, USA, 2003.

[10] M. Benrejeb. Stability Study of Two Level Hierarchical Nonlinear Systems. Plenary lecture in: *The 12th IFAC Symposium on Large Scale Systems: Theory and Applications.* Lille, 2010, 30–41.

[11] M. Benrejeb and M. N. Abdelkrim. On order reduction and stabilization of TSK nonlinear fuzzy models by using arrow form matrix. *Syst. Anal. Model. Simul.* **43** (7) (2003) 977–991.

[12] M. Benrejeb and M. Gasmi. On the use of an arrow form matrix for modeling and stability analysis of singularly perturbed non-linear systems. *Systems Analysis-Modelling-Simulation* **40** (4) (2001) 509–525.

[13] M. Benrejeb and P. Borne. On an algebraic stability criterion for non-linear processes. Interpretation in the frequency domain. In: *Proceedings of the Measurement and Control International Symposium, MECO* **78** (1978) 678–682.

[14] M. Benrejeb, P. Borne and F. Laurent. Sur une application de la reprsentation en flche l'analyse des processus. *RAIRO Automatic* **16** (2) (1982) 133–146.

[15] M. Benrejeb and S. Hammami. New approach of stabilization of nonlinear continuous mono-variable processes characterized by an arrow form matrix. In: *1st International Conference Systems Engineering Design and Applications.* Monastir, 2008.

[16] P. Borne, M. Dambrine, W. Perruquetti and J. P. Richard. Vector Lyapunov functions: nonlinear, time-varying, ordinary and functional differential equations. In: *Advances in Stability Theory at the End of the 20th Century (Stability and Control: Theory, Methods and Applications)* (Ed.: A. A. Martynyuk). Taylor and Francis, New York-London, 2003, 49–73.

[17] R. Geiselhart and F. R. Wirth. Relaxed ISS small-gain theorems for discrete-time systems. *SIAM J. Control Optim.* **54** (2) (2016) 423–449.

[18] R. L. Filali, M. Benrejeb and P. Borne. On observer-based secure communication design using discrete-time hyperchaotic systems. *Commun. Nonlinear Sci. Numer. Simul.* **19** (5) (2014) 1424–1432.

[19] S. Elmadssia, K. Saadaoui and M. Benrejeb. Stability conditions for a class of nonlinear time delay systems. *Nonlinear Dyn. Syst. Theory* **14** (3) (2014) 279–291.

[20] Y. Manai and M. Benrejeb. New Condition of Stabilization of Uncertain Continuous Takagi-Sugeno Fuzzy System based on Fuzzy Lyapunov Function. *International Journal of Intelligent Systems and Applications* **4** (3) (2012) 19–24.

Dynamical Analysis, Stabilization and Discretization of a Chaotic Financial Model with Fractional Order

R. Barkat* and T. Menacer

Laboratory of Applied Mathematics, Mohamed Khider University, Biskra, Algeria

Abstract: In this paper, we use the discretization process of a fractional-order financial system. The conditions of the local asymptotic stability of the equilibrium points of the discretized system are analyzed. Through numerical reproductions, we brighten some dynamical behaviors, such as the chaotic attractor, bifurcation for different values of step size and fractional order parameters. Moreover, the numerical simulations confirm the validity of our theoretical results relative to the time step parameter.

Keywords: *fractional-order differential equations; bifurcation; numerical methods; equilibrium; chaotic behavior; discrete-time systems; asymptotic stability.*

Mathematics Subject Classification (2010): 34A08, 34C23, 49Mxx, 74Gxx, 74H65, 93C55, 93D20.

1 Introduction

In the previous two decades, fractional calculus and its applications have attracted a lot of attention. Many models or systems can be described by the fractional order dynamics, among these are viscoelastic models [16], diffusion wave equations [5], equations of electronic circuits [7], energy supply-request equations [21], muscular blood vessel model [22], equations of seismic tremors [1], image encryption scheme models [15], models for nonlocal scourges [11], and nonlinear dynamical model of finance system [28]. In fact, classical differential equations of integer order are generalized by fractional-order differential equations. Meanwhile, chaos is an important dynamical phenomenon which has received an increased attention of scientists since the pioneering work of Lorenz in 1963 [6]. More recently, chaotic behaviors have been found in some nonlinear fractional-order systems [25]. Moreover, the applications of chaos theory such as synchronization [4, 9] and chaos control of fractional-order hyperchaotic and chaotic systems have recently become central topics for research [10, 29].

---

* Corresponding author: `mailto:barkatradhia1992@gmail.com`

The fractional derivatives have sundry definitions. One of the most commonly used definitions in real applications of fractional derivatives is the Caputo definition [14, 19]

$$D^\alpha f(t) = I^{n-\alpha} D^n f(t), \qquad \alpha > 0, \tag{1}$$

where $D^n f$ represents the n order derivative of $f(t)$, where $n = [\alpha]$ is to round to the nearest integer of α, and I^β is the Riemann-Liouville integral operator of order β

$$I^\beta f(t) = \int_0^t \frac{(t-s)^{\beta-1}}{\Gamma(\beta)} f(s) \, ds, \qquad \beta > 0, \tag{2}$$

where $\Gamma(.)$ is the gamma function. And D^α is the Caputo differential operator of order α. It has been shown that chaos in fractional-order autonomous systems can occur for the orders less than three and this cannot happen in their integer order counterparts according to the Poincar–Bendixon theorem, and there are two popular methods for solving differential equations for fractional order: the frequency domain method [13] and time domain method [17]. In the last years, the second method has proved to be more effective because the first method is not always reliable in showing chaos [23, 24]. An analytical solution of differential equations is often undesirable, and one uses numerical or computational methods.

In [29], a numerical method for nonlinear fractional-order differential equations with constant or time-varying delay is devised. We must indicate that the fractional differential equations tend to inferior the dimensionality of the differential equations, however, introducing time retard in differential equations makes them infinite dimensional. Thus, even a single ordinary differential equation with delay can display chaos.

Many discretization methods have been used to construct the discrete-time model utilizing continuous-time methods such as Euler's method, the Runge–Kutta method, predictor-corrector method and nonstandard finite difference methods [2, 26]. Some of them are approximation for the integral and some for the derivative.

In [8, 27], the discretization method is applied to the logistic fractional-order differential equations. This method is an approximation to the right part direction of the differential equation with the formula: $D^\alpha X(t) = f(X(t))$, $t > 0$, $\alpha \in (0, 1]$.

The organization of this paper is as follows. In Section 2, the equilibrium points are found and the discretized-time financial model with fractional order parameter is established. In Section 3 we studied the local stability of all the equilibrium points of the discretized fractional-order system. In Section 4, we present the numerical simulations, which not only illustrate the validity of the theoretical analysis relative to the time step parameter, but also exhibit the complex dynamical behaviors such as the Hopf bifurcation and chaos phenomenon.

2   The Fractional-Order Financial Model and Its Discretization

The fractional-order finance model [28] is given by the following dynamical system:

$$\begin{cases} D^\alpha x(t) = (y(t) - a) x(t) + z(t), \\ D^\alpha y(t) = 1 - x^2(t) - by(t), \\ D^\alpha z(t) = -(x(t) + cz(t)), \end{cases} \tag{3}$$

where x is the interest rate, y is the investment demand, z is the price index, $a > 0$ denotes the saving amount, $b > 0$ denotes the cost per investment, and $c > 0$ denotes the

elasticity of the demand of commercial markets. Besides, $t > 0$, and α is the fractional order satisfying $\alpha \in (0, 1]$. The equilibrium points of system (3) are given as follows:

$$E_0 = \left(0, \frac{1}{b}, 0\right), \; E_1 = \left(\sqrt{1 - b\left(a + \frac{1}{c}\right)}, \left(a + \frac{1}{c}\right), -\frac{1}{c}\sqrt{1 - b\left(a + \frac{1}{c}\right)}\right), \text{ and } E_2 =$$

$$\left(-\sqrt{1 - b\left(a + \frac{1}{c}\right)}, \left(a + \frac{1}{c}\right), \frac{1}{c}\sqrt{1 - b\left(a + \frac{1}{c}\right)}\right).$$

Now, the discretization process of the fractional-order financial system is given as follows.

Assume that $x(0) = x_0$, $y(0) = y_0$ and $z(0) = z_0$ are the initial conditions of system (3). So, the discretization of system (3) with piecewise constant arguments is given as

$$\begin{cases} D^\alpha x\left(t\right) = \left(y\left(\left[\frac{t}{h}\right]h\right) - a\right) x\left(\left[\frac{t}{h}\right]h\right) + z\left(\left[\frac{t}{h}\right]h\right), \\[2mm] D^\alpha y\left(t\right) = 1 - x^2\left(\left[\frac{t}{h}\right]h\right) - by\left(\left[\frac{t}{h}\right]h\right), \\[2mm] D^\alpha z\left(t\right) = -\left(x\left(\left[\frac{t}{h}\right]h\right) + cz\left(\left[\frac{t}{h}\right]h\right)\right). \end{cases} \quad (4)$$

First, let $t \in [0, h)$, so $t/h \in [0, 1)$. Thus, we obtain

$$\begin{cases} D^\alpha x\left(t\right) = \left(y_0 - a\right) x_0 + z_0, \\ D^\alpha y\left(t\right) = 1 - x_0^2 - by_0, \\ D^\alpha z\left(t\right) = -\left(x_0 + cz_0\right), \end{cases} \quad (5)$$

and the solution of (5) is reduced to

$$\begin{cases} x_1(t) = x_0 + J^\alpha\left(\left(y_0 - a\right) x_0 + z_0\right) = x_0 + \dfrac{t^\alpha}{\Gamma\left(1 + \alpha\right)}\left[\left(y_0 - a\right) x_0 + z_0\right], \\[2mm] y_1(t) = y_0 + J^\alpha\left(1 - x_0^2 - by_0\right) = y_0 + \dfrac{t^\alpha}{\Gamma\left(1 + \alpha\right)}\left[1 - x_0^2 - by_0\right], \\[2mm] z_1(t) = z_0 + J^\alpha\left(-\left(x_0 + cz_0\right)\right) = z_0 + \dfrac{t^\alpha}{\Gamma\left(1 + \alpha\right)}\left[-\left(x_0 + cz_0\right)\right]. \end{cases} \quad (6)$$

Second, let $t \in [h, 2h)$, which makes $t/h \in [1, 2)$. Hence, we get

$$\begin{cases} D^\alpha x(t) = \left(y_1 - a\right) x_1 + z_1, \\ D^\alpha y(t) = 1 - x_1^2 - by_1, \\ D^\alpha z(t) = -\left(x_1 + cz_1\right), \end{cases} \quad (7)$$

which have the following solution

$$\begin{cases} x_2(t) = x_1\left(h\right) + J_h^\alpha\left(\left(y_1 - a\right) x_1 + z_1\right) = x_1\left(h\right) + \dfrac{\left(t - h\right)^\alpha}{\Gamma\left(1 + \alpha\right)}\left[\left(y_1 - a\right) x_1 + z_1\right], \\[2mm] y_2(t) = y_1\left(h\right) + J_h^\alpha\left(1 - x_1^2 - by_1\right) = y_1\left(h\right) + \dfrac{\left(t - h\right)^\alpha}{\Gamma\left(1 + \alpha\right)}\left[1 - x_1^2 - by_1\right], \\[2mm] z_2(t) = z_1\left(h\right) + J_h^\alpha\left(-\left(x_1 + cz_1\right)\right) = z_1\left(h\right) + \dfrac{\left(t - h\right)^\alpha}{\Gamma\left(1 + \alpha\right)}\left[-\left(x_1 + cz_1\right)\right], \end{cases} \quad (8)$$

where $J_h^\alpha = \int_h^t \dfrac{(t-s)^{\alpha-1}}{\Gamma(\alpha)} ds$, $\alpha > 0$. Thus, after repeating the discretization process n times, we obtain

$$
\begin{cases}
x_{n+1}(t) = x_n(nh) + \dfrac{(t-nh)^\alpha}{\Gamma(1+\alpha)} \left[(y_n(nh) - a) x_n(nh) + z_n(nh)\right], \\[2mm]
y_{n+1}(t) = y_n(nh) + \dfrac{(t-nh)^\alpha}{\Gamma(1+\alpha)} \left[1 - x_n^2(nh) - by_n(nh)\right], \\[2mm]
z_{n+1}(t) = z_n(nh) + \dfrac{(t-nh)^\alpha}{\Gamma(1+\alpha)} \left[-(x_n(nh) + cz_n(nh))\right],
\end{cases}
\tag{9}
$$

where $t \in [nh, (n+1)h)$. For $t \to (n+1)h$, system (9) is reduced to

$$
\begin{cases}
x_{n+1} = x_n + \dfrac{h^\alpha}{\Gamma(1+\alpha)} \left[(y_n - a) x_n + z_n\right], \\[2mm]
y_{n+1} = y_n + \dfrac{h^\alpha}{\Gamma(1+\alpha)} \left[1 - x_n^2 - by_n\right], \\[2mm]
z_{n+1} = z_n + \dfrac{h^\alpha}{\Gamma(1+\alpha)} \left[-(x_n + cz_n)\right],
\end{cases}
\tag{10}
$$

which can be expressed as

$$
\begin{cases}
x_{n+1} = x_n + s\left[(y_n - a) x_n + z_n\right], \\
y_{n+1} = y_n + s\left[1 - x_n^2 - by_n\right], \\
z_{n+1} = z_n + s\left[-(x_n + cz_n)\right],
\end{cases}
\tag{11}
$$

in which $s = \dfrac{h^\alpha}{\Gamma(1+\alpha)}$.

3   Stability of the Fixed Points of Discretized Systems

In the following, we discuss the local stability of the equilibrium points of system (11). In fact, the local stability of the discrete-time system (11) is determined by calculating the eigenvalues of the Jacobian matrices corresponding to its equilibrium points. Hence, the Jacobian matrix of system (11) is given as follows:

$$
J_{E_{eq}} = \begin{pmatrix}
1 + s(y_n - a) & sx_n & s \\
-2sx_n & 1 - bs & 0 \\
-s & 0 & 1 - cs
\end{pmatrix}.
\tag{12}
$$

In order to study stability of the equilibrium points of system (11), we recall the following two lemmas and theorem.

Lemma 3.1 *[18] Let $F(\lambda) = \lambda^2 - Tr\lambda + Det$. Suppose that $F(1) > 0$, λ_1, λ_2 are the two roots of $F(\lambda) = 0$. Then*

1. *$|\lambda_1| < 1$ and $|\lambda_2| < 1$ if and only if $F(-1) > 0$ and $Det < 1$.*

2. *$|\lambda_1| < 1$ and $|\lambda_2| > 1$ or $|\lambda_1| > 1$ and $|\lambda_2| < 1$ if and only if $F(-1) < 0$.*

3. *$|\lambda_1| > 1$ and $|\lambda_2| > 1$ if and only if $F(-1) > 0$ and $Det > 1$.*

4. *$\lambda_1 = -1$ and $\lambda_2 \neq 1$ if and only if $F(-1) = 0$ and $Tr \neq 0, 2$.*

5. λ_1 and λ_2 are complex and $|\lambda_1| = |\lambda_2|$ if and only if $Tr^2 - 4Det < 0$ and $Det = 1$.

Lemma 3.2 *[20] Let equation $\lambda^3 + a\lambda^2 + b\lambda + c = 0$, where a, b, $c \in \mathbb{R}$. Let further $A = a^2 - 3b$, $B = ab - 9c$, $C = b^2 - 3ac$, and $\Delta = B^2 - 4AC$. Then*

1. *The equation has three real roots if and only if $\Delta \le 0$.*

2. *The equation has one real root λ_1 and a pair of conjugate complex roots if and only if $\Delta > 0$. Furthermore, the conjugate complex roots $\lambda_{2,3}$ are*

$$\lambda_{2,3} = \frac{1}{6}\left[\sqrt[3]{y_1} + \sqrt[3]{y_2} - 2a \pm \sqrt{3}i\left(\sqrt[3]{y_1} - \sqrt[3]{y_2}\right)\right],$$

where

$$y_{1,2} = aA + \frac{3}{2}\left(-B \pm \sqrt{\Delta}\right).$$

Theorem 3.1 *[20] The equilibrium point E_{eq} has the following topological types of its all values of parameters:*

1. *E_{eq} is asymptotically stable if one of the following conditions holds:*

   1.1. *$\Delta \le 0$, $P(1) > 0$, $P(-1) < 0$ and $-1 < \lambda_{1,2}^* < 1$,*
   1.2. *$\Delta > 0$, $P(1) > 0$, $P(-1) < 0$ and $|\lambda_{2,3}| < 1$.*

2. *E_{eq} is unstable if one of the following conditions holds:*

   2.1. *$\Delta \le 0$, and one of the following conditions holds:*
      2.1.1. *$P(1) > 0$, $P(-1) > 0$ and $\lambda_2^* < -1$ or $\lambda_2^* > 1$,*
      2.1.2. *$P(1) < 0$, $P(-1) < 0$ and $\lambda_2^* < -1$ or $\lambda_2^* > 1$,*
   2.2. *$\Delta > 0$, and one of the following conditions holds:*
      2.2.1. *$P(1) < 0$ and $|\lambda_{2,3}| > 1$,*
      2.2.2. *$P(-1) > 0$ and $|\lambda_{2,3}| > 1$.*

3. *E_{eq} is one-dimensional if one of the following conditions holds:*

   3.1. *$\Delta \le 0$, and one of the following conditions holds:*
      3.1.1. *$P(1) > 0$, $P(-1) < 0$, and $\lambda_1^* < -1$ or $\lambda_2^* > 1$,*
      3.1.2. *$P(1) < 0$, $P(-1) > 0$,*
   3.2. *$\Delta > 0$, and one of the following conditions holds:*
      3.2.1. *$P(1) > 0$, $P(-1) < 0$ and $|\lambda_{2,3}| > 1$,*
      3.2.2. *$P(1) < 0$ and $|\lambda_{2,3}| < 1$,*
      3.2.3. *$P(-1) > 0$ and $|\lambda_{2,3}| < 1$.*

4. *E_{eq} is two-dimensional if one of the following conditions holds:*

   4.1. *$\Delta \le 0$, and one of the following conditions holds:*
      4.1.1. *$P(1) > 0$, $P(-1) > 0$ and $-1 < \lambda_2^* < 1$,*
      4.1.2. *$P(1) < 0$, $P(-1) < 0$ and $-1 < \lambda_1^* < 1$,*
   4.2. *$\Delta > 0$, and one of the following conditions holds:*

      4.2.1. $P(-1) < 0$ *and* $|\lambda_{2,3}| < 1$,

      4.2.2. $P(1) > 0$ *and* $|\lambda_{2,3}| < 1$.

  5. E_{eq} *is non-hyperbolic if one of the following conditions holds*:

     5.1. $\Delta \leq 0$, *and* $P(1) = 0$ *or* $P(-1) = 0$,

     5.2. $\Delta > 0$, *and* $P(1) = 0$ *or* $P(-1) = 0$ *or* $|\lambda_{2,3}| = 1$.

3.1 Stability of fixed point E_0

The Jacobian matrix of E_0 of system (11) is

$$J_{E_0} = \begin{pmatrix} 1 + s\left(\dfrac{1}{b} - a\right) & 0 & s \\ 0 & 1 - bs & 0 \\ -s & 0 & 1 - cs \end{pmatrix}. \tag{13}$$

    The characteristic equation of the Jacobian matrix (13) is

$$(\lambda - (-bs + 1))\left(\lambda^2 - Tr_0\lambda + Det_0\right) = 0, \tag{14}$$

where $Tr_0 = \left(2 - \dfrac{1}{b}s\left(ab + bc - 1\right)\right)$,

$Det_0 = \left(\dfrac{1}{b}\left((b - c + abc)s^2 + (1 - bc - ab)s + b\right)\right)$, and $s_1 = \dfrac{ab + bc - 1}{b - c + abc}$, , $s_4 = \dfrac{2}{b}$,

$$s_2 = -\dfrac{\left(\sqrt{-(2b + ab - bc - 1)(2b - ab + bc + 1)} - ab - bc + 1\right)}{b - c + abc},$$

and $s_3 = \dfrac{\left(\sqrt{-(2b + ab - bc - 1)(2b - ab + bc + 1)} + ab + bc - 1\right)}{b - c + abc}$.

    Theorem 3.2 *If the equilibrium point E_0 exists and $c \geq a + 2$, and $b > \dfrac{c}{ac + 1}$ with $a \geq 0$, then it has the following topological types of its all values of parameters:*

  (i) E_0 is asymptotically stable if $0 < h < \min\left(\sqrt[\alpha]{s_2\Gamma(1+\alpha)}, \sqrt[\alpha]{s_4\Gamma(1+\alpha)}\right)$.

  (ii) E_0 is unstable if $h > \max\left(\sqrt[\alpha]{s_3\Gamma(1+\alpha)}, \sqrt[\alpha]{s_4\Gamma(1+\alpha)}\right)$.

    Proof. By applying stability conditions and using Lemma 3.1 the results (i) and (ii) can be achieved with $s_2 < s_1 < s_3$. □

3.2 Stability of fixed points E_1 and E_2

The Jacobian matrix of model (11) at the equilibrium points E_1 and E_2 is

$$J_{E_1} = \begin{pmatrix} \dfrac{1}{c}(c + s) & s\sqrt{-\dfrac{1}{c}(b - c + abc)} & s \\ -2s\sqrt{-\dfrac{1}{c}(b - c + abc)} & 1 - bs & 0 \\ -s & 0 & 1 - cs \end{pmatrix} \tag{15}$$

and

$$J_{E_2} = \begin{pmatrix} \frac{1}{c}\left(c+s\right) & -s\sqrt{-\frac{1}{c}\left(b-c+abc\right)} & s \\ 2s\sqrt{-\frac{1}{c}\left(b-c+abc\right)} & 1-bs & 0 \\ -s & 0 & 1-cs \end{pmatrix}, \qquad (16)$$

for the convenience of calculations, we denote

$\eta_1 = 2\left(c-b-abc\right)$, $\eta_2 = \frac{1}{c}\left(2c-3b+bc^2-2abc\right)$, and $\eta_3 = -\frac{1}{c}\left(c^2+bc-1\right)$.

The corresponding characteristic equation of J_{E_1} and J_{E_2} can be written as

$$P_1\left(\lambda\right) = \lambda^3 + b_1\lambda^2 + b_2\lambda + b_3, \qquad (17)$$

where $b_1 = -\eta_3 s - 3$, $b_2 = \eta_2 s^2 + 2\eta_3 s + 3$, and $b_3 = \eta_1 s^3 - s^2\eta_2 - \eta_3 s - 1$.

By calculating, we further have

$A = b_1^2 - 3b_2 = -s^2\left(3\eta_2 - \eta_3^2\right)$,

$B = b_1 b_2 - 9b_3 = -s^3\left(9\eta_1 + \eta_2\eta_3\right) + s^2\left(6\eta_2 - 2\eta_3^2\right)$,

$C = b_2^2 - 3b_1 b_3 = \left(\eta_2^2 + 3\eta_1\eta_3\right)s^4 + \left(9\eta_1 + \eta_2\eta_3\right)s^3 + \left(\eta_3^2 - 3\eta_2\right)s^2$,

and

$\Delta = B^2 - 4AC = s^6\Delta^*$,

where $\Delta^* = 3\left(27\eta_1^2 + 18\eta_1\eta_2\eta_3 - 4\eta_1\eta_3^3 + 4\eta_2^3 - \eta_2^2\eta_3^2\right)$.

The derivative of $P_1\left(\lambda\right)$ is $P_1'\left(\lambda\right) = 3\lambda^2 + 2b_1\lambda + b_2$. Obviously, the equation $P_1'\left(\lambda\right) = 0$ has two roots as follows:

$$\lambda_{1,2}^* = \frac{1}{3}\left(-b_1 \pm \sqrt{b_1^2 - 3b_2}\right) = \frac{1}{3}\left(s\eta_3 + 3 \pm s\sqrt{\eta_3^2 - 3\eta_2}\right). \qquad (18)$$

When $\Delta^* \leq 0$, namely, $\Delta \leq 0$, by Lemma 3.2, we have that equation (17) has three real roots λ_1, λ_2 and λ_3. From this, we can easily prove that two roots $\lambda_{1,2}^*$ (let $\lambda_1^* \leq \lambda_2^*$) of equation $P_1'\left(\lambda\right) = 0$ also are real.

When $\Delta^* > 0$, namely, $\Delta > 0$, by Lemma 3.2, we have that equation (17) has one real root λ_1 as follows: $\lambda_1 = -\dfrac{b_1 + y_1^{\frac{1}{3}} + y_2^{\frac{1}{3}}}{3}$, and a pair of conjugate complex roots $\lambda_{2,3}$, and the conjugate complex roots are $\lambda_{2,3} = \dfrac{-2b_1 + y_1^{\frac{1}{3}} + y_2^{\frac{1}{3}}}{6} \pm i\dfrac{\sqrt{3}\left(y_1^{\frac{1}{3}} - y_2^{\frac{1}{3}}\right)}{6}$, where

$$y_{1,2} = b_1 A + \frac{3\left(-B \pm \sqrt{\Delta}\right)}{2} = \frac{s^3}{2}\left(\left(-2\eta_3^3 + 9\eta_2\eta_3 + 27\eta_1\right) \pm \sqrt{\Delta^*}\right).$$

Further, we have $P_1\left(1\right) = \eta_1 s^3$, and $P_1\left(-1\right) = \eta_1 s^3 - 2\eta_2 s^2 - 4\eta_3 s - 8$, and we pose

$s_1 = -\dfrac{\left(\eta_3 + \sqrt{-4\eta_2 + \eta_3^2}\right)}{\eta_2}$, $s_2 = -\dfrac{\left(\eta_3 - \sqrt{-4\eta_2 + \eta_3^2}\right)}{\eta_2}$ and $s_3 = \dfrac{\left(-3\eta_3 - \sqrt{3}\sqrt{-8\eta_2 + 3\eta_3^2}\right)}{2\eta_2}$,

$s_4 = \dfrac{\left(-3\eta_3 + \sqrt{3}\sqrt{-8\eta_2 + 3\eta_3^2}\right)}{2\eta_2}$ and $s_5 = \dfrac{2\eta_2}{\eta_1}$, $s_6 = -\dfrac{\left(2\eta_3 + 2\sqrt{\eta_3^2 - 3\eta_2}\right)}{\eta_2}$ and

$\left(\eta_1\right)_1 = \dfrac{2\left(\eta_3\left(\eta_3^2 - \frac{9}{2}\eta_2\right) - \sqrt{-\left(3\eta_2 - \eta_3^2\right)^3}\right)}{27}$, $\left(\eta_1\right)_2 = \dfrac{2\left(\eta_3\left(\eta_3^2 - \frac{9}{2}\eta_2\right) + \sqrt{-\left(3\eta_2 - \eta_3^2\right)^3}\right)}{27}$.

Now, relative to the dynamical properties of the equilibrium points E_1 and E_2, we have the following result.

Theorem 3.3 *If the equilibrium point E_1 or E_2 exists and $\dfrac{\sqrt{23}}{3} \le a \le \dfrac{\sqrt{27}}{3}$, $\dfrac{\sqrt{11}}{8} \le b \le \dfrac{\sqrt{18}}{10}$ and $\dfrac{\sqrt{35}}{3} \le c \le 2$, then it has the following topological types of its all values of parameters:*

(i) *E_1 or E_2 is asymptotically stable if $0 < h < \sqrt[\alpha]{s_3 \Gamma (1 + \alpha)}$ or $h > \sqrt[\alpha]{s_4 \Gamma (1 + \alpha)}$.*

(ii) *E_1 or E_2 is unstable if $\sqrt[\alpha]{s_3 \Gamma (1 + \alpha)} < h < \sqrt[\alpha]{s_1 \Gamma (1 + \alpha)}$ or $\sqrt[\alpha]{s_2 \Gamma (1 + \alpha)} < h < \sqrt[\alpha]{s_4 \Gamma (1 + \alpha)}$.*

(iii) *E_1 or E_2 is non-hyperbolic if $h = \sqrt[\alpha]{s_3 \Gamma (1 + \alpha)}$ or $h = \sqrt[\alpha]{s_4 \Gamma (1 + \alpha)}$.*

Proof. Here η_1, $\eta_2 > 0$, $\eta_3 < 0$.

We have $\Delta > 0$ if $\eta_1 > (\eta_1)_2$. We also achieve these conditions $\left(-4\eta_2 + \eta_3^2\right) > 0$, $27\eta_1 + 3\eta_2\eta_3 > 0$ and $-\eta_2\eta_3 - \eta_1 > 0$.

We assume $E_1 = \dfrac{\sqrt[3]{y_1} + \sqrt[3]{y_2}}{s} - \eta_3$. And by calculation, we find

$$\|\lambda_{2,3}\|^2 - 1 = \left(E_1^2 + 3\eta_3 E_1 + 9\eta_2\right) s^2 + (9\eta_3 + 3E_1) s, \tag{19}$$

and

$$|\lambda_1| - 1 = \frac{1}{3} s E_1 - 2. \tag{20}$$

The conditions $\|\lambda_{2,3}\| = 1$, $|\lambda_1| = 1$, are realized if and only if $s = s_3$ or $s = s_4$.

And the conditions $\|\lambda_{2,3}\| < 1$, $|\lambda_1| < 1$ are verified if and only if
$0 < s < \left(-3\dfrac{E_1 + 3\eta_3}{E_1^2 + 3\eta_3 E_1 + 9\eta_2}\right)$ and $0 < s < \left(\dfrac{6}{E_1}\right)$.

So

$$0 < s < 2s + s\frac{s\eta_3 + 2}{\eta_2 s^2 + 2\eta_3 s + 4} < -3\frac{E_1 + 3\eta_3}{E_1^2 + 3\eta_3 E_1 + 9\eta_2}, \tag{21}$$

$\dfrac{s\left(\eta_2 s^2 + 3\eta_3 s + 6\right)}{\eta_2 s^2 + 2\eta_3 s + 4}$ is positive if $\left(\eta_2 s^2 + 3\eta_3 s + 6\right) > 0$ and $\left(\eta_2 s^2 + 2\eta_3 s + 4\right) > 0$.

We finally obtain $\|\lambda_{2,3}\| < 1$, $|\lambda_1| < 1$, if $s \in (]0, s_1[\cup]s_2, +\infty[) \cap (]0, s_3[\cup]s_4, +\infty[)$. And the conditions $\|\lambda_{2,3}\| < 1$, $|\lambda_1| > 1$ are verified if and only if $0 < s < \left(-3\dfrac{E_1 + 3\eta_3}{E_1^2 + 3\eta_3 E_1 + 9\eta_2}\right)$ and $s > \left(\dfrac{6}{E_1}\right)$. So

$$0 < s < -3\frac{E_1 + 3\eta_3}{E_1^2 + 3\eta_3 E_1 + 9\eta_2} < -s\frac{s\eta_3 + 2}{\eta_2 s^2 + 2\eta_3 s + 4}, \tag{22}$$

$\dfrac{s\left(\eta_2 s^2 + 3\eta_3 s + 6\right)}{\eta_2 s^2 + 2\eta_3 s + 4}$ is negative if $\left(\eta_2 s^2 + 3\eta_3 s + 6\right) < 0$ and $\left(\eta_2 s^2 + 2\eta_3 s + 4\right) > 0$.

We finally obtain $\|\lambda_{2,3}\| < 1$, $|\lambda_1| > 1$, if $s \in (]0, s_1[\cup]s_2, +\infty[) \cap (]s_3, s_4[)$.

The intersection of the previous fields gives us the following results.

E_1 or E_2 is asymptotically stable if $s \in]0, s_3[$ or $]s_4, +\infty[$, E_1 or E_2 is unstable if $s \in]s_3, s_1[$ or $]s_2, s_4[$, and E_1 or E_2 is non-hyperbolic if $s = s_3$ or $s = s_4$ with $s_3 < s_1 < s_2 < s_4$.

Theorem 3.4 *If the equilibrium point E_1 or E_2 exists and $\dfrac{9}{20} \leq b \leq \dfrac{1}{2}$, $2 \leq c \leq \dfrac{5}{2}$ and $\dfrac{9}{5} \leq a < \dfrac{c-b}{bc}$, then it has the following topological types of its all values of parameters:*

(i) *E_1 or E_2 is asymptotically stable if $0 < h < \sqrt[\alpha]{s_6 \Gamma(1+\alpha)}$.*

(ii) *E_1 or E_2 is unstable if $h > \sqrt[\alpha]{s_5 \Gamma(1+\alpha)}$.*

Proof. Here $\eta_1, \eta_2 > 0$, $\eta_3 < 0$.

We have $\Delta \leq 0$ if $\eta_1 \leq (\eta_1)_2$. We also achieve these conditions $\left(-4\eta_2 + \eta_3^2\right) > 0$, $27\eta_1 + \eta_2 \eta_3 < 0$. We will rely on Theorem 3.1 to find the final conditions:

1. $P_1(1) > 0$ and $P_1(-1) < 0$ are verifed if $s \in \,]0, s_5[$.

2. $P_1(1) > 0$ and $P_1(-1) > 0$ are verifed if $s \in \,]s_5, +\infty[$.

3. $-1 < \lambda_{1,2}^* < 1$ is realized if $s \in \,]0, s_6[$.

4. $\lambda_1^* < -1$ is realized if $s \in \,]s_6, +\infty[$.

The intersection of the previous fields gives us the following results.

Condition (1.1.) of Theorem 3.1 is verified if $s \in \,]0, s_6[$, and condition (3.1.1.) of Theorem 3.1 is verified if $s \in \,]s_5, +\infty[$ with $s_6 < s_5$.

4   Numerical Simulations

In this section, we present the bifurcation diagrams, the phase portraits of the model (11), which confirm the analytical results above and illustrate the dynamic behaviors of our model using the digital relay. A bifurcation occurs when the stability of a point of equilibrium changes [12].

As discussed earlier in Section 3, this paper focuses on varying the time step size parameter h and the fractional-order parameter α in the model (11).

Based on the previous analysis, the parameters of the model (11) can be examined by:

varying h in the range $1.25 \leq h \leq 1.4$ and fixing $a = 1.63$, $b = 0.418$, $c = 1.98$, $\alpha = 0.99$ with the initial conditions $(x_0, y_0, z_0) = (0.3, 2.11, -0.1)$. The resulting points are plotted versus the parameter h (see Figure 1). According to Theorem 3.3, we have $\dfrac{\sqrt{23}}{3} < a < \dfrac{\sqrt{27}}{3}$, $\dfrac{\sqrt{11}}{8} < b < \dfrac{\sqrt{18}}{10}$ and $\dfrac{\sqrt{35}}{3} < c < 2$; and E_1 is asymptotically stable if $1.25 \leq h < \sqrt[\alpha]{s_3 \Gamma(1+\alpha)}$ (see Figure 2(a)), the neighbor trajectories converge to the point E_1. If $h = \sqrt[\alpha]{s_3 \Gamma(1+\alpha)} \simeq 1.3045$, system (11) undergoes a Hopf bifurcation as mentioned above (see Figure 2(b)); the fixed point E_1 becomes unstable if $\sqrt[\alpha]{s_3 \Gamma(1+\alpha)} < h < \sqrt[\alpha]{s_1 \Gamma(1+\alpha)}$ with $\sqrt[\alpha]{s_1 \Gamma(1+\alpha)} \simeq 1.6684$ (see Figure 2(c) and 2(d)).

Second, varying α in the range $0.1 \leq \alpha \leq 0.8$ and fixing $h = 1.393$, the resulting points are plotted versus the parameter α (see Figure 3).

We note that the increase of α causes instability of the fixed point. If $\alpha < 0.44$, the fixed point E_1 is locally asymptotically stable (see Figure 4(a)), the neighbor trajectories converge to the point E_1. If $\alpha = 0.44$, system (11) undergoes a Hopf bifurcation (see
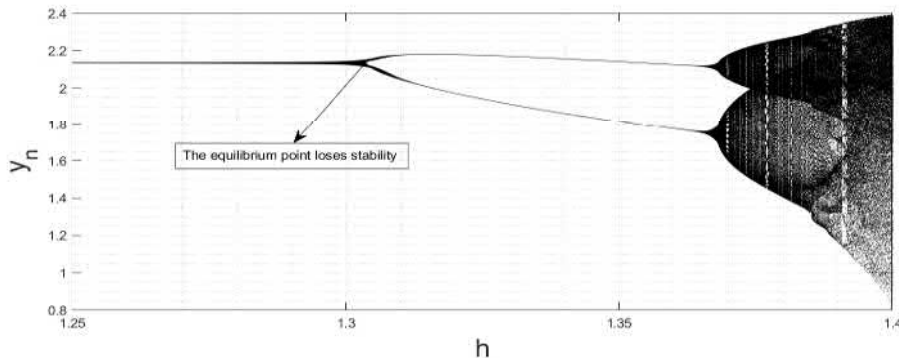
Figure 1: Bifurcation Diagram of Model (11) for $h \in [1.25, 1.4]$.
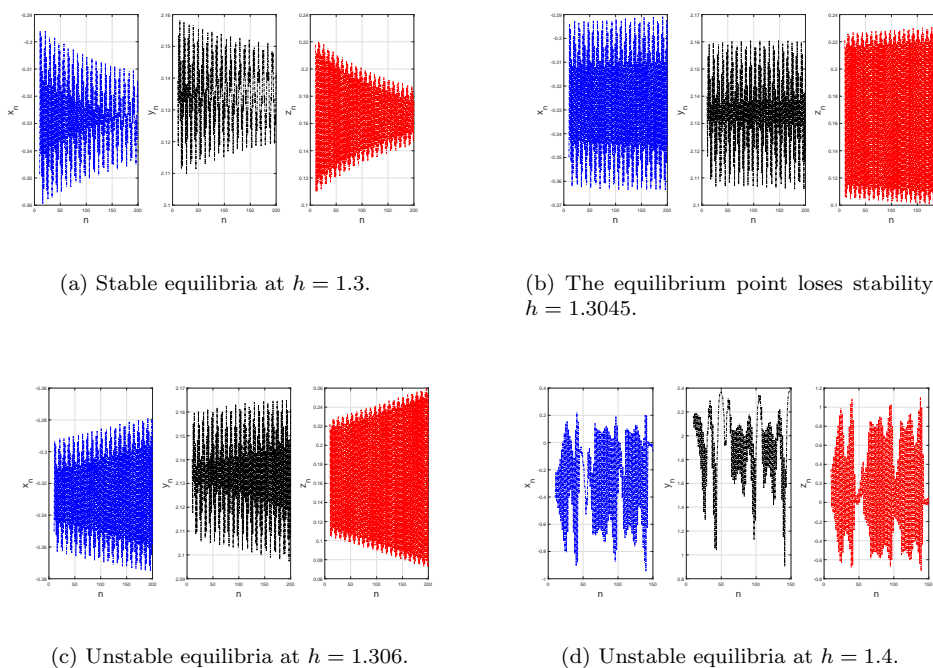
(a) Stable equilibria at $h = 1.3$.

(b) The equilibrium point loses stability at $h = 1.3045$.

(c) Unstable equilibria at $h = 1.306$.

(d) Unstable equilibria at $h = 1.4$.

Figure 2: The Trajectory Diagrams of Model (11) for Various h Corresponding to Figure (1).

Figure 4(b)). The fixed point E_1 becomes unstable if $0.44 < \alpha \le 0.8$, as shown in Figure 4(c) and 4(d).

Third, varying b and fixing $h = 1.399$, $\alpha = 0.99$, the resulting points are plotted versus the parameter b (see Figure 5).

Attracting invariant circles and chaos appear when b decreases, so that the variable belongs to the domain $[0.417, 0.5]$. The phase portraits for various b-values corresponding
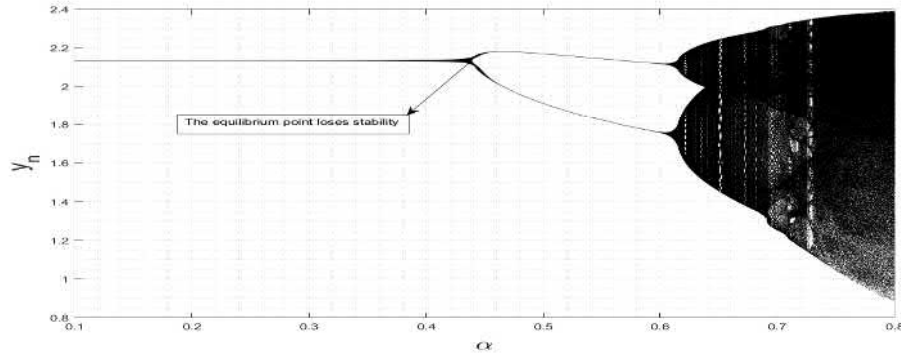
Figure 3: Bifurcation Diagram of Model (11) for $\alpha \in [0.1, 0.8]$.
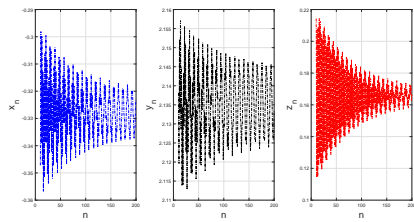
(a) Stable equilibria at $\alpha = 0.42$.
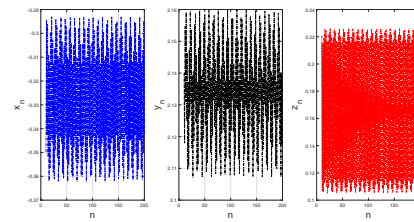
(b) The equilibrium point loses stability at $\alpha = 0.44$.
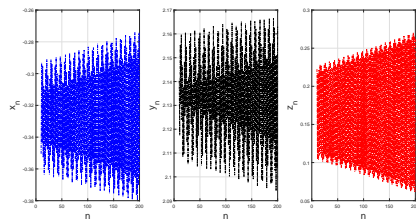
(c) Unstable equilibria at $\alpha = 0.445$.
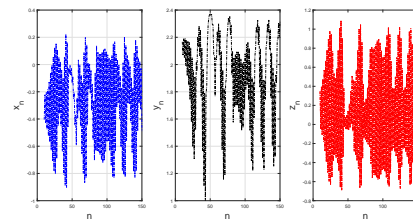
(d) Unstable equilibria at $\alpha = 0.8$.

Figure 4: The Trajectory Diagrams of Model (11) for Various α Corresponding to Figure (3).

to Figure 5 are plotted.

Furthermore, the period-2 orbits ($b = 0.44$) are shown in Figure 6(d), and for the attracting invariant circles ($b = 0.4395$) see Figure 6(c). The quasi-periodic orbits ($b = 0.428$) are observed in Figure 6(b). Attracting chaotic sets are also seen if $b = 0.418$ and are plotted in Figure 6(a).
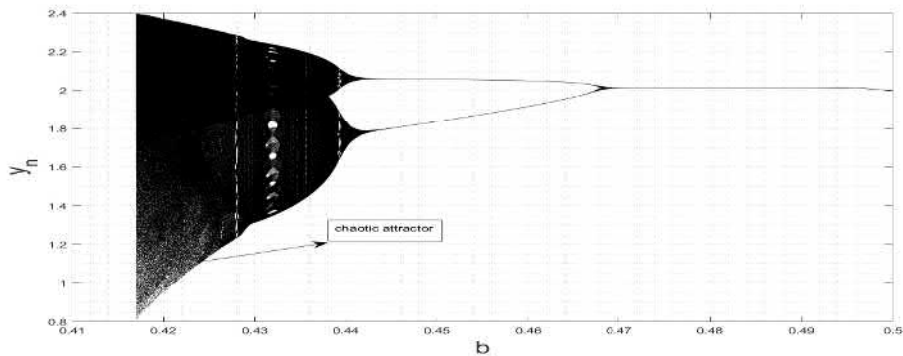
Figure 5: Bifurcation Diagram of Model (11) for $b \in [0.417, 0.5]$.
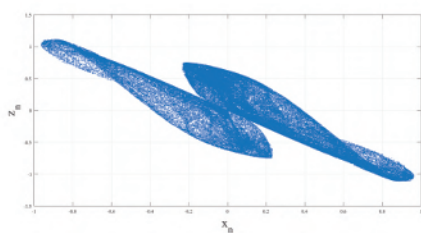
(a) Chaotic attractor at $b = 0.418$.
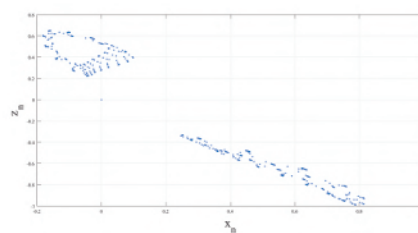
(b) Quasi-periodic orbits at $b = 0.428$.
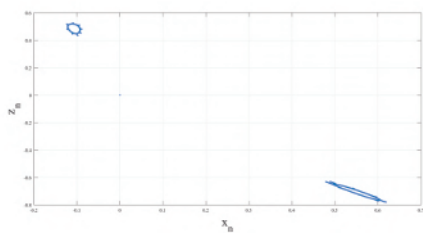
(c) Attracting invariant circles at $b = 0.4395$.
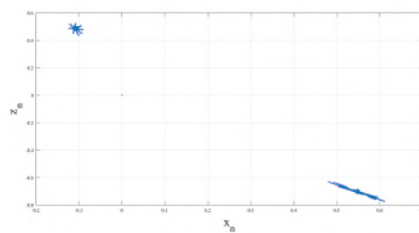
(d) Period-2 orbits at $b = 0.44$.

Figure 6: Phase Portrait Diagrams of Model (11) for Various b Corresponding to Figure (5).

5   Conclusion

In this paper, a discrete-time financial system has been discussed; such a discrete-time model is obtained from the discretization of the fractional-time financial system. The discretization method provides crucial terms such as the time step parameter (h) and fractional-order parameter (α), which are then varied in order to describe the dynamical

behaviors of the model. Note that, whenever we diversify h and α, the system displays many dynamic behaviors including the appearance of bifurcation. Also, the variable b, whenever we change it, shows the bifurcation, attracting invariant circle and chaotic sets. Analytically, sufficient conditions are given to the parameter h for the local stability of equilibrium points. Moreover, numerical continuation is carried out to illustrate the validity of the analytical results.

References

[1] A. E. M. El-Misiery and E. Ahmed. On a fractional model for earthquakes. *Applied Mathematics and Computation* **178** (2) (2006) 207–211.

[2] A. J. Arenas, G. Gonzlez-Parra and B. M. Chen-Charpentier. A nonstandard numerical scheme of predictor–corrector type for epidemic models. *Computers & Mathematics with Applications* **59** (12) (2010) 3740–3749.

[3] A. Khan, N. Aneja and P. Tripathi, J. Biswas. A new hyper chaotic system and study of hybrid projective synchronization behavior. *Nonlinear Dynamics and Systems Theory* **17** (3) (2017) 266–278.

[4] A. Khan and P. Tripathi. Synchronization between a fractional order chaotic system and an integer order chaotic system. *Journal of Applied Mathematics* **13** (4) (2013) 425–436.

[5] A. M. A. El-Sayed. Fractional-order diffusion-wave equation. *International Journal of Theoretical Physics* **35** (2) (1996) 311–322.

[6] A. M. A. El-Sayed, H. M. Nour and A. Elsaid, A. E. Matouk and A. Elsonbaty. Circuit realization, bifurcations, chaos and hyperchaos in a new 4D system. *Applied Mathematics and Computation* **239** (2014) 333–345.

[7] A. M. A. El-Sayed, H. M. Nour and A. Elsaid A. E. Matouk and A. Elsonbaty. Dynamical behaviors, circuit realization, chaos control, and synchronization of a new fractional order hyperchaotic system. *Applied Mathematical Modelling* **40** (5-6) (2006) 3516–3534.

[8] A. M. A. El-Sayed and S. M. Salman. On a discretization process of fractional-order Riccati differential equation. *J. Fract. Calc. Appl.* **4** (2) (2013) 251–259.

[9] A. Ouannas. A new synchronization scheme for general 3D quadratic chaotic systems in discrete-time. *Nonlinear Dynamics and Systems Theory* **15** (2) (2015) 163–170.

[10] C. Li, X. Liao and J. Yu. Synchronization of fractional order chaotic systems. *Physical Review E.* **68** (6) (2003) 067203.

[11] E. Ahmed and A. S. Elgazzar. On fractional order differential equations model for nonlocal epidemics. *Physica A: Statistical Mechanics and its Applications* **379** (2) (2007) 607–614.

[12] H. Cao, Z. Yue and Y. Zhou. The stability and bifurcation analysis of a discrete Holling-Tanner model. *Advances in Difference Equations* **2013** (1) (2013) 330.

[13] H. Sun, A. Abdelwahab and B. Onaral. Linear approximation of transfer function with a pole of fractional power. *IEEE Transactions on Automatic Control* **29** (5) (1984) 441–444.

[14] I. Podlubny. *Fractional Differential Equations.* Academic Press. **198** (1998).

[15] J. Zhao, S. Wang and Y. Chang, X. Li. A novel image encryption scheme based on an improper fractional-order chaotic system. *Nonlinear Dynamics* **80** (4) (2015) 1721–1729.

[16] K. Adolfsson. Nonlinear fractional order viscoelasticity at large strains. *Nonlinear Dynamics* **38** (1-4) (2004) 233–246.

[17] K. Diethelm, N. J. Ford and A. D. Freed. A predictor-corrector approach for the numerical solution of fractional differential equations. *Nonlinear Dynamics* **29** (1-4) (2002) 3–22.

[18] M. A. Abdelaziz, A. I. Ismail, and F. A. Abdullah, M. H. Mohd. Bifurcations and chaos in a discrete SI epidemic model with fractional order. *Advances in Difference Equations* **2018** (1) (2018) 1–19.

[19] M. Caputo. Linear models of dissipation whose Q is almost frequency independent—II. *Geophysical Journal International* **13** (5) (1967) 529–539.

[20] M. El-Shahed, J. J. Nieto and A. M. Ahmed, I. M. E. Abdelstar. Fractional-order model for biocontrol of the lesser date moth in palm trees and its discretization. *Advances in Difference Equations* **2017** (1) (2017) 195.

[21] M. P. Aghababa. Fractional modeling and control of a complex nonlinear energy supply-demand system. *Complexity* **20** (6) (2015) 74–86.

[22] M. P. Aghababa and M. Borjkhani. Chaotic fractional-order model for muscular blood vessel and its control via fractional control scheme. *Complexity* **20** (2) (2014) 37–46.

[23] M. S. Tavazoei and M. Haeri. Limitations of frequency domain approximation for detecting chaos in fractional order systems. *Nonlinear Analysis: Theory, Methods & Applications* **69** (4) (2008) 1299–1320.

[24] M. S. Tavazoei and M. Haeri. Unreliability of frequency-domain approximation in recognising chaos in fractional-order systems. *IET Signal Processing* **1** (4) (2007) 171–181.

[25] P. Muthukumar, P. Balasubramaniam and K. Ratnavelu. Fast projective synchronization of fractional order chaotic and reverse chaotic systems with its application to an affine cipher using date of birth (DOB). *Nonlinear Dynamics* **80** (4) (2015) 1883–1897.

[26] R. E. Mickens. Numerical integration of population models satisfying conservation laws: NSFD methods. *Journal of Biological Dynamics* **1** (4) (2007) 427–436.

[27] R. P. Agarwal, A. M. A. El-Sayed and S. M. Salman. Fractional-order Chua's system: discretization, bifurcation and chaos. *Advances in Difference Equations* **2013** (1) (2013) 320.

[28] W. C. Chen. Nonlinear dynamics and chaos in a fractional-order financial system. *Chaos, Solitons & Fractals* **36** (5) (2008) 1305–1314.

[29] Z. Wang. A numerical method for delayed fractional-order differential equations. *Journal of Applied Mathematics* **2013** (2013), Article ID 256071.

Sinc-Galerkin Method for Solving Higher Order Fractional Boundary Value Problems

A. Darweesh * and K. Al-Khaled

Department of Mathematics and Statistics, Jordan University of Science and Technology, P.O. Box(3030), Irbid (22110), Jordan

Abstract: In this work we use the sinc-Galerkin method to solve higher order fractional boundary value problems. We estimate the second order fractional derivative in the Caputo sense. More precisely, we find a numerical solution for

$$g_1(t)D^\alpha u(t) + g_2(t)D^\beta u(t) + p(t)u^{(4)}(t) + q(t)u(t) = f(t),$$

$$0 < t < 1, \quad 0 < \beta < 1, \quad 1 < \alpha < 2,$$

subject to the boundary conditions $u(0) = 0$, $u'(0) = 0$, $u(1) = 0$, $u'(1) = 0$. Our contribution appears in the estimate of $D^\alpha u$ for higher order α. Numerical examples are described to show the accuracy of this attempt where we applied the sinc-Galerkin method for fractional order differential equations with singularities.

Keywords: *higher order fractional boundary value problems; Caputo derivative; sinc-Galerkin method; numerical solution.*

Mathematics Subject Classification (2010): 34K37, 35A35, 45D05, 65M70.

1 Introduction

Boundary value problems come into view in many areas of science, engineering, and economy. One of the physical modelings for boundary value problems is to suppose a finite length elastic beam, which is fixed at one end, and rested on an elastic bearing at the other end. We may add along its length a load to cause deformations, see [1]. In this work we solve a more general model which has mechanical interpretation that involves higher order fractional derivatives.

---

* Corresponding author: `mailto:ahdarweesh@just.edu.jo`

Several papers discussed the numerical solution of boundary value problems [2–5]. The existence and uniqueness of solutions of such problems are covered in [6–9]. Recently, fractional boundary value problems have been of interest to many mathematicians and scientists, see [10–13]. The present work is motivated by the desire to obtain numerical solutions to the general higher-order fractional boundary value problem of the form

$$\mathbf{L}u : g_1(t)D^\alpha u(t) + g_2(t)D^\beta u(t) + p(t)u^{(4)}(t) + q(t)u(t) = f(t), \tag{1}$$

$$0 < t < 1, \quad 0 < \beta < 1, \quad 1 < \alpha < 2,$$

subject to the conditions

$$u(0) = 0, \quad u'(0) = 0, \quad u(1) = 0, \quad u'(1) = 0, \tag{2}$$

where the notation $y^{(4)}(t)$ stands for the $4th$ derivative of $y(t)$ and $D^\alpha u$ is the Caputo fractional derivative.

Definition 1.1 For $f : [a,b] \to \mathbb{R}$ and $n - 1 < \alpha < n$, the left Caputo fractional derivative of order α is

$$D^\alpha f(t) = \frac{1}{\Gamma(n-\alpha)} \int_a^t (t-\tau)^{n-\alpha+1} \frac{d^n}{d\tau^n} f(\tau)d\tau$$

and the right Riemann-Liouville fractional derivative of order α is

$$D_R^\alpha f(t) = \frac{(-1)^n}{\Gamma(n-\alpha)} \frac{d^n}{dx^n} \int_t^b (t-\tau)^{n-\alpha+1} f(\tau)d\tau.$$

The relation between the left Caputo and right Riemann-Liouville fractional derivatives is given in the following integration by parts formula:

$$\int_a^b g(t)D^\alpha f(t)dt = \int_a^b f(t)D_R^\alpha g(t)dt + \sum_{k=0}^{n-1} D_R^{\alpha-n+k} g(t) \frac{d^{n-k-1}}{dt^{n-k-1}} f(t) \Big|_a^b. \tag{3}$$

One of the most common numerical methods to solve differential equations is the sinc-Galerkin method (SGM). In [14], the authors applied the SGM to solve the general case for the linear fourth-order boundary value problems. For more details about the SGM, see [15–17]. In [18], the author applied the sinc-Galerkin method to solve first order fractional differential equations, in our work we generalize the case to provide a good approximation for higher order fractional boundary value problems. One of the important benefits of the sinc-Galerkin method is dealing with the singularities occurred at the boundaries as we will see in the provided examples. For more details about sinc solutions of analytic problems with singularities, see [19].

The outline of this paper is as follows. In Section 2, we introduce basic definitions and results of the sinc-Galerkin method to formulate the discrete system. Section 3 is devoted to the proof of our main result on the discrete system that is obtained by implementing the sinc-Galerkin method to construct a numerical solution. In Section 4, we demonstrate the accuracy of our suggested scheme by presenting two concrete numerical examples, where the exact solutions are explicitly given. The conclusion is drawn in the last section.

2   The Sinc Function and the Quadrature Formula

The quadrature formula is the main recipe for this paper. It is a rule that approximates integral of some class of functions using the sinc function (see [19, 20]).

The *sinc* function is defined on the whole complex plane $\mathbb{C}$ by

$$\text{sinc}(z) \equiv \begin{cases} \frac{\sin(\pi z)}{\pi z}, & z \neq 0, \\ 1, & z = 0. \end{cases} \tag{4}$$

For $h > 0$ and $k = 0, \pm 1, \pm 2, ...$, the translated sinc function with evenly spaced nodes is given by

$$S(k, h)(z) \equiv \text{sinc}\left(\frac{z - kh}{h}\right). \tag{5}$$

One of the important results on the sinc function is the orthogonality relation

$$\frac{1}{h} \int_{-\infty}^{\infty} S(k, h)(x) S(j, h)(x) dx = \delta_{kj} := \begin{cases} 1, & k = j, \\ 1, & k \neq j. \end{cases} \tag{6}$$

This implies that for any $f \in B(h)$, where $B(h)$ is the Paley-Wiener space (see [19]), we have

$$f(x) = \sum_{k=-\infty}^{\infty} f(hk) S(k, h)(x). \tag{7}$$

The sinc-Galerkin method is originally designed to solve ODEs on the infinite domain $(-\infty, \infty)$. To solve the boundary value problem on the domain (T_1, T_2), we introduce the conformal mapping ϕ that sends (T_1, T_2) onto $(-\infty, \infty)$:

$$\phi(T_1, T_2; z) = \log\left(\frac{z - T_1}{T_2 - z}\right), \tag{8}$$

which maps the eye-shaped domain in the $z-$plane $\mathcal{D}_E$ onto the infinite strip in the $w-$plane, $\mathcal{D}_S$, where

$$\begin{aligned} \mathcal{D}_E &= \{z = x + iy : |arg(\frac{z - T_1}{T_2 - z})| < d \leq \pi/2\}, \\ \mathcal{D}_S &= \{w = u + iv : |v| < d \leq \pi/2\}. \end{aligned}$$

We obtain the basis functions

$$S_k(T_1, T_2; t) := S(k, h) \circ \phi(T_1, T_2; t) = \text{sinc}\left[\frac{\phi(T_1, T_2; t) - kh}{h}\right] \tag{9}$$

over the interval $t \in (T_1, T_2)$. We will use $S_k(t)$ for $S_k(0, 1 : t)$.

To discretize our proposed BVP we use the mesh size h which is the mesh size in $\mathcal{D}_E$ for the uniform grids $\{kh\}$, $-\infty < k < \infty$. Using the conformal mapping ϕ, one can obtain the sinc grid points $t_k \in (T_1, T_2)$ under the action of the inverse image of ϕ :

$$t_k = \phi^{-1}(T_1, T_2; kh) = \frac{e^{kh} + T_1}{T_2 + e^{kh}}.$$

Now we define a class of functions in which the quadrature formula is applied (for more details, see [19, 20]).

Definition 2.1 Let $\phi : \mathcal{D}_E \longrightarrow \mathcal{D}_S$ be a conformal mapping of $\mathcal{D}_E$ onto $\mathcal{D}_S$ with inverse ψ. Let $\Gamma = \{\psi(u) \in \mathcal{D}_E : -\infty < u < \infty\} = (T_1, T_2)$. Then $B(\mathcal{D}_E)$ is the class of functions F which are analytic in $B(\mathcal{D}_E)$ and satisfy

$$\int_{\psi(t+L)} |F(z)| dz \longrightarrow 0, \ \ t \to \pm\infty,$$

where $L = \{iv : |v| < d \leq \pi/2\}$, and on the boundary of $\mathcal{D}_E$, denoted by $\partial\mathcal{D}_E$, satisfy

$$\mathcal{N}(F) = \int_{\partial\mathcal{D}_E} |F(z)| \, dz < \infty.$$

For the choice of the conformal map $\phi(T_1, T_2; z) = \log(\frac{z-T_1}{T_2-z})$ one can state the quadrature formula as follows.

Theorem 2.1 *Let $F \in B(\mathcal{D}_E)$ and ϕ be defined as in 8 such that*

$$|(T_2 - z)(z - T_1)F(z)| \leq C \exp(-\alpha|\phi(z)|)$$

for some $C > 0$, $\alpha > 0$. Choose $N = M + 1, h = \sqrt{2\pi d/(\alpha M)}$. Then the sinc trapezoidal quadrature formula is

$$\int_0^1 F(z)dz \approx h \sum_{j=-M}^{N} \frac{F(z_j)}{\phi'(z_j)} \tag{10}$$

with the exponential order error $\mathcal{O}(\exp(-\sqrt{2\pi d\alpha M}))$.

3   SGM Approach

In this section, we present the SGM method to discretize the fourth-order fractional differential equation for $1 < \alpha < 2$ and $0 < \beta < 1$,

$$\mathbf{L}u := g_1(t)D^\alpha u(t) + g_2(t)D^\beta u(t) + p(t)u^{(4)}(t) + q(t)u(t) = f(t), \ \ 0 < t < 1, \tag{11}$$

subject to the conditions

$$u(0) = 0, \ \ u'(0) = 0, \ \ u(1) = 0, \ \ u'(1) = 0. \tag{12}$$

The completeness of the orthogonal system $\{S_k\}$, which is defined in (9), ensures that we can suggest the approximate solution of the form

$$u_m(t) = \sum_{k=-N_1}^{N_2} c_k S_k(t), \ \ m = N_1 + N_2 + 1, \tag{13}$$

where c_k are the expansion coefficients which will be determined. These coefficients are determined by the orthogonality property of the basis functions $\{S_k\}_{k=-N_1}^{N_2}$. The orthogonality yields the discrete system

$$< \mathbf{L}u_m - f, S_k >= 0, \ \ -N_1 \leq k \leq N_2. \tag{14}$$

One can use the linearity of the inner product to simplify (14) in the form

$$< g_1 D^\alpha u, S_k > + < g_2 D^\beta u, S_k > + < p\, u^{(4)}, S_k > + < q\, u, S_k >$$
$$- < f, S_k > = 0, \quad -N_1 \le k \le N_2. \tag{15}$$

As we mentioned in the previous section, we use the weighted inner product

$$< u(t), v(t) > = \int_0^1 u(t)v(t)w(t)dt,$$

where the weight is

$$w(t) = (1-x)^2 x^2. \tag{16}$$

For the general choice of the weight function see [19], where the author suggested

$$w(t) = 1/(\phi'(t))^m$$

for the general case. In the case of higher order derivatives $D^\alpha u$ and $\frac{d^m}{dt^m}u$, we suggest the weight

$$w(t) = 1/(\phi'(t))^{N_0},$$

where

$$N_0 \le \frac{\max\{n, m\} + 1}{2} < N_0 + 1.$$

The First Term. We estimate the term $< g_1 D^\alpha u, S_k >$ for $1 < \alpha < 2$. We use the integral by parts formula (3) and the boundary conditions $u(0) = u(1) = u'(0) = u'(1) = 0$ to find

$$< g_1 D^\alpha u, S_k > = \int_0^1 g_1(t) D^\alpha[u(t)] S_k(t) w(t) dt$$

$$= \int_0^1 u(t) D_R^\alpha[S_k(t) g_1(t) w(t)] dt + \sum_{k=0}^1 D_R^{\alpha-2+k}[S_k(t) g_1(t) w(t)] \frac{d^{1-k}}{dt^{1-k}} u(t) \Big|_0^1$$

$$= \int_0^1 u(t) D_R^\alpha[S_k(t) g_1(t) w(t)] dt$$

$$= \int_0^1 \left(u(t) \frac{1}{\Gamma(2-\alpha)} \frac{d^2}{dt^2} \int_t^1 (\tau - t)^{1-\alpha} S_k(\tau) g_1(t) w(\tau) d\tau \right) dt.$$

Using the quadrature formula 10, one can write

$$\int_t^1 (\tau - t)^{1-\alpha} S_k(\tau) g_1(t) w(\tau) d\tau \approx h \sum_{r=-N_1}^{N_2} \frac{(\tau_r - t)^{1-\alpha} S_k(\tau_r) g_1(\tau_r) w(\tau_r)}{\phi_t'(\tau_r)},$$

where $h = \pi/\sqrt{N_2}$, and $\tau_k = \phi^{-1}(t, 1; kh)$.

It follows that

$$< g_1 D^\alpha u, S_k > \approx \int_0^1 u(t) \frac{1}{\Gamma(2-\alpha)} \frac{d^2}{dt^2} \left(h \sum_{r=-N_1}^{N_2} \frac{(\tau_r - t)^{1-\alpha} S_k(\tau_r) w(\tau_r)}{\phi_t'(\tau_r)} \right) dt.$$

Another use of the quadrature formula (10) for $t_k = \phi^{-1}(0,1;kh)$ yields

$$< g_1 D^\alpha u, S_j > \approx$$
$$\frac{h^2}{\Gamma(2-\alpha)} \sum_{k=-N_1}^{N_2} \sum_{r=-N_1}^{N_2} \frac{u(t_k)}{\phi'(0,1;t_k)} \frac{d^2}{dt^2} \left(\frac{(\tau_r - t)^{1-\alpha} S_j(\tau_r) g_1(\tau_r) w(\tau_r)}{\phi'(t,1;\tau_r)} \right) \Bigg|_{t=t_k}$$

for $j = -N, ..., N$.

The Second Term. The estimation of the second term is done similarly to that of the first term with the change for $1 < \alpha < 2$ by $0 < \beta < 1$. Hence, the same computations show that

$$< g_2 D^\beta u, S_j > \approx$$
$$\frac{-h^2}{\Gamma(1-\beta)} \sum_{k=-N_1}^{N_2} \sum_{r=-N_1}^{N_2} \frac{u(t_k)}{\phi'(0,1;t_k)} \frac{d}{dt} \left(\frac{(\tau_r - t)^{1-\beta} S_j(\tau_r) g_2(\tau_r) w(\tau_r)}{\phi'(t,1;\tau_r)} \right) \Bigg|_{t=t_k}$$

for $j = -N, ..., N$.

The Third Term. Now we estimate the term $< pu'''', S_k >$ using the sinc quadrature formula in (10). Using the integration by parts and the fact that $w(0) = w(1) = 0$, one can find that

$$< pu'''', S_k > = -\int_0^1 u'''(x) \frac{d}{dx} [p(x) S_k(x) w(x)] dx$$
$$= \int_0^1 u''(x) \frac{d^2}{dx^2} [p(x) S_k(x) w(x)] dx.$$

Now we use the boundary conditions in (2) and the integration by parts two more times to get

$$< u'''', S_k > = \int_0^1 u(x) \frac{d^4}{dx^4} [p(x) S_k(x) w(x)] dx. \tag{17}$$

If we use the chain rule to write $\frac{d^n}{dx^n}[S_k(x)]$ in terms of $\frac{d^n}{d\phi^n}[S_k]$ and $\phi^{(n)}(0,1;x)$, and if we introduce the notation

$$S_k^{(n)}(x) := \frac{d^n}{d\phi^n}[S_k(x)], \ n = 0,1,2,3,4$$

and simplify the calculations as in [19, 20], then we can find the following result:

$$< pu'''', S_k > = \sum_{j=0}^4 \left(\int_0^1 u(x) S_k^{(j)}(x) \eta_j(x) dx \right), \tag{18}$$

where

$$\eta_0(x) = \; 48(-1+2x)P'(x) + 12p''(x) + (-1+x)x$$
$$\times \left(72p''(x) + 8(-1+2x)p^{(3)}(x) + (-1+x)xp^{(4)}(x)\right) + 24p(x),$$

$$\eta_1(x) = \; \frac{18(-1+x)x(-1+2x)p''(x) + 4(-1+x)^2x^2p^{(3)}(x))}{(-1+x)x} +$$
$$\frac{-8\left(1 - 9x + 9x^2\right)p'(x)}{(-1+x)x} - \frac{2(-1+2x)\left(-1 - 6x + 6x^2\right)p(x)}{(-1+x)^2x^2},$$

$$\eta_2(x) = \; \frac{\left(-1 - 12x + 12x^2\right)p(x)}{(-1+x)^2x^2} + \tag{19}$$
$$\frac{-12\left(-2 + 13x - 15x^2 + 2x^3\right)p'(x) + 6(-1+x)^2x^2p''(x)}{(-1+x)^2x^2},$$

$$\eta_3(x) = \; \frac{-2(-1+2x)p(x) - 4(-1+x)xp'(x)}{(-1+x)^2x^2},$$

$$\eta_4(x) = \; \frac{p(x)}{(-1+x)^2x^2}.$$

Applying the sinc quadrature formula (10) to the right-hand side of (18), we obtain

$$< pu'''', S_k > \approx h \sum_{j=-N_1}^{N_2} \sum_{i=0}^{4} \frac{u(x_j)}{\phi'(0,1;x_j)h^i}\delta_{jk}^{(i)}\eta_i(x_j), \tag{20}$$

where $x_k = \phi^{-1}(0,1;kh)$, and $\delta_{jk}^{(i)}$ are given by

$$\delta_{jk}^{(0)} = [S(j,h) \circ \phi(x)]\Big|_{x_k} = \begin{cases} 1, & j = k, \\ \\ 0, & j \neq k, \end{cases}$$

$$\delta_{jk}^{(1)} = h\frac{d}{d\phi}[S(j,h) \circ \phi(x)]\Big|_{x_k} = \begin{cases} 0, & j = k, \\ \\ \frac{(-1)^{k-j}}{(k-j)}, & j \neq k, \end{cases}$$

$$\delta_{jk}^{(2)} = h^2\frac{d^2}{d\phi^2}[S(j,h) \circ \phi(x)]\Big|_{x_k} = \begin{cases} \frac{-\pi^2}{3}, & j = k, \\ \\ \frac{-2(-1)^{k-j}}{(k-j)^2}, & j \neq k, \end{cases} \tag{21}$$

$$\delta_{jk}^{(3)} = h^3\frac{d^3}{d\phi^3}[S(j,h) \circ \phi(x)]\Big|_{x_k} = \begin{cases} 0, & j = k, \\ \\ \frac{(-1)^{k-j}}{(k-j)^3}[6 - \pi^2(k-j)^2], & j \neq k, \end{cases}$$

$$\delta_{jk}^{(4)} = h^4\frac{d^4}{d\phi^4}[S(j,h) \circ \phi(x)]\Big|_{x_k} = \begin{cases} \frac{\pi^4}{5}, & j = k, \\ \\ \frac{-4(-1)^{k-j}}{(k-j)^4}[6 - \pi^2(k-j)^2], & j \neq k. \end{cases}$$

The Last Two Terms. Finally, use (6) and (7). One can write

$$
\begin{aligned}
< qu - f, S_k > &= \int_0^1 (q(x)u(x) - f(x)) \, S_k(x)w(x)dx \\
&= \int_0^1 \left(\frac{q(x)u(x) - f(x)}{\phi'(0,1;x)} w(x) \right) S_k(x)\phi'(0,1;x)dx \\
&= \int_0^1 \left(\sum_{i=-\infty}^{\infty} \frac{q(t_i)u(t_i) - f(t_i)}{\phi'(0,1;t_i)} w(t_i)S_i(x) \right) S_k(x)\phi'(0,1;x)dx \\
&\approx \sum_{i=-N_1}^{N_2} \frac{q(t_i)u(t_i) - f(t_i)}{\phi'(0,1;t_i)} w(t_i) \int_0^1 S_i(x)S_k(x)\phi'(0,1;x)dx \\
&= \sum_{i=-N_1}^{N_2} \frac{q(t_i)u(t_i) - f(t_i)}{\phi'(0,1;t_i)} w(t_i) \int_{-\infty}^{\infty} \text{sinc}(\frac{t-ih}{h})\text{sinc}(\frac{t-ih}{h})dt \\
&= \sum_{i=-N_1}^{N_2} \frac{q(t_i)u(t_i) - f(t_i)}{\phi'(0,1;t_i)} w(t_i)h\delta_{ki} \\
&= h\frac{q(t_k)u(t_k) - f(t_k)}{\phi'(0,1;t_k)} w(t_k).
\end{aligned}
$$

Replacing each term in equation (15) by its approximation, we proved the following theorem.

Theorem 3.1 *Let $\phi(T_1, T_2; x)$, $S_j(x)$, $\eta_j(x)$, $w(x)$, and $\delta_{jk}^{(i)}$ be defined as in (8), (9), (19), (16), and (21), respectively. Discretize $(0,1)$ by $\{t_j\}$, where $t_j = \phi^{-1}(0,1;jh)$ and $(t,1)$ by $\tau_j = \phi^{-1}(t,1;jh)$ for all $0 < t < 1$. We can discretize the BVP*

$$
g_1(x)D^\alpha u(t) + g_2(x)D^\beta u(t) + p(t)u^{(4)}(t) + q(t)u(t) = f(t), \; 0 < t < 1, \; 1 < \alpha < 2, 0 < \beta < 1,
$$

subject to the boundary conditions $u(0) = 0$, $u'(0) = 0$, $u(1) = 0$, $u'(1) = 0$, by the system

$$
\frac{h^2}{\Gamma(2-\alpha)} \sum_{j=-N_1}^{N_2} \sum_{i=-N_1}^{N_2} \frac{u(t_j)}{\phi'(0,1;t_j)} \frac{d^2}{dt^2} \left(\frac{(\tau_i - t)^{1-\alpha} S_k(\tau_i) g_1(\tau_i) w(\tau_i)}{\phi'(t,1;\tau_i)} \right) \Bigg|_{t=t_j} +
$$

$$
\frac{-h}{\Gamma(1-\beta)} \sum_{j=-N_1}^{N_2} \sum_{i=-N_1}^{N_2} \frac{u(t_j)}{\phi'(0,1;t_j)} \frac{d}{dt} \left(\frac{(\tau_i - t)^{-\beta} S_k(\tau_i) g_2(\tau_i) w(\tau_i)}{\phi'(t,1;\tau_i)} \right) \Bigg|_{t=t_j} +
$$

$$
h \sum_{j=-N_1}^{N_2} \sum_{i=0}^{4} \frac{u(t_j)}{\phi'(0,1;t_j)h^i} \delta_{jk}^{(i)} \eta_i(t_j) + h\frac{q(t_k)u(t_k) - f(t_k)}{\phi'(0,1;t_k)} w(t_k) = 0,
$$

for $k = -N_1, ..., 0, ..., N_2$.

4   Numerical Applications

Example 4.1 Consider the following BVP:

$$x^{3/2}D^{1.5}u(x) + u^{(4)}(x) + \frac{1}{1+x^2}u(x) = f(x) \tag{22}$$

with the boundary conditions

$$u(0) = 0, \ \ u'(0) = 0, \ \ u(1) = 0, \ \ u'(1) = 0, \tag{23}$$

where

$$f(x) = 24\left(6 - 20x + 15x^2\right) +$$
$$\frac{(-1+x)^4 x^2}{1+x^2} + \frac{4x^2\left(105 - 840x + 2016x^2 - 1920x^3 + 640x^4\right)}{105\sqrt{\pi}}.$$

The exact solution for this problem is $u(x) = (x-1)^4 x^2$.

For the choice of $w(x) = (1-x)^2 x^2$, we have

$$\eta_0(x) = 24,$$
$$\eta_1(x) = \frac{-2 - 4x\left(2 - 9x + 6x^2\right)}{(-1+x)^2 x^2},$$
$$\eta_2(x) = \frac{-1 + 12(-1+x)x}{(-1+x)^2 x^2},$$
$$\eta_3(x) = -\frac{2}{(-1+x)^2} + \frac{2}{x^2},$$
$$\eta_4(x) = \frac{1}{(-1+x)^2 x^2}.$$

Use $N_1 = N_2 = 30$, and $h = \frac{\pi}{\sqrt{30}}$. Then, the discrete system is given by the resulting system

$$\sum_{j=-30}^{30}\sum_{i=0}^{4}\frac{c_j}{h^i\phi'(0,1;x_j)}\delta_{jk}^{(i)}\eta_i(x_j) + \frac{h}{\Gamma(1/2)}\sum_{j=-30}^{30}\sum_{i=-30}^{30}\frac{c_j}{\phi'(0,1;x_j)}\times$$
$$\frac{d^2}{dt^2}\left(\frac{(\tau_i)^{3/2}(\tau_i - t)^{-1/2}S_k(\tau_i)w(\tau_i)}{\phi'(t,1;\tau_i)}\right)\bigg|_{t=t_j} + \frac{c_k w(x_k)}{(1+x_k^2)\phi'(0,1;x_k)} = \frac{f(x_k)w(x_k)}{\phi'(0,1;x_k)}$$

for $k = -30, -29, ..., 29, 30$. Using Mathematica, one can solve this system and find that
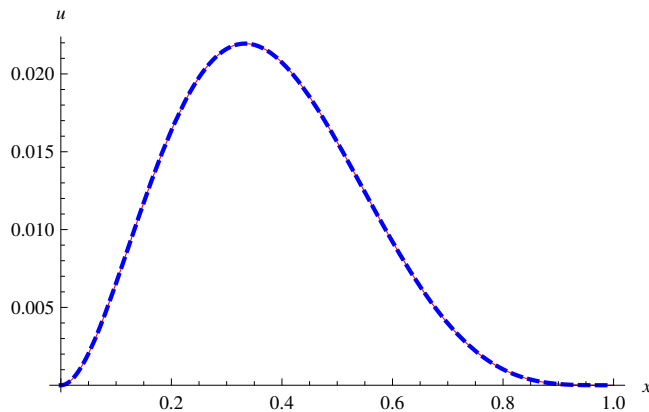
Figure 1: The exact solution is the red color and the approximate solution is the dashed blue color for Example 4.1 when $N_1 = N_2 = 40$ and $h = \pi/\sqrt{60}$.

$c_{-30} = 5.99655 \times 10^{-14}$	$c_{-10} = 0.00001$	$c_{10} = 1.48656 \times 10^{-8}$
$c_{-29} = 1.042706 \times 10^{-13}$	$c_{-9} = 0.0000317$	$c_{11} = 5.5547 \times 10^{-9}$
$c_{-28} = 2.8087 \times 10^{-13}$	$c_{-8} = 0.000097$	$c_{12} = 4.61723 \times 10^{-9}$
$c_{-27} = 4.09977 \times 10^{-13}$	$c_{-7} = 0.000292374$	$c_{13} = 1.82193 \times 10^{-9}$
$c_{-26} = 9.09015 \times 10^{-13}$	$c_{-6} = 0.000848463$	$c_{14} = 1.4434 \times 10^{-9}$
$c_{-25} = 1.15627 \times 10^{-12}$	$c_{-5} = 0.00231724$	$c_{15} = 5.9222 \times 10^{-10}$
$c_{-24} = 2.21194 \times 10^{-12}$	$c_{-4} = 0.00571294$	$c_{16} = 4.5229 \times 10^{-10}$
$c_{-23} = 1.3661 \times 10^{-12}$	$c_{-3} = 0.01192$	$c_{17} = 1.91280 \times 10^{-10}$
$c_{-22} = 3.9494 \times 10^{-13}$	$c_{-2} = 0.0192758$	$c_{18} = 1.420322 \times 10^{-10}$
$c_{-21} = 1.91666 \times 10^{-11}$	$c_{-1} = 0.0217367$	$c_{19} = 6.149521 \times 10^{-11}$
$c_{-20} = 7.5221 \times 10^{-11}$	$c_0 = 0.0156253$	$c_{20} = 4.4668 \times 10^{-11}$
$c_{-19} = 2.9383 \times 10^{-10}$	$c_1 = 0.00690247$	$c_{21} = 1.96808 \times 10^{-11}$
$c_{-18} = 9.7171 \times 10^{-10}$	$c_2 = 0.001944$	$c_{22} = 1.40445 \times 10^{-11}$
$c_{-17} = 3.2402 \times 10^{-9}$	$c_3 = 0.000382$	$c_{23} = 6.2537 \times 10^{-12}$
$c_{-16} = 1.0346 \times 10^{-8}$	$c_4 = 0.0000584$	$c_{24} = 4.3941 \times 10^{-12}$
$c_{-15} = 3.3137 \times 10^{-8}$	$c_5 = 7.59754 \times 10^{-6}$	$c_{25} = 1.9531 \times 10^{-12}$
$c_{-14} = 1.04718 \times 10^{-7}$	$c_6 = 1.01161 \times 10^{-6}$	$c_{26} = 1.34788 \times 10^{-12}$
$c_{-13} = 3.31083 \times 10^{-7}$	$c_7 = 1.41935 \times 10^{-7}$	$c_{27} = 5.7864 \times 10^{-13}$
$c_{-12} = 1.04126 \times 10^{-6}$	$c_8 = 5.67820 \times 10^{-8}$	$c_{28} = 3.84874 \times 10^{-13}$
$c_{-11} = 3.269197 \times 10^{-6}$	$c_9 = 1.7549 \times 10^{-8}$	$c_{29} = 1.4007 \times 10^{-13}$
		$c_{30} = 8.0230 \times 10^{-14}$

Now the numerical solution is $u(x) = \sum_{i=-30}^{30} c_i S_k(x)$. Figure 1, Table 1, and Table 2 show the accuracy of the SGM in Example 4.1.

Example 4.2 Consider the following BVP:

$$xD^{1.5}u(x) + D^{0.5}u(x) + u^{(4)}(x) + \frac{1}{x}u(x) = f(x) \tag{24}$$

with the boundary conditions

$$u(0) = 0, \quad u'(0) = 0, \quad u(1) = 0, \quad u'(1) = 0, \tag{25}$$

x_k	Exact value	Approximate Value	Absolute Error
0.000103361	$1.0679078727 \times 10^{-8}$	$1.034606291 \times 10^{-8}$	$3.33015812 \times 10^{-10}$
0.000325432	$1.057680767 \times 10^{-7}$	$1.047189702 \times 10^{-7}$	$1.04910649 \times 10^{-9}$
0.00102413	$1.044557458 \times 10^{-6}$	$1.041265549 \times 10^{-6}$	$3.291908932 \times 10^{-9}$
0.00321811	0.0000102236	0.0000102134	$1.022024664 \times 10^{-8}$
0.0100649	0.0000972841	0.0000972533	$3.081035295 \times 10^{-8}$
0.0310251	0.000848548	0.000848463	$8.53263208 \times 10^{-8}$
0.0915966	0.00571312	0.00571294	$1.826834860 \times 10^{-7}$
0.241011	0.0192759	0.0192758	$1.500778530 \times 10^{-7}$
0.5	0.015625	0.0156253	$3.16788086 \times 10^{-7}$
0.758989	0.00194364	0.00194426	$6.24294102 \times 10^{-7}$
0.908403	0.0000580864	0.0000584573	$3.70957577 \times 10^{-7}$
0.968975	8.6991642×10^{-7}	$1.011614594 \times 10^{-6}$	$1.416981697 \times 10^{-7}$
0.989935	$1.005642443 \times 10^{-8}$	$5.67820105 \times 10^{-8}$	$4.672558615 \times 10^{-8}$
0.996782	$1.065625857 \times 10^{-10}$	$1.486565724 \times 10^{-8}$	$1.475909466 \times 10^{-8}$
0.998976	$1.097828970 \times 10^{-12}$	$4.61723057 \times 10^{-9}$	$4.616132746 \times 10^{-9}$
0.999675	$1.12087543 \times 10^{-14}$	$1.443447221 \times 10^{-9}$	$1.443436012 \times 10^{-9}$
0.999897	$1.14113473 \times 10^{-16}$	$4.522918397 \times 10^{-10}$	$4.52291725 \times 10^{-10}$

Table 1: Numerical values for Example 4.1 when $N_1 = N_2 = 30$ and $h = \pi/\sqrt{30}$.

x_k	Exact value	Approximate Value	Absolute Error
0.000888742	$7.87057693 \times 10^{-7}$	$7.8614223458 \times 10^{-7}$	$9.15458562 \times 10^{-10}$
0.00179253	$3.19018596 \times 10^{-6}$	$3.1883409387 \times 10^{-6}$	$1.84503042 \times 10^{-9}$
0.00361208	0.0000128597	0.0000128559	$3.71143282 \times 10^{-9}$
0.00726518	0.0000512656	0.0000512581	$7.438059772 \times 10^{-9}$
0.0145589	0.000199884	0.000199869	$1.479564583 \times 10^{-8}$
0.0289613	0.000745729	0.0007457	$2.89922931 \times 10^{-8}$
0.0567902	0.00255258	0.00255252	$5.51198146 \times 10^{-8}$
0.108375	0.00742317	0.00742307	$9.86259941 \times 10^{-8}$
0.19703	0.0161384	0.0161383	$1.562575722 \times 10^{-7}$
0.331262	0.0219466	0.0219464	$1.948937535 \times 10^{-7}$
0.5	0.015625	0.0156248	$1.615772327 \times 10^{-7}$
0.668738	0.00538517	0.00538509	$8.17869846 \times 10^{-8}$
0.80297	0.000971686	0.000971658	$2.849247698 \times 10^{-8}$
0.891625	0.00010967	0.000109661	8.2069107×10^{-9}
0.94321	$9.25355745 \times 10^{-6}$	$9.2513881662 \times 10^{-6}$	$2.16928432 \times 10^{-9}$
0.971039	$6.63350097 \times 10^{-7}$	$6.6280111914 \times 10^{-7}$	$5.4897826 \times 10^{-10}$
0.985441	$4.36286973 \times 10^{-8}$	$4.3493511523 \times 10^{-8}$	$1.35185823 \times 10^{-10}$
0.992735	$2.745695415 \times 10^{-9}$	$2.7132500384 \times 10^{-9}$	$3.2445377 \times 10^{-11}$
0.996388	$1.690005952 \times 10^{-10}$	$1.6151162 \times 10^{-10}$	$7.4889679 \times 10^{-12}$

Table 2: Numerical values for Example 4.1 when $N_1 = N_2 = 40$ and $h = \pi/\sqrt{60}$.
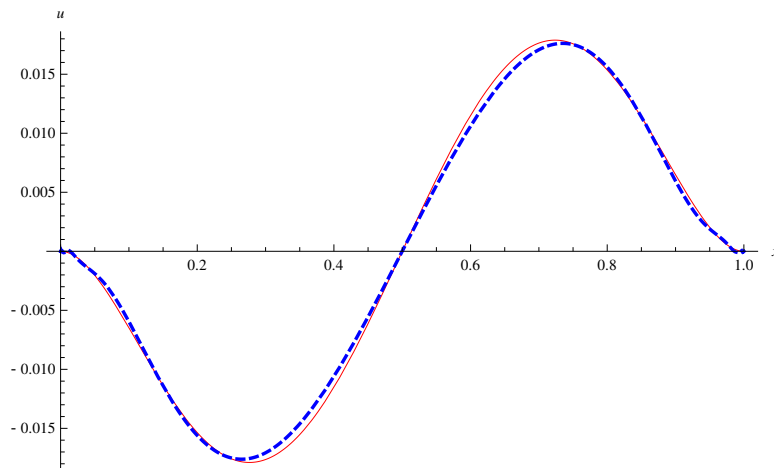
Figure 2: The exact solution is the red color and the approximate solution is the dashed blue color for Example 4.2 when $N_1 = N_2 = 10$ and $h = \frac{\pi}{\sqrt{30}}$.

where

$$f(x) = (-1 + 2x)(24 + (1 - x)^2 x + 96) + \frac{4x^{3/2}}{315\sqrt{\pi}} \left(-525 + 3528x - 6480x^2 + 3520x^3\right).$$

The exact solution for this problem is $u(x) = x^2(-1 + 4x - 5x^2 + 2x^3)$. In this example we consider a fractional differential equation with singularity at $x = 0$ to show the power of SGM with this kind of problems. We consider a different family of parameters, the first $N_1 = N_2 = 10$, and $h = \pi/\sqrt{10}$. Next, we apply the SGM when $N_1 = N_2 = 40$, and $h = \pi/\sqrt{20}$. It is clear from Figures 2 and 3, and Table 3 that we can obtain a high quality approximation for a good choice of the parameters.

5   Conclusion

The sinc-Galerkin method is established for the higher order fractional boundary value problems in this paper. The suggested method utilizes the properties of fractional derivatives in order to solve the higher order BVP. The numerical scheme is computationally captivating. We demonstrated our results by tables and figures, it is proved that the convergence rate of the sinc method is of $\mathcal{O}(\exp(-\kappa\sqrt{N}))$ with some $\kappa > 0$, where N is the number of nodes or bases used in the method. We provided a fractional differential equation with singularities, the method shows the best response to this example.

Acknowledgment
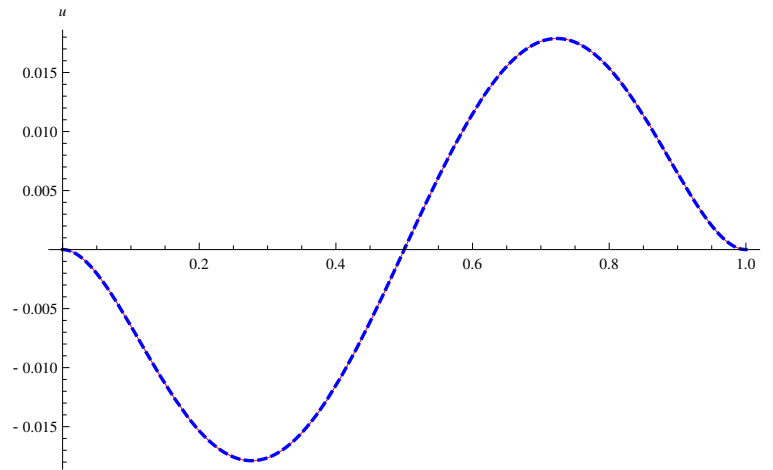
Figure 3: The exact solution is the red color and the approximate solution is the dashed blue color for Example 4.2 when $N_1 = N_2 = 40$ and $h = \frac{\pi}{2\sqrt{30}}$.

x_k	Exact value	Approximate Value	Absolute Error
0.00691383	-0.0000464904	-0.0000460076	$4.828512978699654 \times 10^{-7}$
0.0113114	-0.000122241	-0.00012146	$7.809294063951228 \times 10^{-7}$
0.0184542	-0.000315995	-0.000314746	$1.2489442106647592 \times 10^{-6}$
0.0299707	-0.000794545	-0.000792583	$1.962081982870246 \times 10^{-6}$
0.0483203	-0.0019103	-0.00190731	$2.995110557358835 \times 10^{-6}$
0.0770126	-0.00427437	-0.00427001	$4.365622987672832 \times 10^{-6}$
0.120583	-0.00853317	-0.00852726	$5.90892890370287 \times 10^{-6}$
0.183893	-0.0142393	-0.0142322	$7.096707035069219 \times 10^{-6}$
0.270229	-0.0178716	-0.0178646	$6.9694864587993566 \times 10^{-6}$
0.37831	-0.0134626	-0.013458	$4.585623157854837 \times 10^{-6}$
0.5	$0.$	$1.57961907 \times 10^{-7}$	$1.5796190761125167 \times 10^{-7}$
0.62169	0.0134626	0.0134582	$4.371289509910378 \times 10^{-6}$
0.729771	0.0178716	0.0178646	$6.9222409211575076 \times 10^{-6}$
0.816107	0.0142393	0.0142322	$7.127970986300913 \times 10^{-6}$
0.879417	0.00853317	0.00852723	$5.94465157464398 \times 10^{-6}$
0.922987	0.00427437	0.00426998	$4.386834537174061 \times 10^{-6}$
0.95168	0.0019103	0.0019073	$3.0051297730975847 \times 10^{-6}$
0.970029	0.000794545	0.000792579	$1.966324959320467 \times 10^{-6}$
0.981546	0.000315995	0.000314744	$1.2506400348780188 \times 10^{-6}$
0.988689	0.000122241	0.000121459	$7.815852781527434 \times 10^{-7}$
0.993086	0.0000464904	0.0000460073	$4.83099931514434 \times 10^{-7}$

Table 3: Numerical values for Example 4.2 when $N_1 = N_2 = 40$ and $h = \frac{\pi}{2\sqrt{30}}$.

References

[1] R.A. Usmani. Discrete variable methods for a boundary value problem with engineering applications. *Mathematics of Computation* **32** (144) (1978) 1087–1096.

[2] D. Jiang, H. Liu, and X. Xu. Nonresonant singular fourth-order boundary value problems. *Applied Mathematics Letters*. Elsevier **18** (1) (2005) 69–75.

[3] C. Pang, W. Dong and Z. Wei. Multiple solutions for fourth-order boundary value problem. *Journal of Mathematical Analysis and Applications*. Elsevier **314** (2) (2006) 464–476.

[4] E.A. Al-Said and M. A. Noor. Quartic spline method for solving fourth order obstacle boundary value problems. *Journal of Computational and applied Mathematics*. Elsevier **143** (1) (2002) 107–116.

[5] K. Al-Khaled and M. N. Anwar. Numerical comparison of methods for solving second-order ordinary initial value problems. *Applied Mathematical Modelling*. Elsevier **31** (2) (2007) 292–301.

[6] R. Agarwal. *Boundary value problems for High Ordinary Differential Equations*. World Scientific Singapore, 1986.

[7] P.W. Eloe, J. Henderson and R.A. Khan. Existence and uniqueness conditions for a class of $(k + 4j)$-point n-th order boundary value problems. *Nonlinear Dynamics and Systems Theory* **12** (1) (2012).

[8] D. Dhaigude and P.B. Sandeep. Local Existence and Uniqueness of Solution for Hilfer-Hadamard fractional differential problem. *Nonlinear Dynamics and Systems Theory* **18** (2) (2018) 144–153.

[9] D. Dhaigude and P.B. Sandeep. A Novel Method for Solving Caputo-Time-Fractional Dispersive Long Wave Wu-Zhang System. *Nonlinear Dynamics and Systems Theory* **18** (2) (2018) 182–190.

[10] B. Baeumer, M. Kovács, M. M. Meerschaert and H. Sankaranarayanan. Boundary conditions for fractional diffusion. *Journal of Computational and Applied Mathematics*. Elsevier **336** (2018) 408–424.

[11] W. Ma, S. Meng and Y. Cui. Resonant integral boundary value problems for Caputo fractional differential equations. *Mathematical Problems in Engineering*. Hindawi **7** (2018).

[12] D. Min, L. Liu and Y. Wu. Uniqueness of positive solutions for the singular fractional differential equations involving integral boundary value conditions. *Boundary Value Problems*. Springer **12** (1) (2018) 23–38.

[13] E. Uğurlu, D. Baleanu, and K. Taş. On the solutions of a fractional boundary value problem. *Turkish Journal of Mathematics*. The Scientific and Technological Research Council of Turkey **42** (3) (2018) 1307–1311.

[14] R.C. Smith, and G.A. Bogar, K.L. Bowers and J. Lund. The Sinc-Galerkin method for fourth-order differential equations. *SIAM Journal on Numerical Analysis*. SIAM **28** (3) (1991) 760–788.

[15] S. Ballem and K.K. Viswanadham. *Numerical Solution of Sixth Order Boundary Value Problems by Galerkin Method with Quartic B-splines*. Springer, 2019.

[16] K.M. McArthur, K.L. Bowers and J. Lund. Numerical implementation of the Sinc-Galerkin method for second-order hyperbolic equations. *Numerical Methods for Partial Differential Equations*. Wiley Online Library **3** (3) (1987) 169–185.

[17] M. Youssef and G. Baumann. Troeschs problem solved by Sinc methods. *Mathematics and Computers in Simulation*. Elsevier **162** (2019) 31–44.

[18] A. Secer, S. Alkan, M.A. Akinlar and M. Bayram. *Sinc-Galerkin method for approximate solutions of fractional order boundary value problems.* SpringerOpen **213** (1) (2013) 281–312.

[19] F. Stenger. *Numerical Methods Based on Sinc and Analytic Functions.* Springer Science & Business Media, 2012.

[20] J. Lund and K.L. Bowers. *Sinc Methods for Quadrature and Differential Equations.* Siam, 1992.

Optimization of Linear Quadratic Regulator with Tracking Applied to Autonomous Underwater Vehicle (AUV) Using Cuckoo Search

T. Herlambang [1], D. Rahmalia [2], H. Nurhadi [3,4*], D. Adzkiya [4,5] and S. Subchan [5]

[1] *Department of Information Systems, University of Nahdlatul Ulama Surabaya, Indonesia*
[2] *Department of Mathematics, Darul Ulum University, Lamongan, Indonesia*
[3] *Department of Industrial Mechanical Engineering, Sepuluh Nopember Institute of Technology, Indonesia*
[4] *Center of Excellence for Mechatronics and Industrial Automation Research Center, Sepuluh Nopember Institute of Technology, Indonesia*
[5] *Department of Mathematics, Sepuluh Nopember Institute of Technology, Indonesia*

Abstract: An Autonomous Underwater Vehicle (AUV) is used for exploring marine resources. The AUV has a control system for the surge, sway, or heave position and roll, pitch, or yaw angle. Tracking problems can be solved by using a controller designed using the LQR (Linear Quadratic Regulator). In optimal control for tracking problems using the LQR, the performance index is used as the objective function. The value of objective function depends on weighted matrices and, in general, the weighted matrices are determined by trial and error. In this research, the optimization of weighted matrices will be approached by heuristic methods such as Cuckoo Search (CS). CS simulates the reproduction strategy of cuckoo birds. The nests in CS represent weighted matrices in the LQR and the fitness function represents the performance index. Based on the simulation, the CS algorithm can find optimal weighted matrices in the LQR for the tracking problems. Furthermore, the solution of state and the optimal control can be obtained.

Keywords: *linear quadratic regulator; autonomous underwater vehicle; optimization; Cuckoo search.*

Mathematics Subject Classification (2010): 93C05, 93C15.

---

* Corresponding author: `mailto:hdnurhadi@me.its.ac.id`

1 Introduction

Compared to the whole territory of Indonesia, around seventy percent are in the form of sea. Thus, Indonesia has plenty of marine resources [1, 11]. For exploring marine resources, it is a necessity to have Autonomous Underwater Vehicles (AUV) together with their control [13, 14]. An AUV has three linear motions (surge, sway, heave positions) and three angular rotations (roll, pitch, yaw angle). Both angle and position ought to be controlled for maintaing a stable AUV. The controls for the AUV are rudder (for controlling surge and roll) and fin (for controlling sway, heave, pitch, and yaw) [5].

Control design for tracking problems by using the LQR (Linear Quadratic Regulator) has been developed in many applications. In optimal control for tracking problems using the LQR, the performance index is defined as the objective function. The value of objective function depends on weighted matrices and, generally, weighted matrices are determined by trial and error.

In the previous studies, the optimizations of weighted matrices in the optimal control model have been researched, among which are the optimization of weighted matrices in the optimal control of disease spread [4, 6], optimal control of inverted pendulum [3], fuzzy model for multimachine power systems [15], sliding mode control for wind energy conversion systems [16], PID for quadrotor performance [17]. In this research, the optimization of weighted matrices uses one of the heuristic methods called Cuckoo Search (CS).

The Cuckoo Search (CS) algorithm was proposed in [7, 8]. It simulates the reproduction strategy of cuckoo birds. They lay their eggs in the other bird's nest so that when the eggs are hatched, their chicks are fed by the other birds. Sometimes they remove existing eggs of the host nest in order to have higher probability of hatching their own eggs. Some species of cuckoo birds are specialized to mimic the pattern and color of the eggs of host birds so that the host birds could not recognize their eggs which have higher probability of hatching.

The contributions of this paper are as follows. In this paper, we use the CS algorithm to compute the weighted matrices that will be used in the LQR. After the optimized weighted matrices are obtained using CS, the weighted matrices will be used to compute the solution of state and optimal control for tracking problems by using the LQR. In the LQR, the performance index is defined as the objective function. In the simulations, a sinusoidal signal is used as the reference for surge position, sway position, heave position, roll angle, pitch angle, and yaw angle. Then we compare the reference and the trajectory generated by the closed-loop system.

2 Mathematical Modelling of AUV

In this section, first we derive the mathematical model of the AUV from the equation of motions. Then we extend the original model so that it can be used to solve the problem discussed in this paper.

2.1 State space model of AUV

In this subsection, we develop the mathematical model of the AUV from the equation of motions. The specifications and profile of the AUV used in this research are shown in Table 1 and Figure 1. As mentioned in the Introduction, the AUV has six degrees of freedom (6-DOF), that is, surge, sway, heave, roll, pitch and yaw [12]. The following
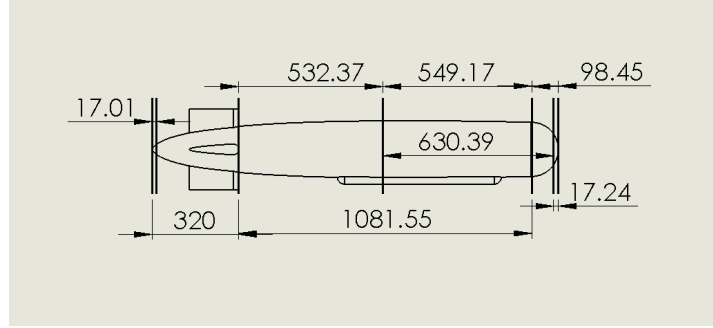
Figure 1: Profile of UNUSAITS AUV [13].

equations describe the dynamics of each motion for the AUV. The dynamics are described in the form of ordinary differential equations.

The dynamics of surge is

$$m[\dot{u} - vr + wq - x_G(q^2 + r^2) + y_G(pq - \dot{r}) + z_G(pr + \dot{q})] = X_{|u|u}u|u| + X_{\dot{u}}\dot{u} + X_{wq}wq$$
$$+ X_{qq}qq + X_{vr}vr + X_{rr}rr + X_{prop}. \tag{1}$$

The dynamics of sway is

$$m[\dot{v} - wp + ur - y_G(r^2 + p^2) + z_G(qr - \dot{p}) + x_G(pq + \dot{r})] = Y_{res} + Y_{|v|v}v|v| + Y_{r|r|}r|r|$$
$$+ Y_{\dot{v}}\dot{v} + Y_{\dot{r}}\dot{r} + Y_{ur}ur + Y_{wp}wp + Y_{pq}pq + Y_{uv}uv + Y_{uu\delta_r}u^2\delta_r. \tag{2}$$

The dynamics of heave is

$$m[\dot{w} - uq + vp - z_G(p^2 + q^2) + x_G(rp - \dot{q}) + y_G(rq + \dot{p})] = Z_{res} + Z_{|w|w}w|w| + Z_{q|q|}q|q|$$
$$+ Z_{\dot{w}}\dot{w} + Z_{\dot{q}}\dot{q} + Z_{uq}uq + Z_{vp}vp + Z_{rp}rp + Z_{uw}uw + Z_{uu\delta_s}u^2\delta_s. \tag{3}$$

The dynamics of roll is

$$I_x\dot{p} + (I_z - I_y)qr + m[y_G(\dot{w} - uq + vp) - z_G(\dot{v} - wp + ur)] = K_{res} + K_{p|p|}p|p| + K_{\dot{p}}\dot{p}$$
$$+ K_{prop}. \tag{4}$$

The dynamics of pitch is

$$I_y\dot{q} + (I_x - I_z)rp + m[z_G(\dot{u} - vr + wq) - x_G(\dot{w} - uq + vp)] = M_{res} + M_{w|w|}w|w|$$
$$+ M_{q|q|}q|q| + M_{\dot{w}}\dot{w} + M_{\dot{q}}\dot{q} + M_{uq}uq + M_{vp}vp + M_{rp}rp + M_{uw}uw + M_{uu\delta_s}u^2\delta_s. \tag{5}$$

The dynamics of yaw is

$$I_z\dot{r} + (I_y - I_z)pq + m[x_G(\dot{v} - wp + ur) - y_G(\dot{u} - vr + wq)] = N_{res} + N_{v|v|}v|v|$$
$$+ N_{r|r|}r|r| + N_{\dot{v}}\dot{v} + N_{\dot{r}}\dot{r} + N_{ur}ur + N_{wp}wp + N_{pq}pq + N_{uv}uv + N_{uu\delta_r}u^2\delta_r. \tag{6}$$

The parameters in (1)-(6) are as follows: m is the mass of the AUV, I_x, I_y, I_z are the moment of inertia at the x-axis, y-axis, and z-

Weight	16 Kg
Length	1500 mm
Diameter	200 mm
Controller	Ardupilot Mega 2.0
Communication	Wireless Xbee 2.4 GHz
Camera	TTL Camera
Battery	Li-Pro 11.8 V
Propulsion	12V DC Motor
Propeller	3 Blades OD : 50 mm
Speed	3.1 knots (1.5 m/s)
Maximum depth	8 m

Table 1: Specification of UNUSAITS AUV [13].

axis, respectively, x_G, y_G, z_G are the longitudinal, athwart, and vertical position of the center of gravity, respectively. The others are [5]:

X : surge force x : surge position u : surge velocity
Y : sway force y : sway position v : sway velocity
Z : heave force z : heave position w : heave velocity
K : roll moment ϕ : roll angle p : roll rate
M : pitch moment θ : pitch angle q : pitch rate
N : yaw moment ψ : yaw angle r : yaw rate

Then we linearize the model around an equilibrium point by using the Jacobian method. The linearized state space model can be expressed as follows:

$$\dot{X}_v = A_v X_v + B_v U_v, \tag{7}$$

$$Y_v = C_v X_v. \tag{8}$$

For the AUV model, the surge velocity u, sway velocity v, heave velocity w, roll rate p, pitch rate q, and yaw rate r can be written in the general form of the state space model as follows:

$$\begin{bmatrix} \dot{u} \\ \dot{v} \\ \dot{w} \\ \dot{p} \\ \dot{q} \\ \dot{r} \end{bmatrix} = A_v \begin{bmatrix} u \\ v \\ w \\ p \\ q \\ r \end{bmatrix} + B_v \begin{bmatrix} \delta_1 \\ \delta_2 \\ \delta_3 \\ \delta_4 \\ \delta_5 \\ \delta_6 \end{bmatrix}, \quad \begin{bmatrix} Y_{v1} \\ Y_{v2} \\ Y_{v3} \\ Y_{v4} \\ Y_{v5} \\ Y_{v6} \end{bmatrix} = C_v \begin{bmatrix} u \\ v \\ w \\ p \\ q \\ r \end{bmatrix}, \tag{9}$$

where the matrices A_v, B_v, C_v are

$$A_v = \dots \tag{10}$$

$$B_v = \dots \tag{11}$$

$$C_v = \begin{bmatrix} 1 & 0 & 0 & 0 & 0 & 0 \\ 0 & 1 & 0 & 0 & 0 & 0 \\ 0 & 0 & 1 & 0 & 0 & 0 \\ 0 & 0 & 0 & 1 & 0 & 0 \\ 0 & 0 & 0 & 0 & 1 & 0 \\ 0 & 0 & 0 & 0 & 0 & 1 \end{bmatrix}. \tag{12}$$

2.2   Development of state space model of AUV

State space model (7)-(8) can produce a solution of surge velocity u, sway velocity v, heave velocity w, roll rate p, pitch rate q, and yaw rate r. We will develop a state space model in order to produce a solution of surge position x, sway position y, heave position z, roll angle ϕ, pitch angle θ, and yaw angle ψ.

Assume that velocity is the first derivative of position and rate is the first derivative of angle, then we obtain

$$\dot{x} = u, \quad \dot{y} = v, \quad \dot{z} = w, \quad \dot{\phi} = p, \quad \dot{\theta} = q, \quad \dot{\psi} = r. \tag{13}$$

There are six controls U_v in the surge velocity, sway velocity, heave velocity, roll rate, pitch rate, and yaw rate:

$$U_v = \begin{bmatrix} \delta_1 & \delta_2 & \delta_3 & \delta_4 & \delta_5 & \delta_6 \end{bmatrix}^T. \tag{14}$$

There is no control for the surge position, sway position, heave position, roll angle, pitch angle, and yaw angle. In the output matrix, we only observe the surge position, sway position, heave position, roll angle, pitch angle, and yaw angle to be minimized in the performance index of the LQR optimal control. Therefore, the state space model (9) can be extended to become the following equations:

$$\begin{bmatrix} \dot{X}_v \\ \dot{X}_p \end{bmatrix} = \begin{bmatrix} A_v & \bar{0} \\ I & \bar{0} \end{bmatrix} \begin{bmatrix} X_v \\ X_p \end{bmatrix} + \begin{bmatrix} B_v \\ \bar{0} \end{bmatrix} U_v, \tag{15}$$

$$\begin{bmatrix} Y_v \\ Y_p \end{bmatrix} = \begin{bmatrix} \bar{0} & \bar{0} \\ \bar{0} & I \end{bmatrix} \begin{bmatrix} X_v \\ X_p \end{bmatrix}, \tag{16}$$

where $X_p = \begin{bmatrix} x & y & z & \phi & \theta & \psi \end{bmatrix}^T$, I is an identity matrix, and $\bar{0}$ is the matrix whose all elements are zero.

In state space model (15) and (16), the size of matrix $\begin{bmatrix} A_v & \bar{0} \\ I & \bar{0} \end{bmatrix}$ is 12×12, the size of input matrix $\begin{bmatrix} B_v \\ \bar{0} \end{bmatrix}$ is 12×6, and the size of output matrix $\begin{bmatrix} \bar{0} & \bar{0} \\ \bar{0} & I \end{bmatrix}$ is 12×12.

3   Linear Quadratic Regulator

The Linear Quadratic Regulator (LQR) will be used in determining the optimal control of AUV. The optimal control problem is to find an optimal control $u^*(t)$, such that the corresponding trajectory $x^*(t)$ minimizes the given performance index J [10].

3.1   Tracking problems for discrete-time systems using LQR

In this research, we describe the tracking problems and its solution by using the LQR. The objective of tracking problems is that the output of the system follows a desired trajectory r that minimizes a performance index J. The discrete-time model for tracking problems by using the LQR is defined as follows.

The state $\dot{x}(t)$ and output equation $y(t)$ in discrete time can be constructed in the following equations:

$$x_{k+1} = Ax_k + Bu_k, \tag{17}$$

$$y_k = Cx_k, \tag{18}$$

and the performance index that is defined as the objective function is defined as follows:

$$J = \frac{1}{2}e_N^T P e_N + \frac{1}{2}\sum_{k=0}^{N-1}(e_k^T Q e_k + u_k^T R u_k), \qquad (19)$$

where $e_N = Cx_N - r_N$ and $e_k = Cx_k - r_k$.

The error weighted matrices $P \geq 0$ and $Q \geq 0$ must be symmetric and positive semidefinite, whereas the control weighted matrix $R > 0$ must be symmetric and positive definite.

3.2 Tracking algorithm by using LQR

The tracking algorithm and computation by using the LQR for discrete-time systems are as follows [2]:

1. Compute K_k, S_k, v_k, K_k^v backward with the final conditions $S_N = C^T P C$ and $v_N = C^T P r_N$.
   For $k = N-1, N-2, \ldots, 0$ do

$$K_k = (B^T S_{k+1} B + R)^{-1} B^T S_{k+1} A, \qquad (20)$$

$$S_k = C^T Q C + A^T S_{k+1}(A - B K_k), \qquad (21)$$

$$v_k = (A - B K_k)^T v_{k+1} + C^T Q r_k, \qquad (22)$$

$$K_k^v = (B^T S_{k+1} B + R)^{-1} B^T, \qquad (23)$$

   End For

2. Compute x_k forward with the initial conditions x_0.
   For $k = 1, 2, \ldots, N-1$ do

$$x_{k+1} = Ax_k + B(-K_k x_k + K_k^v v_{k+1}), \qquad (24)$$

   End For

3. Compute the optimal control u_k:

$$u_k = -K_k x_k + K_k^v v_{k+1}. \qquad (25)$$

4. Compute the performance index J as the objective function:

$$J = \frac{1}{2}e_N^T P e_N + \frac{1}{2}\sum_{k=0}^{N-1}(e_k^T Q e_k + u_k^T R u_k), \qquad (26)$$

   where $e_N = Cx_N - r_N$ and $e_k = Cx_k - r_k$.

4 Cuckoo Search

The Cuckoo Search (CS) algorithm was proposed in [7]. It imitates the reproduction strategy of cuckoo birds. The cuckoo birds lay their eggs in the other bird's nest. So, when the eggs are hatched, their chicks are fed by the other birds. Sometimes they remove existing eggs of the host nest in order to increase the probability of hatching their own eggs. Some species of cuckoo birds are specialized to mimic the pattern and color of the host bird's eggs, so the host birds could not recognize their eggs, meaning it ensures high probability of the hatching [8].

4.1 Behavior of the cuckoo

Based on the behavior of cuckoo birds, the CS algorithm uses three idealized rules:

1. Each cuckoo lays one egg at a time and dumps it in a randomly selected nest.

2. The best nest with high quality eggs will be carried over to the next generation.

3. The number of available host nests is fixed and a host bird can discover a strange egg with a probability $p_a \in [0, 1]$. In this case, the host bird can either throw the egg away or abandon the nest to build a completely new nest in a new location.

In the original CS, there is no distinction between an egg, a nest, or a cuckoo. Each nest corresponds to one egg which also represents one cuckoo.

4.2 Cuckoo Search algorithm on LQR

In tracking problems by using the LQR, there are three weighted matrices which will be optimized, i.e., $P \geq 0$, $Q \geq 0$ which must be symmetric and positive semidefinite, and $R > 0$ which must be symmetric and positive definite.

We assume $P = \bar{0}$. Because of the only surge position, sway position, heave position, roll angle, pitch angle, and yaw angle which will be minimized, one has $Q = \begin{bmatrix} \bar{0} & \bar{0} \\ \bar{0} & Q_x \end{bmatrix}$ with Q_x being

$$Q_x = \begin{bmatrix} q_7 & 0 & 0 & 0 & 0 & 0 \\ 0 & q_8 & 0 & 0 & 0 & 0 \\ 0 & 0 & q_9 & 0 & 0 & 0 \\ 0 & 0 & 0 & q_{10} & 0 & 0 \\ 0 & 0 & 0 & 0 & q_{11} & 0 \\ 0 & 0 & 0 & 0 & 0 & q_{12} \end{bmatrix}, \tag{27}$$

where $q_i > 0$, $i = 7, 8, \ldots, 12$.

Because there are six controls U_v in the surge velocity, sway velocity, heave velocity, roll rate, pitch rate, and yaw rate

$$U_v = \begin{bmatrix} \delta_1 & \delta_2 & \delta_3 & \delta_4 & \delta_5 & \delta_6 \end{bmatrix}^T, \tag{28}$$

$R > 0$ can be constructed as follows:

$$R = \begin{bmatrix} r_1 & 0 & 0 & 0 & 0 & 0 \\ 0 & r_2 & 0 & 0 & 0 & 0 \\ 0 & 0 & r_3 & 0 & 0 & 0 \\ 0 & 0 & 0 & r_4 & 0 & 0 \\ 0 & 0 & 0 & 0 & r_5 & 0 \\ 0 & 0 & 0 & 0 & 0 & r_6 \end{bmatrix}, \tag{29}$$

where $r_i > 0$, $i = 1, 2, \ldots, 6$.

Therefore, the representation of decision variable which will be used in CS as the host nest is

$$X = \begin{bmatrix} q_7 & q_8 & q_9 & \ldots & q_{12} & r_1 & r_2 & r_3 & \ldots & r_6 \end{bmatrix}, \tag{30}$$

where the fitness function is defined as the performance index J in (26). Based on the behavior of cuckoo birds, the CS algorithm for optimizing weighted matrices in the LQR with tracking can be designed as follows.

Generate the initial population of host nests x_i, $i = 1, 2, \ldots, maxpop$, randomly. Each of them represents a candidate solution to the optimization problem with the objective function $f(x)$ [9].

For $t = 1, 2, \ldots, tmax$

1. Calculate the global random walk and generate a new nest x_i^{t+1} using the Levy flight:

$$x_i^{t+1} = x_i^t + \alpha \otimes Levy(s, \lambda),$$

   where $\alpha > 0$ is the step size scaling factor. The search steps in terms of random $Levy(s, \lambda)$ should be drawn from the Levy distribution. In addition, $\otimes$ denotes the entry-wise multiplication.

$$Levy \sim \frac{\lambda \Gamma(\lambda) \sin\left(\frac{\lambda}{2}\pi\right)}{\pi} \frac{1}{s^{1+\lambda}}, \quad s > 0.$$

   The letter Γ represents the gamma function $\Gamma(z) = \int_0^\infty t^{z-1} e^{-z} dt$. If $z = k$ is a positive integer, then $\Gamma(k) = (k-1)!$.

2. Evaluate the fitness of x_i^{t+1}

3. Choose a new nest j randomly from $maxpop$ initial nests. If the fitness of x_i^{t+1} is better than x_i^t, replace j by x_i^{t+1}

4. Abandon some of the worst nests and build new ones. It depends on the discovery probability parameter p_a. Generate a uniformly distributed random number $\varepsilon \sim U(0, 1)$.
   If $\varepsilon < p_a$
   Create a new nest using the local random walk

$$x_i^{t+1} = x_i^t + \alpha \otimes H(p_a - \varepsilon) \otimes (x_j^t - x_k^t),$$

   where $\alpha > 0$ and $H(p_a - \varepsilon)$ is a Heaviside function.
   Evaluate the fitness of x_i^{t+1} and find the best one
   End If

5. Update the best solution

End For

5 Simulation Results

Based on the AUV data, the state space model in (15) uses the following matrices A_v and B_v:

$$A_v = \begin{bmatrix} 0.098 & 0.032 & -0.179 & 0.119 & -0.037 & -0.148 \\ -0.001 & 0.098 & 0.077 & 0.083 & 0.039 & 0.026 \\ -0.089 & 0.030 & -0.066 & 0.008 & -0.113 & -0.128 \\ 0.139 & -0.027 & 0.019 & -0.988 & -0.371 & 0.139 \\ 0.047 & 0.004 & -0.032 & -0.993 & -0.469 & 0.031 \\ 0.139 & -0.114 & -0.054 & -0.879 & -0.411 & 0.119 \end{bmatrix},$$

$$B_v = \begin{bmatrix} 0.0177 & 0.0003 & -0.0003 & 0 & -0.0003 & 0.0003 \\ 0.0012 & 1.49 \times 10^{-5} & -1.80 \times 10^{-5} & -0.6070 & -1.80 \times 10^{-5} & 1.49 \times 10^{-5} \\ 0.0156 & 0.0002 & -0.0002 & 0.6070 & -0.0002 & 0.0002 \\ -0.0153 & -0.0002 & 0.0002 & 5.8592 & 0.0002 & -0.0002 \\ -0.0019 & -2.97 \times 10^{-5} & 0.0005 & 6.4357 & 0.0005 & -2.97 \times 10^{-5} \\ -0.0164 & 0.0002 & 0.0003 & 6.4357 & 0.0003 & 0.0002 \end{bmatrix}.$$

5.1 Cuckoo Search simulation on standard LQR without tracking

Tracking problems by using the LQR will be used in the AUV model for determining the solution of state as in (24) and the optimal control as in (25). There are weighted matrices whose elements will be optimized by the CS algorithm. In the CS simulation, the parameters used are:

- The number of nests = 10.

- Maximum iteration = 50.

- Discovery probability parameter $p_a = 0.5$.

Figure 2(a) is an optimization process of the CS algorithm for optimizing the weighted matrices of LQR. First, there are some nests at a random position. At the optimization process using the Levy flight, by abandoning some of the worst nests and building new nests, the position of the best nest is found. The Optimal Performance Index as the fitness function is 1.1081 with the elements of weighted matrices being

$$\begin{aligned} X &= \begin{bmatrix} q_7 & q_8 & q_9 & \ldots & q_{12} & r_1 & r_2 & r_3 & \ldots & r_6 \end{bmatrix} \\ &= [1.0197 \quad 2.0534 \quad 1.0841 \quad 1.1568 \quad 1.8789 \quad 1.4099 \quad 0.0711 \quad 0.5264 \quad 0.2167 \quad \ldots \\ &\qquad 0.3140 \quad 0.2686 \quad 0.8924]. \end{aligned}$$

After the optimal weighted matrices are obtained, they will be applied in the LQR simulation of the AUV model. Figure 2(b) is the optimal control of LQR, with the solutions of state as in Figure 2(c).

5.2 Cuckoo Search simulation on LQR with tracking

Tracking problems by using the LQR will be used in the AUV model for determining the solution of state as in (24) and the optimal control as in (25). In tracking problems by using the LQR, the reference used is $\sin t$, $t = 1, 2, \ldots, T$ for each position and angle. There are weighted matrices whose elements will be optimized by the CS algorithm. In the CS simulation, the parameters used are:
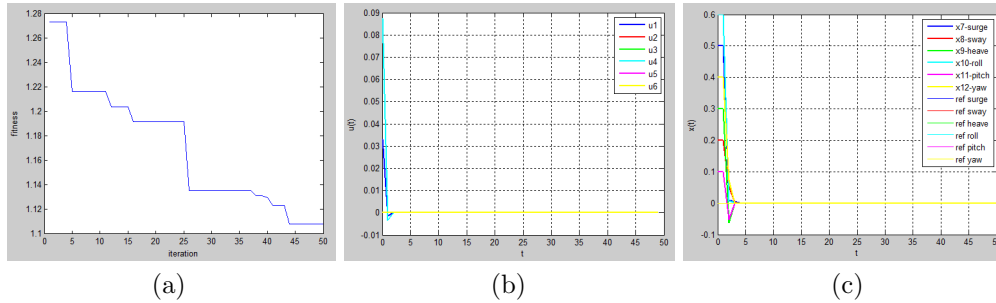
Figure 2: (a) The CS optimization process (b) The optimal control of LQR (c) The solution of state of LQR.

- The number of nests = 10.

- Maximum iteration = 50.

- Discovery probability parameter $p_a = 0.5$.

Figure 3(a) is an optimization process of the CS algorithm for optimizing the weighted matrices of the LQR with tracking $\sin t$, $t = 1, 2, \ldots, T$, for the surge position and zero otherwise.

First, there are some nests at a random position. At the optimization process using the Levy flight, by abandoning some of the worst nests and building new nests, the position of the best nest is found. The Optimal Performance Index as the fitness function is 11.0361 with the elements of weighted matrices being

$$X = \begin{bmatrix} q_7 & q_8 & q_9 & \ldots & q_{12} & r_1 & r_2 & r_3 & \ldots & r_6 \end{bmatrix}$$
$$= [1.0387 \quad 1.4831 \quad 1.9183 \quad 1.6391 \quad 3.8579 \quad 2.3461 \quad 0.0003 \quad 0.0883 \quad 0.6869 \quad \ldots$$
$$0.4850 \quad 0.7080 \quad 0.0933].$$

After the optimal weighted matrices are obtained, they will be applied in tracking problems by using the LQR for the AUV model. Figure 3(b) is the optimal control of tracking problems by using the LQR on the surge position, with the solutions of state as in Figure 3(c). Figure 3(d) is the comparison between the solution of the surge position and its reference.

Figure 4(a) is an optimization process of the CS algorithm for optimizing the weighted matrices of tracking problems by using the LQR with reference $\sin t$, $t = 1, 2, \ldots, T$, for the sway position and zero otherwise. First, there are some nests at a random position. At the optimization process using the Levy flight, by abandoning some of the worst nests and building new nests, the position of the best nest is found. The Optimal Performance Index as the fitness function is 13.7676 with the elements of weighted matrices being

$$X = \begin{bmatrix} q_7 & q_8 & q_9 & \ldots & q_{12} & r_1 & r_2 & r_3 & \ldots & r_6 \end{bmatrix}$$
$$= [1.8594 \quad 1.0174 \quad 1.4118 \quad 1.4144 \quad 1.6101 \quad 1.2758 \quad 0.8354 \quad 0.2502 \quad 0.5636 \quad \ldots$$
$$0.3001 \quad 0.0801 \quad 0.5326].$$

After the optimal weighted matrices are obtained, they will be applied in the simulation of tracking problems by using the LQR for the AUV model. Figure 4(b) is the
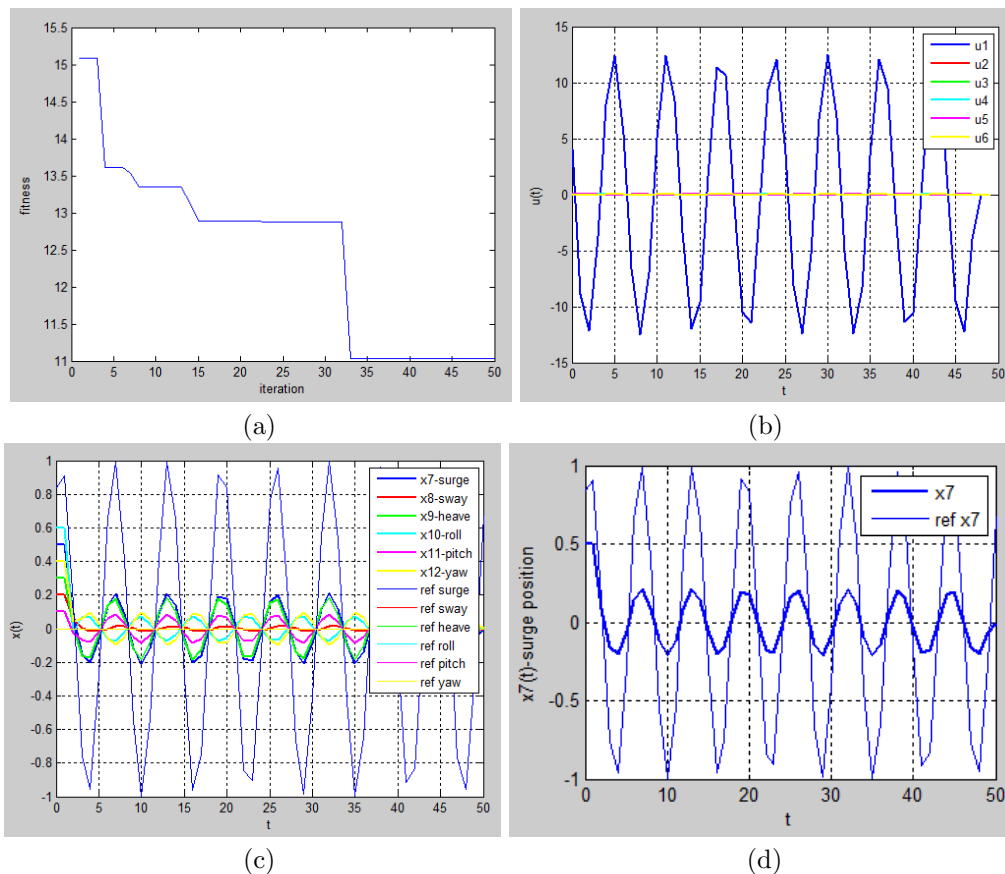
Figure 3: (a) The CS optimization process (b) The optimal control of tracking problems by using the LQR on the surge position (c) The solution of state of tracking problems by using the LQR on the surge position (d) Comparison between the reference and the surge position.

optimal control of tracking problems by using the LQR on the sway position, with the solutions of state as in Figure 4(c). Figure 4(d) is the comparison between the solution of the sway position and its reference.

Figure 5(a) is an optimization process of the CS algorithm for optimizing the weighted matrices of tracking problems by using the LQR with reference $\sin t$, $t = 1, 2, \ldots, T$, for the heave position and zero otherwise. First, there are some nests at a random position. At the optimization process using the Levy flight, by abandoning some of the worst nests and building new nests, the position of the best nest is found. The Optimal Performance Index as the fitness function is 12.3018 with the elements of weighted matrices being

$$X = \begin{bmatrix} q_7 & q_8 & q_9 & \ldots & q_{12} & r_1 & r_2 & r_3 & \ldots & r_6 \end{bmatrix}$$
$$= [2.8670 \quad 2.5503 \quad 1.0348 \quad 1.1602 \quad 3.4523 \quad 1.2199 \quad 0.0003 \quad 0.0255 \quad 0.0590 \quad \ldots$$
$$0.2296 \quad 0.2725 \quad 0.0403].$$

After the optimal weighted matrices are obtained, they will be applied in the simulation of tracking problems by using the LQR for the AUV model. Figure 5(b) is the
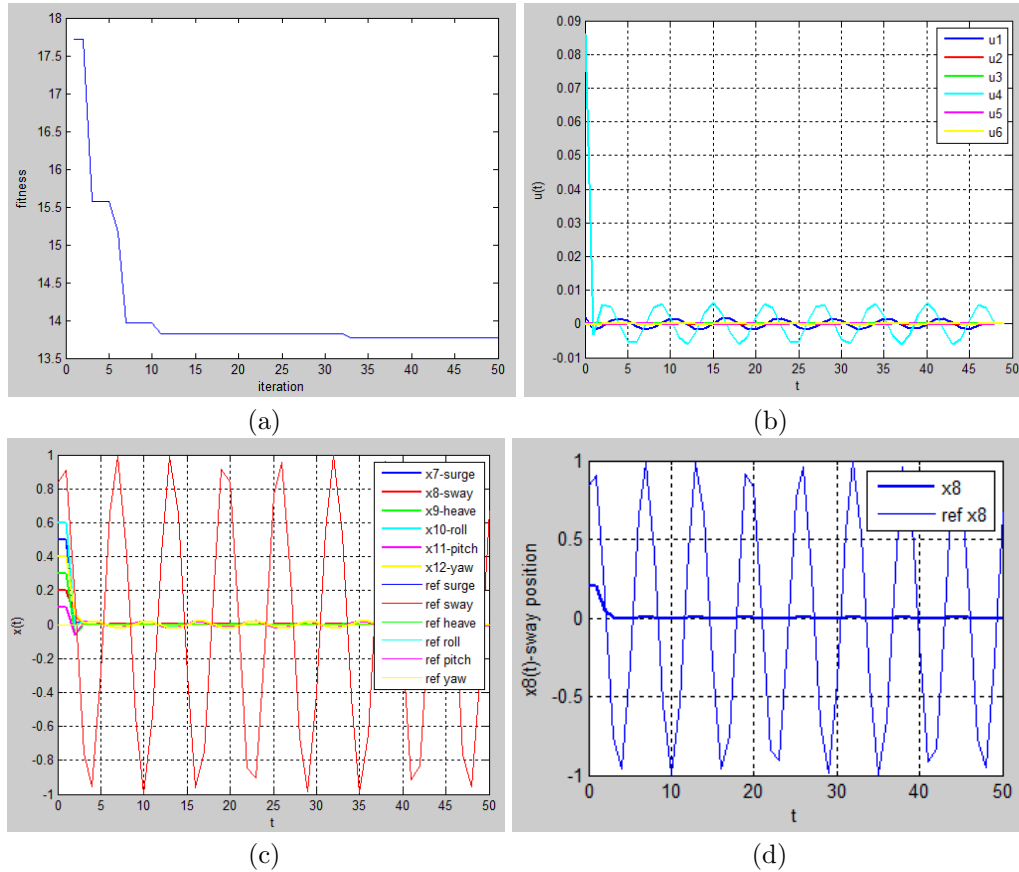
Figure 4: (a) The CS optimization process (b) The optimal control of tracking problems by using the LQR on the sway position (c) The solution of state of tracking problems by using the LQR on the sway position (d) Comparison between the reference and the sway position.

optimal control of tracking problems by using the LQR on the heave position, with the solutions of state as in Figure 5(c). Figure 5(d) is the comparison between the solution of the heave position and its reference.

Figure 6(a) is an optimization process of the CS algorithm for optimizing the weighted matrices of tracking problems by using the LQR with reference $\sin t$, $t = 1, 2, \ldots, T$, for the roll angle and zero otherwise. First, there are some nests at a random position. At the optimization process using the Levy flight, by abandoning some of the worst nests and building new nests, the position of the best nest is found. The Optimal Performance Index as the fitness function is 9.9797 with the elements of weighted matrices being

$$X = \begin{bmatrix} q_7 & q_8 & q_9 & \ldots & q_{12} & r_1 & r_2 & r_3 & \ldots & r_6 \end{bmatrix}$$
$$= [2.2584 \quad 1.3483 \quad 1.2542 \quad 1.0173 \quad 1.1281 \quad 1.1688 \quad 0.7712 \quad 0.8242 \quad 0.0241 \quad \ldots$$
$$0.6006 \quad 0.6243 \quad 0.0782].$$

After the optimal weighted matrices are obtained, they will be applied in the simulation of tracking problems by using the LQR for the AUV model. Figure 6(b) is the
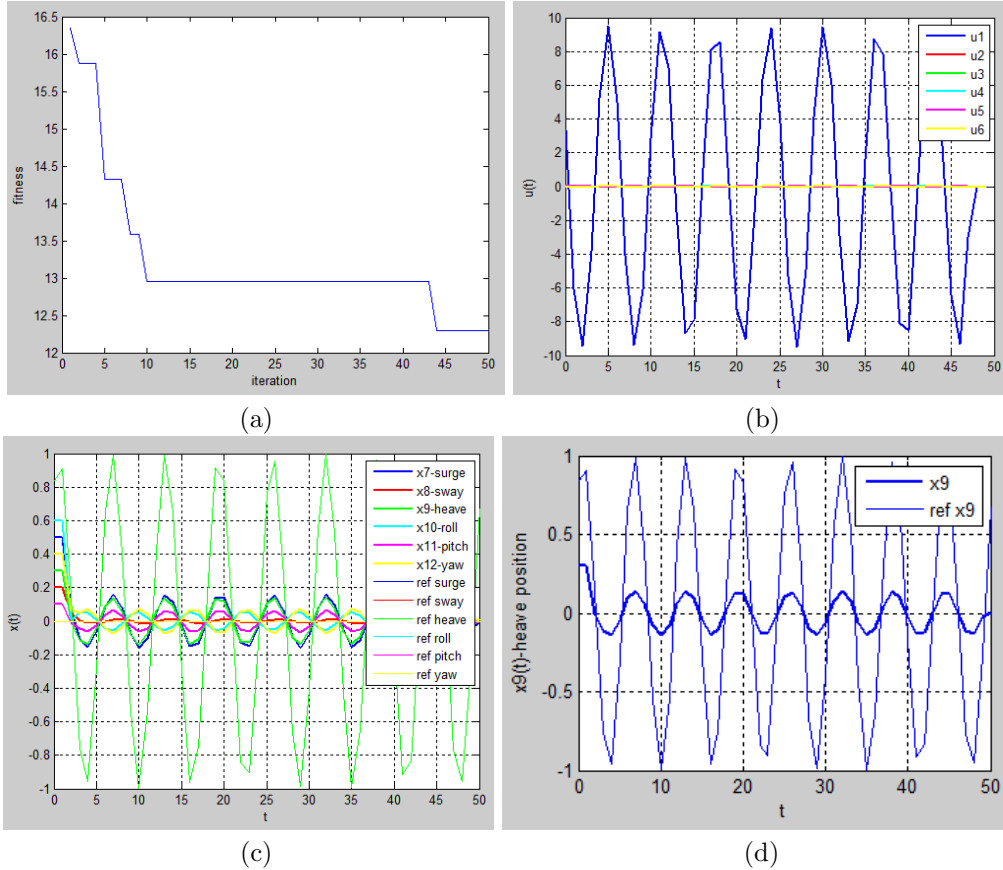
Figure 5: (a) The CS optimization process (b) The optimal control of tracking problems by using the LQR on the heave position (c) The solution of state of tracking problems by using the LQR on the heave position (d) Comparison between the reference and the heave position.

optimal control of tracking problems by using the LQR on the roll angle, with the solutions of state as in Figure 6(c). Figure 6(d) is the comparison between the solution of the roll angle and its reference.

Figure 7(a) is an optimization process of the CS algorithm for optimizing the weighted matrices of the LQR with tracking $\sin t$, $t = 1, 2, \ldots, T$, for the pitch angle and zero otherwise. First, there are some nests at a random position. At the optimization process using the Levy flight, by abandoning some of the worst nests and building new nests, the position of the best nest is found. The Optimal Performance Index as the fitness function is 10.2451 with the elements of weighted matrices being

$$
\begin{aligned}
X &= \begin{bmatrix} q_7 & q_8 & q_9 & \ldots & q_{12} & r_1 & r_2 & r_3 & \ldots & r_6 \end{bmatrix} \\
&= [2.0025 \quad 2.0480 \quad 2.2970 \quad 1.0217 \quad 1.0020 \quad 1.0005 \quad 0.4297 \quad 0.5129 \quad 0.7946 \quad \ldots \\
&\qquad 0.2648 \quad 0.3575 \quad 0.9104].
\end{aligned}
$$

After the optimal weighted matrices are obtained, they will be applied in the simulation of tracking problems by using the LQR for the AUV model. Figure 7(b) is the
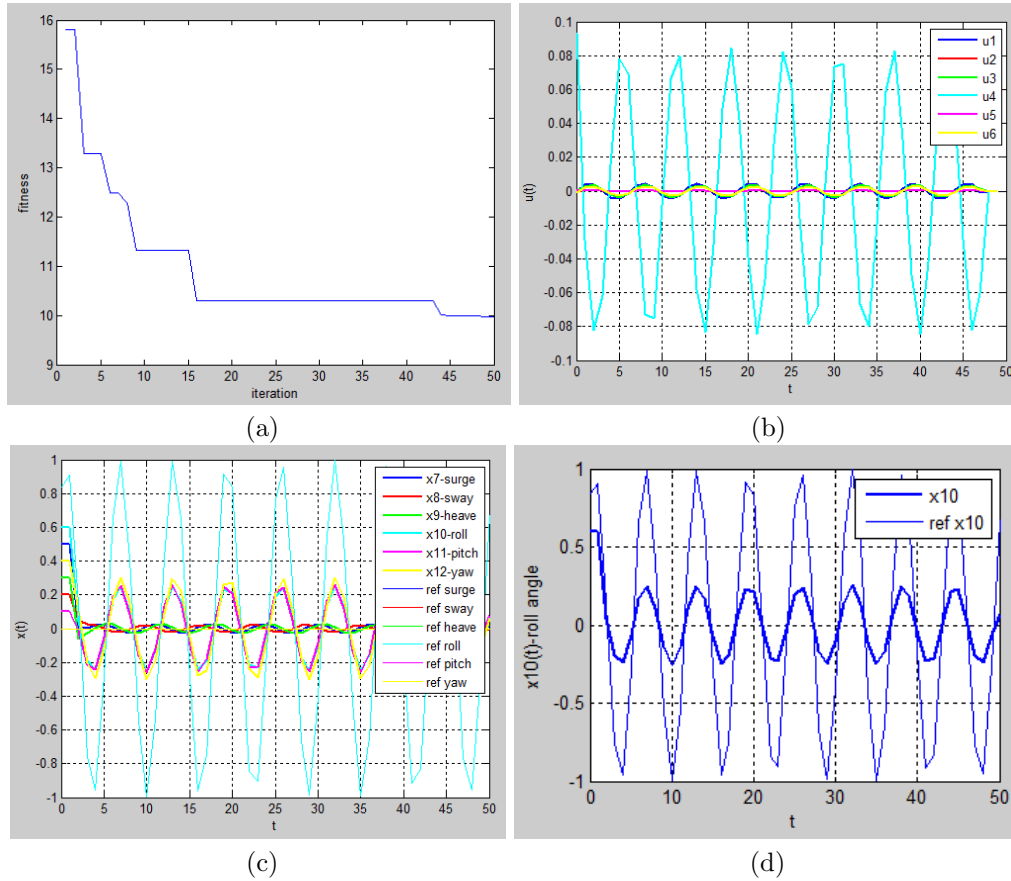
Figure 6: (a) The CS optimization process (b) The optimal control of tracking problems by using the LQR on the roll angle (c) The solution of state of tracking problems by using the LQR on the roll angle (d) Comparison between the reference and the roll angle.

optimal control of the LQR with tracking on the pitch angle, with the solutions of state as in Figure 7(c). Figure 7(d) is the comparison between the solution of the pitch angle and its reference.

Figure 8(a) is an optimization process of the CS algorithm for optimizing the weighted matrices of tracking problems by using the LQR with reference $\sin t$, $t = 1, 2, \ldots, T$, for the yaw angle and zero otherwise. First, there are some nests at a random position. At the optimization process using the Levy flight, by abandoning some of the worst nests and building new nests, the position of the best nest is found. The Optimal Performance Index as the fitness function is 8.7282 with the elements of weighted matrices being

$$
\begin{aligned}
X &= \begin{bmatrix} q_7 & q_8 & q_9 & \ldots & q_{12} & r_1 & r_2 & r_3 & \ldots & r_6 \end{bmatrix} \\
&= \begin{bmatrix} 1.1022 & 1.5842 & 1.1603 & 1.1180 & 1.1842 & 1.0430 & 0.3255 & 0.0185 & 0.6339 & \ldots \\
& 0.0825 & 0.9782 & 0.6808 \end{bmatrix}.
\end{aligned}
$$

After the optimal weighted matrices are obtained, they will be applied in the simu-

(a)

(b)

(c)

(d)
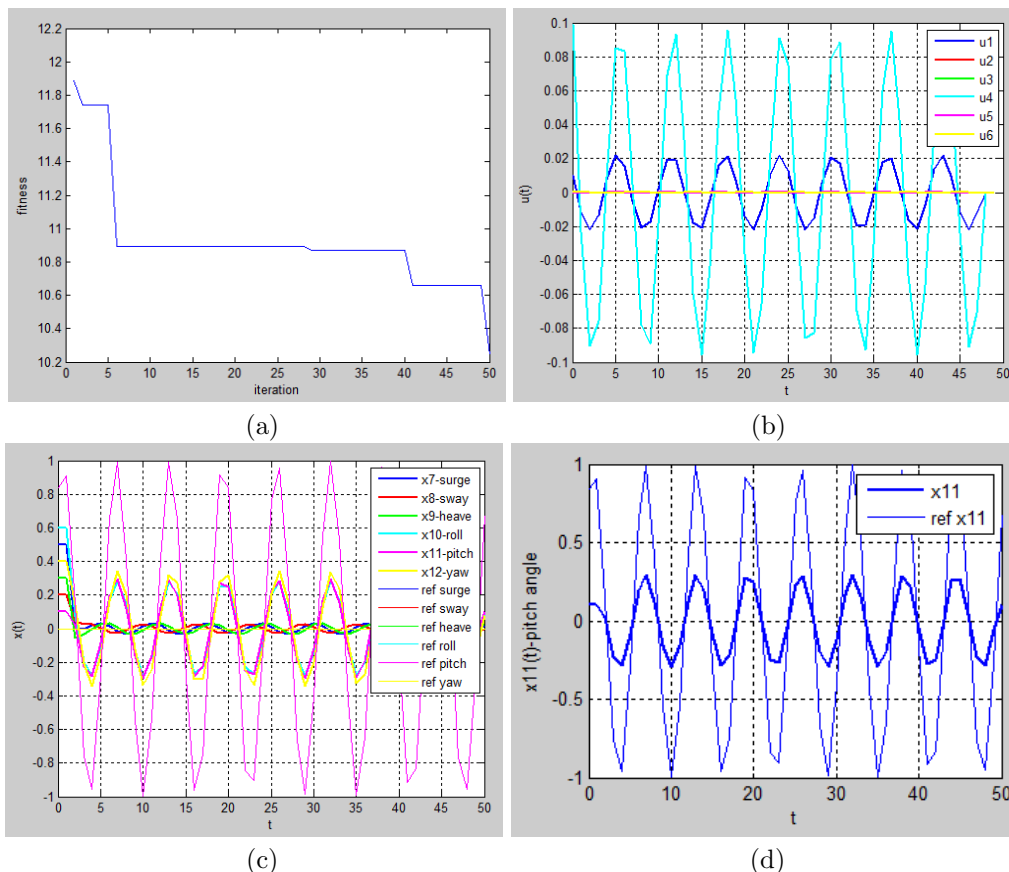
Figure 7: (a) The CS optimization process (b) The optimal control of tracking problems by using the LQR on the pitch angle (c) The solution of state of tracking problems by using the LQR on the pitch angle (d) Comparison between the reference and the pitch angle.

lation of tracking problems by using the LQR for the AUV model. Figure 8(b) is the optimal control of tracking problems by using the LQR on the yaw angle, with the solutions of state as in Figure 8(c). Figure 8(d) is the comparison between the solution of the yaw angle and its reference.

6   Conclusion

Tracking problems by using the LQR have been applied to the AUV model for determining the solution of state consisting of the surge position, sway position, heave position, roll angle, sway angle and yaw angle and the optimal control. In the tracking problems by using the LQR, there are weighted matrices which need to be optimized. The Cuckoo Search (CS) algorithm can be applied in optimization to obtain the weighted matrices. Based on simulation, the CS algorithm can find optimal weighted matrices in tracking problems by using the LQR. Furthermore, the solution of state and the optimal control can be obtained.
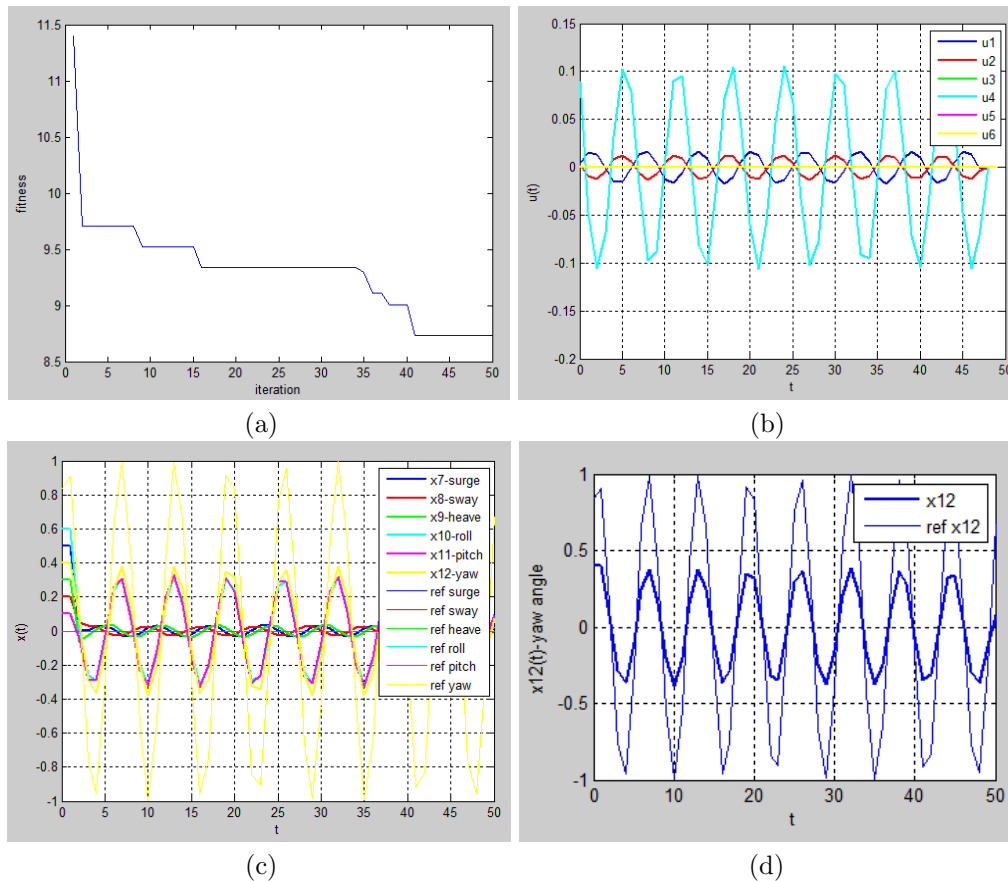
Figure 8: (a) The CS optimization process (b) The optimal control of tracking problems by using the LQR on the yaw angle (c) The solution of state of tracking problems by using the LQR on the yaw angle (d) Comparison between the reference and the yaw angle.

Acknowledgment

References

[1] T. Herlambang, H. Nurhadi and Subchan. Preliminary Numerical Study on Designing Navigation and Stability Control Systems for ITS AUV. *Applied Mechanics and Materials* **493** (2014) 420–452.

[2] F. L. Lewis, D. Vrabie and V. L. Syrmos. *Optimal Control*. John Wiley & Sons, 2012.

[3] K. Ogata. *Modern Control Engineering (5th Edition)*. Pearson, 2009.

[4] D. Rahmalia and T. Herlambang. Weight Optimization of Optimal Control Influenza Model Using Artificial Bee Colony. *International Journal of Computing Science and Applied Mathematics* **4** (1) (2018) 27–31.

[5] T. Herlambang, D. Rahmalia and T. Yulianto. Particle Swarm Optimization (PSO) and Ant Colony Optimization (ACO) for Optimizing PID Parameters on Autonomous Underwater Vehicle (AUV) Control System. *Journal of Physics: Conference Series* **1211** (1) (2019) 012039.

[6] T. Herlambang and D. Rahmalia. Application of ant colony optimization on weight selection of optimal control seir epidemic model. In: *Proceeding Book 7th Annual Basic Science Initernational Conference* Malang, Indonesia, 2017, 196–199.

[7] X.-S. Yang, S. Deb and S.K. Mishra. Multi-species cuckoo search algorithm for global optimization. *Cognitive Computation* **10** (6) (2018) 1085-1095.

[8] X.-S. Yang, Z. Cui, R. Xiao, A.H. Gandomi and M. Karamanoglu. *Swarm Intelligence and Bio-inspired Computation: Theory and Applications*. Newnes, 2013.

[9] R. Salgotra, U. Singh and S. Saha. New cuckoo search algorithms with enhanced exploration and exploitation properties. *Expert Systems with Applications* **95** (2018) 384–420.

[10] D.S. Naidu. *Optimal Control Systems*. CRC press, 2002.

[11] T. Herlambang, E.B. Djatmiko and H. Nurhadi. Navigation and guidance control system of AUV with trajectory estimation of linear modelling. In: *International Conference on Advanced Mechatronics, Intelligent Manufacture, and Industrial Automation (ICAMIMIA)* Surabaya, Indonesia, 2015, 184–187.

[12] C. Yang. *Modular modelling and control for autonomous vehicle (AUV)*. Department of Mechanical Engineering, National University of Singapore, 2007.

[13] T. Herlambang, S. Subchan and H. Nurhadi. Design of Motion Control Using Proportional Integral Derivative for UNUSAITS AUV. *International Review of Mechanical Engineering (IREME)* **12** (11) (2018) 928–938.

[14] K. Oktafianto, T. Herlambang, Mardlijah and H. Nurhadi. Design of Autonomous Underwater Vehicle motion control using Sliding Mode Control method. In: *Proc. International Conf. on Advanced Mechatronics, Intelligent Manufacture, and Industrial Automation (ICAMIMIA)* Surabaya, Indonesia, 2015, 162–166.

[15] A. Abbadi, F. Hamidia, A. Morsli and A. Tlemcani. Optimal Voltage Controller using T-S Fuzzy Model for Multimachine Power Systems. *Nonlinear Dynamics and Systems Theory* **19** (2) (2019) 217–226.

[16] S. Boulkhrachef, A. Moualdia, D.J. Boudana and P. Wira. Higher-Order Sliding Mode Control of a Wind Energy Conversion System. *Nonlinear Dynamics and Systems Theory* **19** (4) (2019) 486–496.

[17] F. Ouendi, S. Houti and M. Tadjine. Comparison of Quadrotor Performance Using Forwarding and PID-Backstepping Control. *Nonlinear Dynamics and Systems Theory* **19** (3) (2019) 427–443.

Natural Daftardar-Jafari Method for Solving Fractional Partial Differential Equations

H. Jafari [1], M.N. Ncube [1,*] and L. Makhubela [2]

[1] *Department of Mathematical Sciences, University of South Africa, UNISA0003, South Africa*
[2] *African Research House, 46 Veronica Street, Kloofendal, Roodepoort, South Africa*

Abstract: In this paper we introduce a new method, the natural Daftardar-Jafari method for solving fractional differential equations. This method is a combination of the natural transform and an iterative technique. The fractional derivative is considered in the Caputo sense.

Keywords: *fractional partial differential equations, natural transform, Daftardar-Jafari method, Caputo fractional derivative.*

Mathematics Subject Classification (2010): 34A08, 35R11.

1 Introduction

Fractional Differential Equations(FDEs) have received so much attention in the past two decades due to their ability to model well situations that arise in different fields such as engineering, science and medicine [1]. The importance of FDEs has prompted researchers to look into the methods of their solution that are easy to implement and possess a considerable degree of accuracy. However, despite some significant progress that has been made in terms of the methods for solving FDEs, the fact remains that there are no agreed upon universal methods to solve them.

The Laplace transform method was used in [1] to solve linear ordinary and partial differential equations of fractional order. The Adomian decomposition method (ADM) was used in [2] to solve a system of non linear fractional differential equations. The fractional reduced differential transform method (FRDTM) was applied to the Klein-Gordon differential equation of fractional order in [3].

---

* Corresponding author: `mailto:mnncube@gmail.com`

Then, fairly recently, researchers have explored the possibility of blending integral transforms and decomposition methods, this adventure has proved to be useful. The Laplace decomposition method (LDM), a combination of the Laplace transform and the ADM, was used in [4] to solve fractional diffusion and fractional wave equations. The natural decomposition method (NDM), a combination of the natural transform and the ADM, was used in [5] to solve fractional models.

The uniqueness and existence of fractional differential equations have also been explored extensively by many researchers. In [6], the uniqueness and existence of Sobolev type differential equations of fractional order were studied. In [7], the uniqueness and existence of fractional reaction diffusion equation were also studied.

In this paper, we explore the feasibility of blending the natural transform and an iterative technique suggested by Daftardar and Jafari to come up with the natural transform Daftardar and Jafari method (NDJM). The natural transform was used to solve Maxwell's equations in [8] and to solve a fluid flow problem in [9].

The rest of the paper is structured as follows: firstly, we give some mathematical framework, secondly, we give a general description of our proposed method, thirdly, we offer examples to demonstrate the use of the method, and lastly, we draw up a conclusion.

2   Preliminaries, Analysis of the Method and Examples

In this section we give the mathematical framework that will form the basis of the discussions in this paper, we then provide a description of our proposed method and give some examples.

2.1   Preliminaries

Definition 2.1 The natural transform of the function $y(t)$ is defined as [9]

$$\mathcal{N}[y(t)] = \psi(s,u) = \int_0^\infty e^{-st} y(ut)dt, \qquad t,s,u > 0, \tag{1}$$

s and u are natural transform parameters.

To get the original function $y(t)$ we take the inverse natural transform as

$$y(t) = \mathcal{N}^{-1}[\psi(s,u)].$$

The natural transform has the following important properties [9]:

(i) It is a linear operator. Given functions $y_1(t)$ and $y_2(t)$ with defined natural transforms and constants $c_1, c_2 \in \mathbb{R}$, then

$$\mathcal{N}[c_1 y_1(t) + c_2 y_2(t)] = c_1 \mathcal{N}[y_1(t)] + c_2 \mathcal{N}[y_2(t)],$$

(ii) It exhibits time scaling property,

$$\mathcal{N}[y(ct)] = \frac{1}{c}\psi\left(\frac{s}{c},u\right) \qquad t > 0, \quad c \in \mathbb{R}, \quad c \neq 0,$$

(iii) The natural transform of the pth derivative of the function $y(t)$ is

$$\mathcal{N}[y^{(p)}(t)] = \left(\frac{s}{u}\right)^p \psi(s,u) - \sum_{i=0}^{p-1} \frac{1}{s} \left(\frac{s}{u}\right)^{p-i} y^{(i)}(0).$$

Table 2.1 provides some useful information on the natural transforms of some basic functions.

$y(t)$	$\psi(s,u)$
1	$\frac{1}{s}$
$\sin \omega t$	$\frac{u\omega}{s^2+u^2\omega^2}$
$\cos \omega t$	$\frac{s}{s^2+u^2\omega^2}$
e^{ct}	$\frac{1}{s-cu}$
$\sinh ct$	$\frac{cu}{s^2-c^2u^2}$
$\cosh ct$	$\frac{s}{s^2-c^2u^2}$
$\frac{1}{\Gamma(n)}t^{n-1}$	$u^{n-1}s^{-n}$

Table 1: The short table of natural transforms of basic functions.

Definition 2.2 The Caputo fractional derivative of the function $y(t)$ of order μ is defined as [10]

$$\mathcal{D}_t^\mu y(t) = \begin{cases} \frac{1}{\Gamma(p-\mu)} \int\limits_0^t \frac{y^{(p)}(s)ds}{(t-s)^{\mu-p+1}} & \text{if} \quad p-1 < \mu \le p, \quad p \in \mathbb{N}; \\ \frac{d^p}{dt^p} y(t) & \text{if} \quad \mu = p. \end{cases} \tag{2}$$

Definition 2.3 The Mittag-Leffler function in two parameters is defined as [10]

$$E_{\mu,\alpha}(\xi) = \sum_{k=0}^{\infty} \frac{\xi^k}{\Gamma(\mu k + \alpha)} \qquad \mu, \alpha > 0. \tag{3}$$

If $\alpha = 1$ in the above definition, we get the one parameter Mittag-Leffler function.

Definition 2.4 The natural transform of the Caputo fractional derivative of order μ of the function $y(t)$ is defined as [10]

$$\mathcal{N}[\mathcal{D}_t^\mu y(t)] = \left(\frac{s}{u}\right)^\mu \psi(s,u) - \sum_{i=0}^{p-1} \frac{1}{s} \left(\frac{s}{u}\right)^{\mu-i} y^{(i)}(0), \qquad \mu \in (p-1;p]. \tag{4}$$

2.2　Analysis of the method

$$\mathcal{D}_t^\mu y(\xi,t) + R(y(\xi,t)) + F(y(\xi,t)) = \eta(\xi,t) \tag{5}$$

with the initial conditions

$$y^{(i)}(\xi,0) = \frac{\partial^i y(\xi,0)}{\partial t^i}, \quad i = 0, 1, 2, ..., p-1. \tag{6}$$

$\mathcal{D}_t^\mu$ is the Caputo fractional derivative with respect to t, $R(y(\xi,t))$ represents the linear operator, $F(y(\xi,t))$ represents non linear terms and $\eta(\xi,t)$ is taken as the source term.

The first step in the NDJM is to take the natural transform on both sides of (5)

$$\mathcal{N}[\mathcal{D}_t^\mu y(\xi,t)] + \mathcal{N}[R(y(\xi,t))] + \mathcal{N}[F(y(\xi,t))] = \mathcal{N}[\eta(\xi,t)], \tag{7}$$

simplifying the above equation and applying the initial conditions yield

$$\begin{aligned}
\psi(\xi,s,u) &= \left(\frac{u}{s}\right)^\mu \sum_{i=0}^{p-1} \frac{1}{s}\left(\frac{s}{u}\right)^{\mu-i} y^{(i)}(0) + \left(\frac{u}{s}\right)^\mu \mathcal{N}[\eta(\xi,t)] \\
&\quad - \left(\frac{u}{s}\right)^\mu [\mathcal{N}[R(y(\xi,t))] + \mathcal{N}[F(y(\xi,t))]].
\end{aligned} \tag{8}$$

In the second step, we take the inverse natural transform on both sides of (8) to get

$$\begin{aligned}
y(\xi,t) &= \mathcal{N}^{-1}\left[\left(\frac{u}{s}\right)^\mu \sum_{i=0}^{p-1} \frac{1}{s}\left(\frac{s}{u}\right)^{\mu-i} y^{(i)}(0) + \left(\frac{u}{s}\right)^\mu \mathcal{N}[\eta(\xi,t)]\right] \\
&\quad - \mathcal{N}^{-1}\left[\left(\frac{u}{s}\right)^\mu [\mathcal{N}[R(y(\xi,t))] + \mathcal{N}[F(y(\xi,t))]]\right],
\end{aligned}$$

the above equation can be rewritten as

$$y(\xi,t) = \mathcal{Q}(\xi,t) - \mathcal{N}^{-1}\left[\left(\frac{u}{s}\right)^\mu [\mathcal{N}[R(y(\xi,t))] + \mathcal{N}[F(y(\xi,t))]]\right], \tag{9}$$

where $\mathcal{Q}(\xi,t)$ is the term due to the initial conditions and the source term.

In the third and final step, we apply an iterative method suggested by Daftardar and Jafari known as the Daftardar-Jafari method (DJM) [11], the solution to (5)-(6) is written as an infinite series,

$$y(\xi,t) = \sum_{n=0}^\infty y_n(\xi,t), \tag{10}$$

substituting (10) into (9) gives

$$\sum_{n=0}^\infty y_n(\xi,t) = \mathcal{Q}(\xi,t) - \mathcal{N}^{-1}\left[\left(\frac{u}{s}\right)^\mu \left[\mathcal{N}\left[R\left(\sum_{n=0}^\infty y_n\right)\right] + \mathcal{N}\left[F\left(\sum_{n=0}^\infty y_n\right)\right]\right]\right]. \tag{11}$$

The non linear term is decomposed as in [11],

$$F\left(\sum_{n=0}^\infty y_n(\xi,t)\right) = F(y_0(\xi,t)) + \sum_{n=1}^\infty \left[F\left(\sum_{k=0}^n y_k\right) - F\left(\sum_{k=0}^{n-1} y_k\right)\right]. \tag{12}$$

Substituting (12) into (11) gives

$$\begin{aligned}
\sum_{n=0}^\infty y_n(\xi,t) &= \mathcal{Q}(\xi,t) - \mathcal{N}^{-1}\left[\left(\frac{u}{s}\right)^\mu \mathcal{N}\left[R\sum_{n=0}^\infty y_n(\xi,t)\right]\right] \\
&\quad - \mathcal{N}^{-1}\left[\left(\frac{u}{s}\right)^\mu \mathcal{N}\left[F(y_0(\xi,t)) + \sum_{n=1}^\infty \left[F\left(\sum_{k=0}^n y_k\right) - F\left(\sum_{k=0}^{n-1} y_k\right)\right]\right]\right].
\end{aligned} \tag{13}$$

The following iteration is then deduced:

$$
\begin{aligned}
y_0(\xi, t) &= \mathcal{Q}(\xi, t), \\
y_1(\xi, t) &= -\mathcal{N}^{-1}\left[\left(\frac{u}{s}\right)^\mu \mathcal{N}[R(y_0(\xi, t))]\right] - \mathcal{N}^{-1}\left[\left(\frac{u}{s}\right)^\mu \mathcal{N}\left[F(y_0(\xi, t))\right]\right], \\
y_2(\xi, t) &= -\mathcal{N}^{-1}\left[\left(\frac{u}{s}\right)^\mu \mathcal{N}[R(y_1(\xi, t))]\right] - \mathcal{N}^{-1}\left[\left(\frac{u}{s}\right)^\mu \mathcal{N}\left[F(y_1 + y_0) - F(y_0)\right]\right], \\
y_n(\xi, t) &= -\mathcal{N}^{-1}\left[\left(\frac{u}{s}\right)^\mu \mathcal{N}[R(y_{n-1})]\right] \\
&\quad -\mathcal{N}^{-1}\left[\left(\frac{u}{s}\right)^\mu \mathcal{N}\left[F(y_0 + ... + y_{n-1}) - F(y_0 + ... + y_{n-2})\right]\right], \quad n = 3, 4, ...
\end{aligned}
$$

Our $n+1$ term approximate solution of (5)-(6) is given by $y(\xi, t) = y_0 + y_1 + ... + y_n$.

2.3   Examples

Example 2.1 Consider the one dimensional time fractional diffusion equation with given initial condition [12]

$$
\mathcal{D}_t^\mu y(\xi, t) = \frac{1}{2}\xi^2 y_{\xi\xi}(\xi, t), \quad \mu \in (1, 2], \quad (\xi, t) \in [0, 1] \times [0, 1], \tag{14}
$$

$$
y(\xi, 0) = \xi, \quad y_t(\xi, 0) = \xi^2.
$$

$R(y(\xi, t)) = \frac{1}{2}\xi^2 y_{\xi\xi}(\xi, t)$, $F(y(\xi, t)) = 0$ and $\eta(\xi, t) = 0$, we take the natural transform on both sides of (14) and use the initial conditions, this yields

$$
\psi(\xi, s, u) = \frac{\xi}{s} + \frac{u\xi^2}{s^2} + \left(\frac{u}{s}\right)^\mu \mathcal{N}\left(\frac{1}{2}\xi^2 y_{\xi\xi}(\xi, t)\right). \tag{15}
$$

We then take the inverse natural transform of (15) to get

$$
y(\xi, t) = \xi + t\xi^2 + \mathcal{N}^{-1}\left[\left(\frac{u}{s}\right)^\mu \left[\mathcal{N}\left(\frac{1}{2}\xi^2 y_{\xi\xi}\right)\right]\right]. \tag{16}
$$

The NDJM then leads to the following terms:

$$
\begin{aligned}
y_0 &= \xi + t\xi^2, \\
y_1 &= \mathcal{N}^{-1}\left[\left(\frac{u}{s}\right)^\mu \left[\mathcal{N}\left(\frac{1}{2}\xi^2 v_{0\xi\xi}\right)\right]\right] = \frac{\xi^2 t^{\mu+1}}{\Gamma(\mu+2)}, \\
y_2 &= \mathcal{N}^{-1}\left[\left(\frac{u}{s}\right)^\mu \left[\mathcal{N}\left(\frac{1}{2}\xi^2 v_{1\xi\xi}\right)\right]\right] = \frac{\xi^2 t^{2\mu+1}}{\Gamma(2\mu+2)}, \\
y_3 &= \mathcal{N}^{-1}\left[\left(\frac{u}{s}\right)^\mu \left[\mathcal{N}\left(\frac{1}{2}\xi^2 v_{2\xi\xi}\right)\right]\right] = \frac{\xi^2 t^{3\mu+1}}{\Gamma(3\mu+2)}, \\
&\vdots \\
y_n &= \mathcal{N}^{-1}\left[\left(\frac{u}{s}\right)^\mu \left[\mathcal{N}\left(\frac{1}{2}\xi^2 v_{(n-1)\xi\xi}\right)\right]\right] = \frac{\xi^2 t^{n\mu+1}}{\Gamma(n\mu+2)}.
\end{aligned}
$$

Then our solution to (14) is given by

$$
\begin{aligned}
y(\xi, t) &= \xi + \xi^2\left(1 + \frac{x^2 t^{\mu+1}}{\Gamma(\mu+2)} + \frac{\xi^2 t^{2\mu+1}}{\Gamma(2\mu+2)} + \frac{\xi^2 t^{3\mu+1}}{\Gamma(3\mu+2)} + ...\right) \\
&= \xi + \xi^2\left(\sum_{n=0}^\infty \frac{t^{n\mu+1}}{\Gamma(n\mu+2)}\right).
\end{aligned}
$$

We obtain the same solution as in [12] where the Laplace homotopy perturbation method was used to solve the problem.

Example 2.2 Consider the one dimensional time fractional diffusion equation with given initial condition [13]

$$\mathcal{D}_t^\mu y(\xi, t) = y_{\xi\xi}(\xi, t), \quad \mu \in (0, 1], \quad x \in \mathbb{R}, \quad t > 0, \tag{17}$$
$$y(\xi, 0) = \sin(\xi).$$

In this example, $R(y(\xi, t)) = y_{\xi\xi}(\xi, t)$, $F(y(\xi, t)) = 0$ and $\eta(\xi, t) = 0$. We take the natural transform on both sides of (17) and utilise the initial condition to get

$$\psi(\xi, s, u) = \frac{\sin(\xi)}{s} + \left(\frac{u}{s}\right)^\mu \mathcal{N}[y_{\xi\xi}(\xi, t)]. \tag{18}$$

We then take the inverse natural transform on both sides of the above equation, this yields

$$v(x, t) = \sin(\xi) + \mathcal{N}^{-1}\left[\left(\frac{u}{s}\right)^\mu \mathcal{N}[v_{\xi\xi}(\xi, t)]\right], \tag{19}$$

from (19), the NDJM then leads to

$$
\begin{aligned}
y_0 &= \sin(\xi), \\
y_1 &= \mathcal{N}^{-1}\left[\left(\frac{u}{s}\right)^\mu \mathcal{N}[y_{0\xi\xi}(\xi, t)]\right] = -\frac{t^\mu \sin(\xi)}{\Gamma(\mu + 1)}, \\
y_2 &= \mathcal{N}^{-1}\left[\left(\frac{u}{s}\right)^\mu \mathcal{N}[y_{1\xi\xi}(\xi, t)]\right] = \frac{t^{2\mu} \sin(\xi)}{\Gamma(2\mu + 1)}, \\
y_3 &= \mathcal{N}^{-1}\left[\left(\frac{u}{s}\right)^\mu \mathcal{N}[y_{2\xi\xi}(\xi, t)]\right] = -\frac{t^{3\mu} \sin(\xi)}{\Gamma(3\mu + 1)}, \\
&\vdots \\
y_n &= \mathcal{N}^{-1}\left[\left(\frac{u}{s}\right)^\mu \mathcal{N}[y_{(n-1)\xi\xi}(\xi, t)]\right] = \frac{(-t^\mu)^n \sin(\xi)}{\Gamma(n\mu + 1)}.
\end{aligned}
$$

Thus our solution to (17) is given by

$$
\begin{aligned}
y(x, t) &= \sin(\xi)\left(1 - \frac{t^\mu}{\Gamma(\mu + 1)} + \frac{t^{2\mu}}{\Gamma(2\mu + 1)} - \frac{t^{3\mu}}{\Gamma(3\mu + 1)} + \ldots\right) \\
&= \sin(\xi)\sum_{n=0}^\infty \frac{(-t^\mu)^n}{\Gamma(n\mu + 1)} = \sin(\xi)E_\mu(-t^\mu).
\end{aligned}
$$

This is the same solution as that obtained in [13] using the DJM.

Example 2.3 Consider the following one dimensional nonlinear time fractional diffusion equation with the given initial condition [13]:

$$\mathcal{D}_t^\mu y(\xi, t) = y_{\xi\xi}(\xi, t) + 2y^2(\xi, t), \quad \mu \in (0, 1], \quad x \in \mathbb{R}, \quad t > 0, \tag{20}$$
$$y(\xi, 0) = e^{-\xi}.$$

$R(y(\xi, t)) = y_{\xi\xi}(\xi, t)$, $F(y(\xi, t)) = 2y^2(\xi, t)$ and $\eta(\xi, t) = 0$, we take the natural transform on both sides of (20) and utilize the initial condition to get

$$\psi(\xi, s, u) = \frac{e^{-\xi}}{s} + \left(\frac{u}{s}\right)^{\mu} \mathcal{N}[y_{\xi\xi}(\xi, t)] + \left(\frac{u}{s}\right)^{\mu} \mathcal{N}[2y^2(\xi, t)], \tag{21}$$

$$y(\xi, t) = e^{-\xi} + \mathcal{N}^{-1}\left[\left(\frac{u}{s}\right)^{\mu} \mathcal{N}[y_{\xi\xi}(\xi, t)]\right] + \mathcal{N}^{-1}\left[\left(\frac{u}{s}\right)^{\mu} \mathcal{N}[2\xi^2(\xi, t)]\right]. \tag{22}$$

The NDJM then entails that we have the following iteration:

$$
\begin{aligned}
y_0 &= e^{-\xi}, \\
y_1 &= \mathcal{N}^{-1}\left[\left(\frac{u}{s}\right)^{\mu} \mathcal{N}[y_{0\xi\xi}(\xi, t)]\right] + \mathcal{N}^{-1}\left[\left(\frac{u}{s}\right)^{\mu} \mathcal{N}[F(y_0)]\right], \\
&= \frac{e^{-\xi} t^{\mu}}{\Gamma(\mu+1)} + \frac{2e^{-2\xi} t^{\mu}}{\Gamma(\mu+1)}, \\
y_2 &= \mathcal{N}^{-1}\left[\left(\frac{u}{s}\right)^{\mu} \mathcal{N}[y_{1\xi\xi}(\xi, t)]\right] + \mathcal{N}^{-1}\left[\left(\frac{u}{s}\right)^{\mu} \mathcal{N}[F(y_1 + y_0) - F(y_0)]\right], \\
&= \frac{e^{-\xi} t^{2\mu}}{\Gamma(2\mu+1)} + \frac{8e^{-2\xi} t^{2\mu}}{\Gamma(2\mu+1)} + \frac{4e^{-2\xi} t^{2\mu}}{\Gamma(2\mu+1)} + \frac{8e^{-3\xi} t^{2\mu}}{\Gamma(2\mu+1)} \\
&+ \frac{2\Gamma(2\mu+1)e^{-2\xi} t^{3\mu}}{\Gamma(\mu+1)^2 \Gamma(3\mu+1)} + \frac{8\Gamma(2\mu+1)e^{-3\xi} t^{3\mu}}{\Gamma(\mu+1)^2 \Gamma(3\mu+1)} + \frac{8\Gamma(2\mu+1)e^{-4\xi} t^{3\mu}}{\Gamma(\mu+1)^2 \Gamma(3\mu+1)}.
\end{aligned}
$$

Our approximate solution to (20) is then given by $y(\xi, t) = y_0 + y_1 + y_2$, we note that this is the same solution as in [13] where the DJM was used.

3 Conclusion

In this paper we managed to successfully introduce a new method, the natural Daftardar-Jafari method for solving partial differential equations of fractional order. We have shown that this new technique produces the same results as the other methods that are already in existence. This method is also applicable to ordinary and partial differential equations of integer order.

References

[1] I. Podlubny. *An Introduction to Fractional Derivatives, Fractional Differential Equations, to Methods of Their Solution and Some of Their Applicatons.* Academic Press, New York, NY, 1999.

[2] H. Jafari and V. Daftardar-Gejji. Solving a system of non linear fractional differential equations using Adomian decomposition method. *J. Comp. Appl. Math.* **196** (2006) 644–651.

[3] E. Abuteen, A. Fraihat, M. Al-Smadi, H. Khalil and A. R. Khan. Approximate series solution of nonlinear fractional Klein-Gordon equations using fractional reduced differential transform method. *J. Math. Stat.* **12** (2016) 23–33.

[4] H. Jafari, C. M. Khalique and M. Nazari. Application of the Laplace decomposition method for solving Linear and nonlinear fractional diffusion wave equations. *Appl. Math. Letters.* **24** (2011) 1799–1805.

[5] A. S. Abdel-Rady, S. Z. Rida, A. A. M. Arafa and H. R. Abedl-Rahim. Natural transform for solving fractional models. *J. Appl. Math. Phy.* **3** (2015) 1633–1644.

[6] R. Chaudhary and D. N. Pandey. Existence results for Sobolev type fractional differential
     equation with nonlocal integral boundary conditions. *Nonlinear Dynamics and Systems
     Theory* **18** (3) (2018) 259–272.

[7] P. G. Chhetri and A. S. Vatsala. Generalised Monotone Method for Riemann-Liouville
     fractional reaction diffusion equation with applications.*Nonlinear Dynamics and Systems
     Theory* **16** (3) (2016) 235–245.

[8] F. B. M. Balgacem and R. Silambarasan. Maxwell's equations by means of the natural
     transform. *Math. Eng. Sc. Aero.* **3** (2012) 313–323.

[9] Z.H. Khan and W. Khan. N-Transform properties and applications. *NUST Journal Engi-
     neering Sciences* **1** (2008) 127-133.

[10] S. MaitamaS and I. Abdullahi. A new analytical method for solving linear and nonlinear
     fractional partial differential equations. *Progr. Fract. Differ.* **2** (4) (2016) 247–256.

[11] V. Daftardar-Gejji and H. Jafari. An iterative method for solving non linear functional
     equations. *J. Math. Anal. Appl.* **316** (2006) 753–763.

[12] V. F. Morales-Delgado, J. F. Gómez-Aguilar, H. Yépez-Martínez, D. Baleanu, R. F.
     Escobar-Jimenez and V. H. Olivares-Peregrino. Laplace homotopy analysis method for
     solving linear partial differential equations using a fractional derivative with and without
     a singular kernel. *Adv. Differ. Equ.* (2016) 2016:164.

[13] V. Daftardar-Gejji and S. Bhalekar. Solving fractional diffusion-wave equations uing a new
     iterative method. *Int. J. Theo. Appl.* **11** (2) (2008) 193–202.

Increased Order Generalized Combination Synchronization of Non-Identical Dimensional Fractional-Order Systems by Introducing Different Observable Variable Functions

S. Kaouache [1*], N. E. Hamri [1], A. S. Hacinliyan [2], E. Kandiran [3], B. Deruni [4] and A. C. Keles [5]

[1] *Laboratory of Mathematics and Their Interactions, Abdelhafid Boussouf University Center, Mila 43000, Algeria*
[2] *Department of Physics and Department of Information Systems and Technologies, Yeditepe University, 26 Agustos Yerlesimi, Kayisdagi Caddesi, 34755 Atasehir Istanbul, Turkey*
[3] *Department of Software Development, Yeditepe University, 26 Agustos Yerlesimi, Kayisdagi Caddesi, 34755 Atasehir Istanbul, Turkey*
[4] *7, Harmanlik Street, Yakacik, Kartal 34876, Turkey*
[5] *Departmnt of Information Systems and Technologies, Yeditepe University, 26 Agustos Yerlesimi, Kayisdagi Caddesi, 34755 Atasehir Istanbul, Turkey*

Abstract: An increased order generalized combination synchronization (IOGCS) of non-identical dimensional fractional-order systems with suitable different observable variable functions is proposed and analyzed in this paper. This synchronization scheme is applied for the combination of two fractional-order unified drive systems and the fractional-order Liu response system. In view of the stability property of linear fractional-order systems, an effective nonlinear control scheme is designed to achieve the desired synchronization. Theoretical analysis and numerical simulations are shown to demonstrate the effectiveness of the proposed method.

Keywords: *increased order generalized combination synchronization; chaotic system; fractional-order system; stability property of fractional-order system.*

Mathematics Subject Classification (2010): 34A34, 37B55, 93C55, 93D05.

* Corresponding author: mailto:s.kaouache@centre-univ-mila.dz

1   Introduction

Fractional calculus can be dated back to the 17th century as studied by Podlubny [1]. Over the last decades, fractional calculus has applied in various fields such as control processing [2], reaction difusion equation [3], biological phenomena [4] and so on.

Chaos synchronization schemes for fractional-order dynamical systems have also been investigated in several fields such as secure communication and data encryption [5, 6]. Up to now, a variety of approaches of chaos synchronization have been developed, such as complete synchronization [7], generalized synchronization [8], inverse matrix projective synchronization [9], modified projective synchronization [10], coexistence of different types of chaos synchronization [11], and $Q - S$ synchronization [12].

However, most of researchers mainly focused on the usual drive-response synchronization model, which has one drive system and one response system.

Recently, studying synchronization between the combination of two (or more) drive systems and one response system becomes an interesting problem due to its potential applications in secure communication [13].

Now, some results on the combination synchronization of several chaotic fractional order systems are obtained. For example, the combination synchronization of three classic chaotic systems using active backstepping design is investigated in [14]. The combination synchronization of three identical or different nonlinear complex hyperchaotic systems is achieved in [15]. The reduced order function projective combination synchronization of three Josephson junctions using the backstepping technique is investigated in [16]. An adaptive function projective combination synchronization of three different fractional order chaotic systems is investigated in [17]. The generalized combination complex synchronization for fractional-order chaotic complex systems is investigated in [18]. And the generalized combination synchronization of three different dimensional fractional chaotic and hyperchaotic systems by using three scaling matrices is achieved in [19]. However, these studies are mainly concerned with the combination synchronization between chaotic systems with respect to the scaling matrices. Therefore the combination synchronization of non-identical dimensional chaotic fractional order systems with respect to the variable functions becomes an interesting and challenging work.

By exploiting the idea of the stability property of linear fractional order systems, an effective nonlinear controller for the IOGCS of three fractional-order chaotic systems with suitable different observable variable functions is designed in this paper, and the stability criterion for the above-mentioned systems is found. To simplify our discussions, the synchronization scheme is applied for the combination of two fractional-order unified drive systems and the fractional-order Liu response system.

The rest of the paper is organized as follows. In Section 2, based on the stability property of linear fractional order systems, a powerful scheme is proposed to realize the IOGCS of non-identical fractional order dynamical chaotic systems. In Section 3, numerical simulations show that the method can ensure the occurrence of the IOGCS between the fractional-order unified chaotic system and fractional-order Liu system. Finally, conclusion is given in Section 4.

2   Problem Formulation of the IOGCS

In this section, we introduce the concept of the IOGCS of three non-identical dimension fractional-order systems with suitable different observable variable functions. The model

can be given as follows

$$D^\alpha x = f(x), \tag{1}$$

$$D^\alpha y = g(y), \tag{2}$$

$$D^\alpha z = h(z) + u, \tag{3}$$

where D^α is the Caputo differential operator [1] which is defined as

$$D^\alpha \xi(t) = J^{n-\alpha} \xi^{(n)}(t), \ \ \alpha \in (n-1, n), \tag{4}$$

where J^α is the α-order Riemann–Liouville integral operator which is defined as

$$J^\alpha \xi(t) = \frac{1}{\Gamma(\alpha)} \int_0^t (t-\tau)^{\alpha-1} \xi(\tau) d\tau, \tag{5}$$

and

$$\Gamma(\alpha) = \int_0^{+\infty} z^{\alpha-1} \exp(-z) dz \tag{6}$$

is the gamma function, $x = (x_1, x_2, ..., x_n)^T \in \mathbb{R}^n$ and $y = (y_1, y_2, ..., y_n)^T \in \mathbb{R}^n$ are the state variables of two drive systems, $z = (z_1, z_2, ..., z_m)^T \in \mathbb{R}^m (n < m)$ is the state variable of the response system, $f, g : \mathbb{R}^n \to \mathbb{R}^n$ and $h : \mathbb{R}^m \to \mathbb{R}^m$ are the continuous vector-valued functions and $u = (u_1, u_2, ..., u_m)^T \in \mathbb{R}^m$ is the controller vector which will be designed.

The definition of the proposed synchronization is given as follows.

Definition 2.1 The two drive systems (1)-(2) and the response system (3) are said to achieve the IOGCS if there exists a suitable controller u and three continuous smooth vector functions $Q, R : \mathbb{R}^n \to \mathbb{R}^m$ and $S : \mathbb{R}^m \to \mathbb{R}^m$, such that the error vector

$$e(t) = Q(x(t)) + R(y(t)) - S(z(t)) \tag{7}$$

will approach zero for large enough t, i.e.,

$$\lim_{t \to +\infty} \|Q(x(t)) + R(y(t)) - S(z(t))\| = 0, \tag{8}$$

where $\|.\|$ represents the matrix norm.

Remark 2.1 From Definition 2.1, one can show that the IOGCS of three different fractional-order chaotic systems can be extended to more chaotic systems.

In this paper, we consider the fractional-order unified system (Lorenz, Chen and Lü systems) [20] as the first drive system, which is described by

$$\begin{cases} D^\alpha x_1 = (25\delta + 10)(x_2 - x_1), \\ D^\alpha x_2 = (-35\delta + 28)x_1 - x_1 x_3 + (29\delta - 1)x_2, \\ D^\alpha x_3 = x_1 x_2 - (\frac{\delta + 8}{3})x_3. \end{cases} \tag{9}$$

The second drive system is described also by the fractional-order unified system

$$\begin{cases} D^\alpha y_1 = (25\delta + 10)(y_2 - y_1), \\ D^\alpha y_2 = (-35\delta + 28)y_1 - y_1 y_3 + (29\delta - 1)y_2, \\ D^\alpha y_3 = y_1 y_2 - (\frac{\delta + 8}{3})y_3, \end{cases} \tag{10}$$

and the controlled response system is chosen as the fractional-order Liu system [21]

$$\begin{cases} D^\alpha z_1 = a(z_2 - z_1) + u_1, \\ D^\alpha z_2 = bz_1 + z_1 z_3 - z_4 + u_2, \\ D^\alpha z_3 = -cz_3 - z_1 z_2 + z_4 + u_3, \\ D^\alpha z_4 = dz_1 + z_2 + u_4, \end{cases} \tag{11}$$

where x_i, y_i $(i = 1, 2, 3)$ and z_j $(j = 1, 2, 3, 4)$ are the state variables of the master systems and the slave system, respectively, $\delta \in [0,1]$, D^α is the Caputo differential operator $(0 < \alpha \le 1)$,u_1, u_2, u_3 and u_4 are the nonlinear controllers to be designed.

To simplify our discussions, we take the observable variable functions $Q, R : \mathbb{R}^3 \to \mathbb{R}^4$ and $S : \mathbb{R}^4 \to \mathbb{R}^4$ as

$$Q(x_1, x_2, x_3) = (x_1 - x_2, x_2, x_3 + 1, 2), \tag{12}$$

$$R(y_1, y_2, y_3) = (y_1 - y_2, y_2, y_3, 0) \tag{13}$$

and

$$S(z_1, z_2, z_3, z_4) = (z_1, z_2, z_3 + 1, z_4 - cz_3 + 2). \tag{14}$$

The error states are defined by

$$\begin{cases} e_1 = x_1 - x_2 + y_1 - y_2 - z_1, \\ e_2 = x_2 + y_2 - z_2, \\ e_3 = x_3 + y_3 - z_3, \\ e_4 = -z_4 + cz_3. \end{cases} \tag{15}$$

Then the error dynamical systems between the drive systems (9), (10) and the response system (11) can be written as

$$\begin{cases} D^\alpha e_1 = (10\delta - 38)e_1 + (7\delta - 27)e_2 + (10\delta + a - 38)z_1 + \\ \qquad + (7\delta - a - 27)z_2 + x_1 x_3 + y_1 y_3 - u_1, \\ D^\alpha e_2 = (29\delta - 1)e_2 - e_4 + (29\delta - 1)z_2 + (-35\delta + 28)(x_1 + y_1) + \\ \qquad - (x_1 x_3 + y_1 y_3) - bz_1 - z_1 z_3 + cz_3 - u_2, \\ D^\alpha e_3 = -(\dfrac{\delta + 8}{3})e_3 + e_4 + x_1 x_2 + y_1 y_2 + z_1 z_2 + -(\dfrac{\delta + 8}{3})z_3 - u_3, \\ D^\alpha e_4 = -ce_4 - dz_1 - z_2 - cz_1 z_2 - u_4 + cu_3. \end{cases} \tag{16}$$

To get the IOGCS to occur, the zero solutions of the error system must be stable, that is to say, the error evolution of the systems (9), (10) and (11) should tend to zero as $t \to +\infty$. So, a suitable controller $u_i, i = 1, 2, 3, 4$ should be designed which guarantees that system (16) stabilizes towards the origin. To this end, we need the following theorem and hypothesis.

Theorem 2.1 *[22] Consider the fractional-order linear system*

$$D^\alpha x = Ax, \tag{17}$$

where $x \in \mathbb{R}^n$ is the state vector. The previous system is asymptotically stable if and only if $|\arg(\lambda_i\,(A))| > \alpha\dfrac{\pi}{2}$ for $i = 1, 2, ..., n$, where $\arg(\lambda_i\,(A))$ denotes the argument of the eigenvalue λ_i of A.

Hypothesis: *We assume that the controllers $u_i, i = 1, 2, 3, 4$ are chosen as*

$$\begin{cases} u_1 = (10\delta + a - 38)z_1 + (7\delta - a - 27)z_2 + x_1x_3 + y_1y_3 + k_1e_1, \\ u_2 = (29\delta - 1)z_2 + (-35\delta + 28)(x_1 + y_1) - (x_1x_3 + y_1y_3) - bz_1 - (z_1 - c)z_3 + k_2e_2, \\ u_3 = x_1x_2 + y_1y_2 + z_1z_2 - (\dfrac{\delta + 8}{3})z_3, \\ u_4 = -dz_1 - z_2 + c\left(x_1x_2 + y_1y_2 + -(\dfrac{\delta + 8}{3})z_3\right), \end{cases}$$

(18)

where k_1 and k_2 are the feedback gains satisfying

$$k_1 > 10\delta - 38 \ \text{ and } \ k_2 > 29\delta - 1. \tag{19}$$

Now, due to Theorem 2.1, we have the following results.

Theorem 2.2 *If the controllers $u_i, i = 1, 2, 3, 4$ are given by (18), and the feedback gains k_1 and k_2 are given by (19), then*

$$\lim_{t \to +\infty} \|Q\left(x(t)\right) + R\left(y(t)\right) - S\left(z(t)\right)\| = 0,$$

that is to say, the IOGCS occurs between the systems (9), (10) and (11) with respect to the variable functions Q, R and S.

Proof. By hypothesis (18), the error system (16) becomes

$$\begin{cases} D^\alpha e_1 = (10\delta - 38 - k_1)e_1 + (7\delta - 27)e_2, \\ D^\alpha e_2 = (29\delta - 1 - k_2)e_2 - e_4, \\ D^\alpha e_3 = -(\dfrac{\delta + 8}{3})e_3 + e_4, \\ D^\alpha e_4 = -ce_4, \end{cases}$$

(20)

and the characteristic equation is

$$\frac{1}{3}\left(\lambda + c\right)\left(3\lambda + \delta + 8\right)\left(\lambda - 29\delta + k_2 + 1\right)\left(\lambda - 10\delta + k_1 + 38\right) = 0. \tag{21}$$

It is easy to obtain its characteristic roots as

$$\lambda_1 = -c, \ \lambda_2 = -(\frac{\delta + 8}{3}), \ \lambda_3 = 29\delta - 1 - k_2 \text{ and } \lambda_4 = 10\delta - 38 - k_1. \tag{22}$$

Since $\delta \in [0, 1]$ and by hypothesis (19), all roots of (21) are negative. Therefore,

$$|\arg \lambda_i \,| > \alpha\frac{\pi}{2} \text{ for } i = 1, 2, 3, 4 \text{ and } 0 < \alpha < 1.$$

In view of Theorem 2.1, the error system (20) is asymptotically stable, which implies that the desired synchronization is achieved.

3   Numerical Simulations

In order to verify the theoretical results obtained in the above section, the corresponding numerical simulations will be performed. In the simulations, we take: $\alpha = 0.97$, $\delta = 1$,

$k_1 = -27$, $k_2 = 29$. The initial values of the two drive and the response systems are chosen as $(x_1(0), x_2(0), x_3(0))^T = (0.1, 0.1, 0.1)^T$, $(y_1(0), y_2(0), y_3(0))^T = (0.1, 0.1, 0.1)^T$ and $(z_1(0), z_2(0), z_3(0), z_4(0))^T = (0.3, 0.3, 0, -0.3)^T$, respectively. The initial conditions for the error system are thus $(e_1(0), e_2(0), e_3(0), e_4(0))^T = (-0.3, -0.1, 0.2, 0.3)^T$.

Figures 1, 2, 3 and 4 display the chaotic behaviors of the Lorenz system (9) (when $\delta = 0$), the Lü system (9) (when $\delta = 0.8$), the Chen system (9) (when $\delta = 1$), and the Liu system (11) (when $a = 10$, $b = 35$, $c = 1.4$ and $d = 5$), respectively. Figure 5 shows the curves of the synchronization errors (20) under the controllers (18).
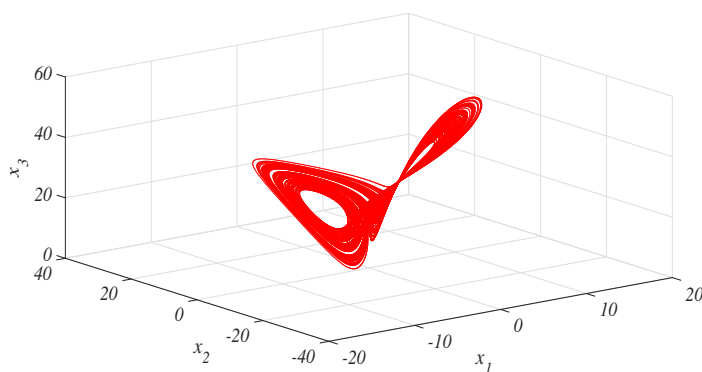
Figure 1: The chaotic attractor of the Lorenz system (9), when $\delta = 0$.
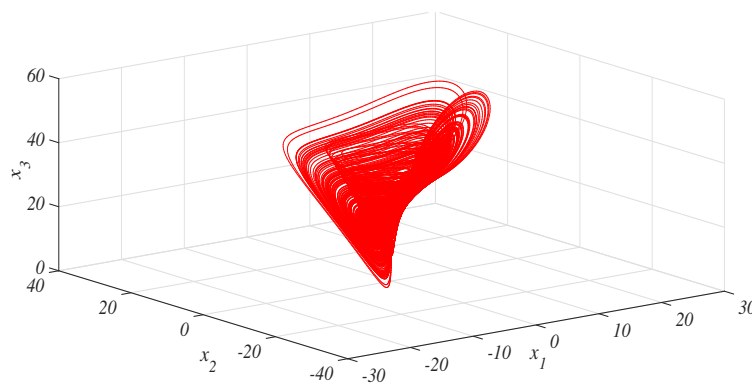
Figure 2: The chaotic attractor of the Lü system (9), when $\delta = 0.8$.

Remark 3.1 From Figure 5, it can be seen that the components of the error system (20) decay towards zero as $t \to +\infty$, which implies that the desired synchronization is achieved with our designed scheme.
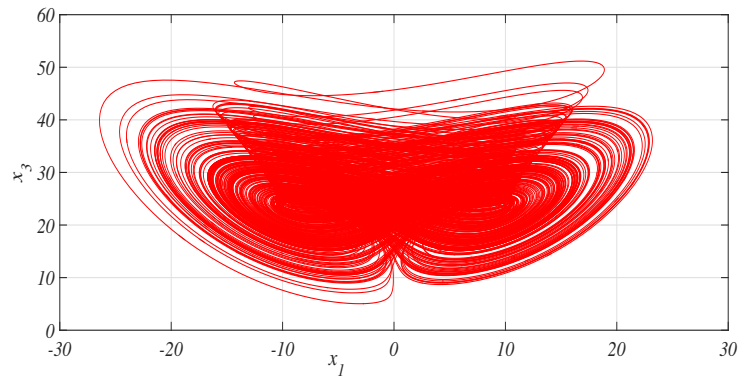
Figure 3: The chaotic attractor of the Chen system (9), when $\delta = 1$.
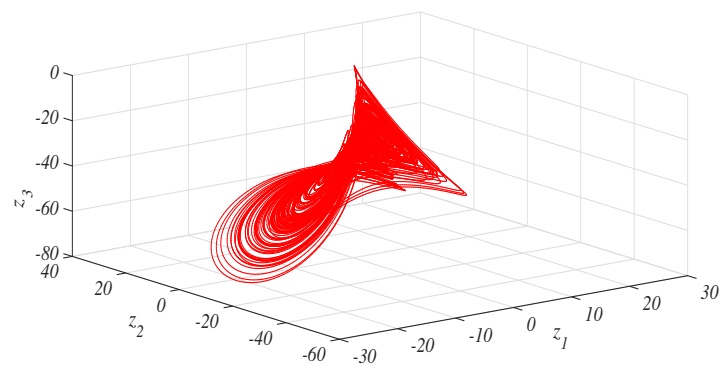
Figure 4: The hyperchaotic attractor of the Liu system (11).
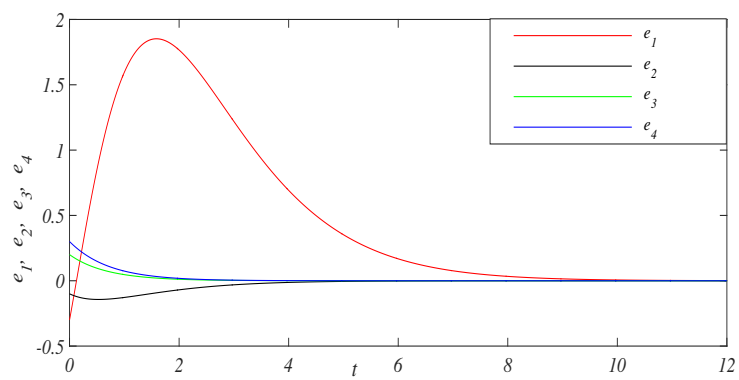
Figure 5: The curves of the synchronization errors (20).

4 Conclusion

In this paper, we have investigated a new type of combination synchronization, called IOGCS, between two drive systems of dimension 3 and a slave system of dimension 4 by introducing suitable observable variable functions. In view of the stability theory of linear fractional-order systems, a suitable controller is designed to achieve the desired synchronization. The method of this scheme has been applied for the combination of two fractional-order unified drive systems and the fractional-order Liu response system. Finally, numerical simulations are provided to verify the effectiveness of the proposed scheme.

Acknowledgements

References

[1] I. Podlubny. Fractional Differential Equations. *Academic Press*, New York, 1999.

[2] B. Labed, S. Kaouache and M.S. Abdelouahab. Control of a novel class of uncertain fractional-order hyperchaotic systems with external disturbances via sliding mode controller. *Nonlinear Dynamics and Systems Theory* **20** (2) (2020) 203–213.

[3] P.G. Chetri and A.S. Vatsala. Generalized monotone method for Riemann-Liouville fractional reaction difusion equation with applications. *Nonlinear Dynamics and Systems Theory* **18** (3) (2018) 259–272.

[4] E. Kaslik, S. Sivasundaram. Nonlinear dynamics and chaos in fractional-order neural networks. *Neural Netw.* **32** (2012) 245–256.

[5] H. Delavari and M. Mohadeszadeh. Robust finite-time synchronization of non-identical fractional-order hyperchaotic systems and its application in secure communication. *IEEE/CAA Journal of Automatica Sinica* **6** (1) (2019) 228–235.

[6] E. Inzunza-Gonzalez and C. Cruz-Hernandez. Double hyperchaotic encryption for security in biometric systems. *Nonlinear Dynamics and Systems Theory* **13** (1) (2013) 55–68.

[7] A. Khan, and P. Tripathi. Synchronization between a fractional order chaotic system and an integer order chaotic system. *Nonlinear Dynamics and Systems Theory* **13** (4) (2013) 425–436.

[8] S. Kaouache and M.S. Abdelouahab. Generalized synchronization between two chaotic fractional non-commensurate order systems with different dimensions. *Nonlinear Dynamics and Systems Theory* **18** (3) (2018) 273–284.

[9] S. Kaouache and M.S. Abdelouahab. Inverse matrix projective synchronization of novel hyperchaotic system with hyperbolic sine function non-linearity. *DCDIS B: Applications and Algorithms* **27** (2020) 145–154.

[10] S. Kaouache, and M.S. Abdelouahab. Modified projective synchronization between integer order and fractional order hyperchaotic systems. *Jour. of Adv. Research in Dynamical and Control Systems* **10** (5) (2018) 96–104.

[11] S. Boudiar, A. Ouannas, S. Bendoukha and A. Zara. Coexistence of different types of chaos synchronization between non-identical and different dimensional dynamical systems. *Nonlinear Dynamics and Systems Theory* **18** (3) (2018) 253–258.

[12] Y. Chai, L. Chen, R. Wu and J. Dai. $Q - S$ synchronization of the fractional-order unified system. *Pramana Journal of Physics* **80** (3) (2013) 449–461.

[13] R.Z. Luo and Y.L. Wang. Finite-time stochastic combination synchronization of three different chaotic systems and its application in secure communication. *Chaos* **22** (2012) 023109.

[14] R. Luo, Y. Wang and S. Deng. Combination synchronization of three classic chaotic systems using active backstepping design. *Chaos: An Interdisciplinary Journal of Nonlinear Science* **21** (4) (2011) Article ID 043114.

[15] Z.Y. Wu and X.C. Fu. Combination synchronization of three different order nonlinear systems using active backstepping design. *Nonlin. Dyn.* **73** (2013) 1863–1872.

[16] K.S. Ojo, A.N. Njah, S.T. Ogunjo and O.I. Olusola. Reduced Order Function Projective Combination Synchronization of Three Josephson Junctions Using Backstepping Technique. *Nonlinear Dynamics and Systems Theory* **14** (2) (2014) 119–133.

[17] H. Xi, Y. Li and X. Huang. Adaptive function projective combination synchronization of three different fractional order chaotic systems. *Optik* **126** (24) (2015) 5346?-5349.

[18] C. Jiang, S. Liu and D. Wang. Generalized combination complex synchronization for fractional-order chaotic complex systems. *Entropy* **17** (8) (2015) 5199?-5217.

[19] S. Kaouache, M.S. Abdelouahab and N.E. Hamri. Generalized combination synchronization of three different dimensional fractional chaotic and hyperchaotic systems using three scaling matrices. *Jour. of Adv. Research in Dynamical and Control Systems* **12** (4) (2020) 330–337.

[20] J.W. Wang and Y.B. Zhang. Designing synchronization schemes for chaotic fractional-order unified systems. *Chaos Solitons and Fractals* **30** (5) (2006) 1265–1272.

[21] L. Liu, C. Liu and Y. Zhang. Analysis of a novel four-dimensional hyperchaotic system. *Chin. J. Phys.* **46** (2008) 386–393.

[22] D. Matignon. Stability results of fractional differential equations with applications to control processing. In: *IMACS, IEEE-SMC,* Lille, France, 1996.

Gradient Optimal Control Problems for a Class of Infinite Dimensional Systems

M. O. Sidi* and S. A. Beinane

RT-M2A Laboratory, Mathematics Department, College of Science, Jouf University, P.O. Box: 2014, Sakaka, Saudi Arabia.

Abstract: In this work, we address the issue of optimal control for a class of bilinear systems. The goal is to achieve approximately a desired gradient on the whole domain by seeking the minimum of a function. Next, optimization methods are used to reach the desired subregion gradient at time T. The proposed methods are illustrated by a theoretical approach and algorithm.

Keywords: *infinite dimensional systems; gradient problems; regional problems; algorithm.*

Mathematics Subject Classification (2010): 37M05, 65K05, 93C10.

1 Introduction

Infinite-dimensional systems are present in many problems. The analysis of such systems regroup many concepts such as stability, exact controllability, approximate controllability [2, 4, 5]. Nonlinear dynamics is of interest to mathematicians because most systems are nonlinear in nature. The multiplication of state and control in bilinear dynamics make them an important subclass of nonlinear systems, such nonlinearity appears in many dynamical process, for example, a convective-diffusive fluid problem used in [6] to remove a contaminant from water and control of velocity in a Kirchhoff plate, see [4]. Bichiou et al. in [3] treated an approach for the minimum time control of dynamical systems. Alharbi et al. in [1] studied the immune system using vitamins intervention. Regional controllability is a very important generalization referring to the optimal control problems in which the target is studied particularly on a subregion ω.

---

* Corresponding author: `mailto:maawiya81@gmail.com`

An important real situation that requires such notions, arises when the control is required to attain a level of temperature in a specified zone of furnace, see [5]. El Jai et al. give the most important motivation of regional controllability in [5], proving that there exists a system which is regional controllable but not global controllable. Backgrounds in dynamical systems of linear and semi-linear type are established by Zerrik and Ould Sidi in [10] when studying the control of the gradient state of a regional target.

One of the important motivations are the thermal isolation problems, where the control is maintained to reduce the gradient temperature on the boundary. Very interesting developments of this field are found in [7], in particular the characterization of the control achieving gradient controllability.

The partial analysis of bilinear systems was initiated by Zerrik and Ould Sidi in [11,12] and [13]. Using a minimizing sequence, they study the existence of solutions for the problems governed by such systems. Zine and Ould Sidi in [14,15] and Zine in [16] worked on bilinear hyperbolic distributed systems. Ould Sidi in [8] gives necessary conditions for optimal control problems with more regular control functions.

In this work, we address the issue of optimal control for a class of bilinear systems. The goal is to achieve approximately a desired gradient on the whole domain by seeking the minimum of a function. Next, optimization methods help us to reach the desired subregion gradient at time T. The proposed methods are illustrated by a theoretical approach and algorithm.

2 Gradient Optimal Control Problem

We choose an open bounded domain $\Omega \subset I\!R^n (n \in \{1, 2, 3\})$ and $\partial\Omega$ is its regular boundary. Let $T > 0$ and $\Theta = \Omega \times]0, T[$, $\Sigma = \partial\Omega \times]0, T[$ and $Q \in L^2(0, T; L^2(\Omega))$ be the control. We consider the following bi-linear equation:

$$\begin{cases} \dfrac{\partial z}{\partial t} + \Delta^2 z = Q(x,t)\nabla z, & \Theta, \\ z(x,0) = z_0(x), & \Omega, \\ z = \dfrac{\partial z}{\partial \nu} = 0, & \Sigma. \end{cases} \tag{1}$$

Δ^2 is the bi-Laplace operator, ∇ is the gradient operator defined by

$$\begin{aligned} \nabla : H^1(\Omega) &\longrightarrow (L^2(\Omega))^n \\ z &\longrightarrow \nabla z = (\dfrac{\partial z}{\partial x_1}, ..., \dfrac{\partial z}{\partial x_n}). \end{aligned}$$

The state space is

$$W = \{z \in L^2(0, T; H_0^1(\Omega)) / \dfrac{\partial z(x,t)}{\partial t} \in L^2(0, T; H^{-2}(\Omega))\}.$$

For $Q \in L^2(0, T; L^2(\Omega))$ and $z_0(x) \in L^2(\Omega)$, from the results in [9] the equation (1) has a unique solution z_Q in $W \cap L^\infty(0, T; L^2(\Omega))$.

The gradient problem of (1) is

$$\min_{Q \in L^2(0,T;L^2(\Omega))} J_\varepsilon(Q). \tag{2}$$

For $\varepsilon > 0$, the gradient quadratic cost J_ε is defined by

$$
\begin{aligned}
J_\varepsilon(Q) &= \frac{1}{2}\left\|\nabla z - z^d\right\|^2_{(L^2(0,T;L^2(\Omega)))^n} + \frac{\varepsilon}{2}\int_\Theta \left\|Q(x,t)\right\|^2_{\mathbb{R}^n} dxdt \\
&= \frac{1}{2}\sum_{i=1}^n \left\|\frac{\partial z}{\partial x_i} - z_i^d\right\|^2_{L^2(0,T;L^2(\Omega))} + \frac{\varepsilon}{2}\int_\Theta \left\|Q(x,t)\right\|^2_{\mathbb{R}^n} dxdt,
\end{aligned}
\tag{3}
$$

where $z^d = (z_1^d, ...z_n^d)$ is the desired gradient in $L^2(0,T;L^2(\Omega))$.

In the literature, quadratic problems such as (1) command the system state to a desired function, see [4,6]. The main objective of our work is to steer the gradient of (1) to $z^d(x)$ minimizing (3), and to characterize the optimal control $Q \in L^2(0,T;L^2(\Omega))$.

3   Solving Method

This section studies the existence and proposes a solution of (2).

Theorem 3.1
There exists $(z^*, Q^*) \in \mathcal{C}([0,T];H_0^1(\Omega)) \times L^2([0,T])$, where z^* is the solution of

$$
\begin{cases}
\dfrac{\partial z}{\partial t} + \Delta^2 z = Q^*(x,t)\nabla z, & \Theta, \\
z(x,0) = z_0(x), & \Omega, \\
z = \dfrac{\partial z}{\partial \nu} = 0, & \Sigma,
\end{cases}
\tag{4}
$$

and Q^* is the optimal control of (2).

Proof. The set $\{J_\varepsilon(Q) \mid Q \in L^2(0,T;L^2(\Omega))\}$ is a positive nonempty set of $\mathbb{R}$, then it admits a lower bound. We choose $(Q_n)_n$ as a minimum such that

$$
J^* = \lim_{n \to +\infty} J(Q_n) = \inf_{Q \in L^2(0,T;L^2(\Omega))} J_\varepsilon(Q).
$$

$J_\varepsilon(Q_n)$ is then bounded, it follows that $\|Q_n\|_{L^2(0,T;L^2(\Omega))} \leq C$, for a positive constant C. Using lemma in [16], we can deduce that

$$
\begin{aligned}
Q_n &\rightharpoonup Q^*, & L^2(0,T;L^2(\Omega)), \\
z_n &\rightharpoonup z^*, & W, \\
\Delta^2 z_n &\rightharpoonup \chi, & W, \\
Q_n\nabla z_n &\rightharpoonup \Lambda, & W, \\
\frac{\partial z_n(x,t)}{\partial t} &\rightharpoonup \Psi, & W.
\end{aligned}
\tag{5}
$$

The limit in $\dfrac{\partial z_n(x,t)}{\partial t} + \Delta^2 z_n = Q_n\nabla z_n$, we get $\dfrac{\partial z^*(x,t)}{\partial t} = \Psi$.

The linearity of the operator $z \mapsto \Delta^2 z$ and the operator ∇ gives $\Delta^2 z^* = \chi$ and $Q^*\nabla z^* = \Lambda$. Hence we obtain

$$
\frac{\partial z^*}{\partial t} + \Delta^2 z^* = Q^*(x,t)\nabla z^*.
$$

We use the lower semi-continuity of $J_\varepsilon(Q)$:

$$
\begin{aligned}
J_\varepsilon(Q^*) &= \inf_n \sum_{i=1}^n \frac{1}{2}\int_0^T \int_\Omega \left(\frac{\partial z_n}{\partial x_i} - z_i^d\right)^2 dx + \frac{\varepsilon}{2}\int_\Theta \left\|Q_n(t)\right\|^2_{\mathbb{R}^n} dxdt \\
&\leq \lim_{n \to \infty} J_\varepsilon(Q_n) = \inf_Q J_\varepsilon(Q).
\end{aligned}
\tag{6}
$$

Thus Q^* is a solution of (2). To characterize the solution of problem (2), we study the differential of cost $J_\varepsilon(Q)$

Lemma 3.1 *For the map*

$$
\begin{array}{ccl}
L^2(0,T;L^2(\Omega)) & \longrightarrow & \mathcal{C}(0,T;H^1(\Omega)), \\
Q & \longrightarrow & z(Q)
\end{array}
$$

the solution of (4) is differentiable and its differential ψ verifies the system

$$
\begin{cases}
\dfrac{\partial \psi}{\partial t} = -\Delta^2 \psi(x,t) + Q^*(x,t)\nabla\psi + h(x,t)\nabla z, & \Theta, \\
\psi(x,0) = \psi_0(x) = 0, & \Omega, \\
\psi = \dfrac{\partial \psi}{\partial \nu} = 0, & \Sigma,
\end{cases}
\tag{7}
$$

with $z^* = z(Q^*)$, $h \in U$, and $d(z(Q^*))h$ is the differential of $Q \to z(Q)$.

Proof. The solution of the equation (7) verifies

$$
||\psi||_W \le k_1 ||z||_{L^\infty(0,T;H_0^1(\Omega))} ||h||_{L^2(0,T;L^2(\Omega))}.
$$

Also,

$$
||\psi'||_W \le k_2 ||z^*||_{L^\infty(0,T;H_0^1(\Omega))} ||h||_{L^2(0,T;L^2(\Omega))}.
$$

Thus,

$$
||\psi||_{\mathcal{C}([0,T];H_0^1(\Omega))} \le k_3 ||h||_{L^2(0,T;L^2(\Omega))}.
$$

Consequently, we have $h \in L^2(0,T;L^2(\Omega)) \to \psi \in \mathcal{C}((0,T);H_0^1(\Omega))$ is bounded, see [12]. Let $z_h = z(Q^*+h)$ and $\varphi = z_h - z^*$, then φ verifies

$$
\begin{cases}
\dfrac{\partial \varphi(x,t)}{\partial t} = -\Delta^2 \varphi + Q^*(x,t)\nabla\varphi(x,t) + h(x,t)\nabla z_h, & \Theta, \\
\varphi(x,0) = \varphi_0(x) = 0, & \Omega, \\
\varphi = \dfrac{\partial \varphi}{\partial \nu} = 0, & \Sigma.
\end{cases}
\tag{8}
$$

Thus

$$
||\varphi||_{L^\infty([0,T];H_0^1(\Omega))} \le k_4 ||h||_{L^2(0,T;L^2(\Omega))}.
$$

Put $\phi = \varphi - \psi$ which verifies the system

$$
\begin{cases}
\dfrac{\partial \phi}{\partial t} = -\Delta^2 \phi + Q^*(x,t)\nabla\phi(x,t) + h(x,t)\nabla\varphi, & \Theta, \\
\phi(x,0) = 0, & \Omega, \\
\phi = \dfrac{\partial \phi}{\partial \nu} = 0, & \Sigma.
\end{cases}
\tag{9}
$$

$\phi \in \mathcal{C}(0,T;H_0^1(\Omega))$, and we have

$$
||\phi||_{\mathcal{C}([0,T];H_0^1(\Omega))} \le k ||h||^2_{L^2(0,T;L^2(\Omega))}.
$$

Consequently,

$$
||z(Q^*+h) - z(Q^*) - d(z(Q^*))h||_{\mathcal{C}(0,T;H_0^1(\Omega))} = ||\phi||_{\mathcal{C}([0,T];H_0^1(\Omega))} \le k ||h||^2_{L^2(0,T;L^2(\Omega))}.
$$

Next, we consider the family of optimality systems

$$
\begin{cases}
-\dfrac{\partial p_i}{\partial t} = -\Delta^2 p_i - Q_\varepsilon^*(x,t)\nabla p_i + (\dfrac{\partial z}{\partial x_i} - z_i^d), & \Theta, \\
p_i(x,T) = 0, & \Omega, \\
p_i = \dfrac{\partial p_i}{\partial \nu} = 0, & \Sigma.
\end{cases}
\tag{10}
$$

The next result gives the differential of $J_\varepsilon(Q)$.

Lemma 3.2 *For $Q_\varepsilon \in L^2(0,T;L^2(\Omega))$, which is the solution of the problem (2), we have*

$$
\lim_{\beta \longrightarrow 0} \frac{J_\varepsilon(Q_\varepsilon + \beta h) - J_\varepsilon(Q_\varepsilon)}{\beta} = \sum_{i=1}^n \int_\Omega \int_0^T \frac{\partial \psi(x,t)}{\partial x_i}(\frac{\partial z}{\partial x_i} - z_i^d)dtdx
$$
$$
+ \varepsilon \int_\Omega \int_0^T hQ_\varepsilon dtdx.
\tag{11}
$$

Proof. The functional $J_\varepsilon(Q_\varepsilon)$ from (3) can be written in the following form

$$
J_\varepsilon(Q_\varepsilon) = \frac{1}{2}\sum_{i=1}^n \int_\Omega \int_0^T (\frac{\partial z}{\partial x_i} - z_i^d)^2 dtdx + \frac{\varepsilon}{2}\int_\Omega \int_0^T Q_\varepsilon^2(t)dtdx.
\tag{12}
$$

Let $z_\beta = z(Q_\varepsilon + \beta h)$ and $z = z(Q_\varepsilon)$, from (12) we deduce

$$
\lim_{\beta \longrightarrow 0}\frac{J_\varepsilon(Q_\varepsilon + \beta h) - J_\varepsilon(Q_\varepsilon)}{\beta} = \lim_{\beta \longrightarrow 0}\sum_{i=1}^n \frac{1}{2}\int_\Omega \int_0^T \frac{(\frac{\partial z_\beta}{\partial x_i} - z_i^d)^2 - (\frac{\partial z}{\partial x_i} - z_i^d)^2}{\beta}dtdx
$$
$$
+ \lim_{\beta \longrightarrow 0}\frac{\varepsilon}{2}\int_\Omega \int_0^T \frac{(Q_\varepsilon + \beta h)^2 - Q_\varepsilon^2}{\beta}(t)dtdx.
\tag{13}
$$

Thus

$$
\lim_{\beta \longrightarrow 0}\frac{J_\varepsilon(Q_\varepsilon + \beta h) - J_\varepsilon(Q_\varepsilon)}{\beta}
$$
$$
= \lim_{\beta \longrightarrow 0}\sum_{i=1}^n \frac{1}{2}\int_\Omega \int_0^T \frac{(\frac{\partial z_\beta}{\partial x_i} - \frac{\partial z}{\partial x_i})}{\beta}(\frac{\partial z_\beta}{\partial x_i} + \frac{\partial z}{\partial x_i} - 2z_i^d)dtdx
$$
$$
+ \lim_{\beta \longrightarrow 0}\int_\Omega \int_0^T (\varepsilon h Q_\varepsilon + \beta\varepsilon h^2)dtdx
$$
$$
= \sum_{i=1}^n \int_\Omega \int_0^T \frac{\partial \psi(x,t)}{\partial x_i}(\frac{\partial z(x,t)}{\partial x_i} - z_i^d)dtdx + \int_\Omega \int_0^T \varepsilon h Q_\varepsilon dtdx.
\tag{14}
$$

We characterize the solution of (2) by the following theorem.

Theorem 3.2 *If $Q_\varepsilon \in L^2(0,T;L^2(\Omega))$ and $z_\varepsilon = z(Q_\varepsilon)$ is the output of (1), then*

$$
Q_\varepsilon(t) = \frac{-1}{\varepsilon}(\nabla z^*(x,t))(Div(p))
\tag{15}
$$

is the solution of (2), where $p = (p_1....p_n)$ and $p_i \in C([0,T];H_0^1(\Omega))$ is the unique solution of (10).

Proof. Let $h \in L^\infty(0,T;L^2(\Omega))$ and $Q_\varepsilon + \beta h \in L^2(0,T;L^2(\Omega))$ for $\beta > 0$. The extremal of J_ε is achieved at Q_ε, then

$$0 \leq \lim_{\beta \longrightarrow 0} \frac{J_\varepsilon(Q_\varepsilon + \beta h) - J_\varepsilon(Q_\varepsilon)}{\beta}. \tag{16}$$

From Lemma (3.2), we deduce

$$
\begin{aligned}
0 &\leq \lim_{\beta \longrightarrow 0} \frac{Q_\varepsilon(u_\varepsilon + \beta h) - Q_\varepsilon(u_\varepsilon)}{\beta} \\
&= \sum_{i=1}^{n} \int_\Omega \int_0^T \frac{\partial \psi(x,t)}{\partial x_i}(\frac{\partial z(x,t)}{\partial x_i} - z_i^d)dtdx + \int_\Omega \int_0^T \varepsilon h Q_\varepsilon dtdx,
\end{aligned}
\tag{17}
$$

and using the system (10), we have

$$
\begin{aligned}
0 &\leq \sum_{i=1}^{n} \int_\Omega \int_0^T \frac{\partial \psi(x,t)}{\partial x_i}(-\frac{\partial p_i(x,t)}{\partial t} \\
&+ \Delta^2 p_i(x,t) + Q_\varepsilon^*(x,t)\nabla p_i(x,t))dtdx + \int_\Omega \int_0^T \varepsilon h Q_\varepsilon dtdx \\
&= \sum_{i=1}^{n} \int_\Omega \int_0^T \frac{\partial}{\partial x_i}(\frac{\partial \psi}{\partial t} + \Delta^2 \psi - Q_\varepsilon^*(x,t)\nabla \psi)p_i(x,t)dtdx + \int_\Omega \int_0^T \varepsilon h Q_\varepsilon dtdx \\
&= \sum_{i=1}^{n} \int_\Omega \int_0^T \frac{\partial}{\partial x_i}(h(x,t)\nabla z)p_i dtdx + \int_\Omega \int_0^T \varepsilon h Q_\varepsilon dtdx \\
&= \int_\Omega \int_0^T h(x,t)[\nabla z(\sum_{i=1}^{n} \frac{\partial p_i(x,t)}{\partial x_i}) + \varepsilon Q_\varepsilon dtdx].
\end{aligned}
\tag{18}
$$

For h = h(t), an arbitrary control with $Q_\varepsilon + \beta h \in L^2(0,T;L^2(\Omega))$, and all small β, we deduce

$$Q_\varepsilon(t) = \frac{-1}{\varepsilon}(\nabla z)(\sum_{i=1}^{n} \frac{\partial p_i}{\partial x_i}) = \frac{-1}{\varepsilon}(\nabla z)(Div(p)). \tag{19}$$

4 Regional Gradient Optimal Control Problem

For $\omega \in \Omega$, we define the restriction operator to ω by

$$
\begin{aligned}
\chi_\omega : (L^2(\Omega))^n &\longrightarrow (L^2(\omega))^n \\
z &\longrightarrow \chi_\omega z = z|_\omega.
\end{aligned}
$$

The adjoint of χ_ω is defined by

$$\chi_\omega^* z = \begin{cases} z \ in \ \Omega, \\ 0 \in \Omega \setminus \omega, \end{cases}$$

and

$$
\begin{aligned}
\widetilde{\chi}_\omega : (L^2(\Omega)) &\longrightarrow (L^2(\omega)) \\
z &\longrightarrow \widetilde{\chi}_\omega z = z|_\omega.
\end{aligned}
$$

Definition 4.1 A system state is said to be weakly partial gradient controllable on $\omega \subset \Omega$ if for $\forall \; \varepsilon > 0$, we can find a control $Q \in L^2(0, T; L^2(\Omega))$ such that

$$\|\chi_\omega \nabla z_Q(T) - z^d\|_{(L^2(\omega))^n} \leq \varepsilon,$$

where $z^d = (z_1^d, ..., z_n^d)$ is the desired gradient in $(L^2(\omega))^n$.

Let us consider the partial gradient control problem

$$\min_{Q \; \in L^2(0, T; L^2(\Omega))} J_\varepsilon(Q), \tag{20}$$

where the regional gradient quadratic cost J_ε is defined by

$$
\begin{aligned}
J_\varepsilon(Q) &= \frac{1}{2} \left\| \chi_\omega \nabla z(T) - z^d \right\|_{(L^2(\omega))^n}^2 + \frac{\varepsilon}{2} \int_\Theta \left\| Q(x, t) \right\|_{\mathbb{R}^n}^2 dx dt \\
&= \frac{1}{2} \sum_{i=1}^{n} \left\| \widetilde{\chi}_\omega \frac{\partial z(T)}{\partial x_i} - z_i^d \right\|_{(L^2(\omega))}^2 + \frac{\varepsilon}{2} \int_\Theta \left\| Q(x, t) \right\|_{\mathbb{R}^n}^2 dx dt.
\end{aligned}
\tag{21}
$$

Next, we consider the family of optimality systems

$$
\begin{cases}
-\dfrac{\partial p_i}{\partial t} = -\Delta^2 p_i - Q_\varepsilon^*(x, t) \nabla p_i, & \Theta, \\[2mm]
p_i(x, T) = \left(\dfrac{\partial z(T)}{\partial x_i} - \widetilde{\chi}_\omega^* z_i^d \right), & \Omega, \\[2mm]
p_i(x, t) = \dfrac{\partial p_i(x, t)}{\partial \nu} = 0, & \Sigma.
\end{cases}
\tag{22}
$$

Lemma 4.1 *If $Q_\varepsilon \in L^2(0, T; L^2(\Omega))$ is the optimal control solution of (20), p_i is the solution of (22), and ψ is the solution of (7), we have*

$$
\begin{aligned}
&\lim_{\beta \longrightarrow 0} \frac{J_\varepsilon(Q_\varepsilon + \beta h) - J_\varepsilon(Q_\varepsilon)}{\beta} \\
&= \sum_{i=1}^{n} \int_\Omega \widetilde{\chi}_\omega^* \widetilde{\chi}_\omega \left[\int_0^T \frac{\partial p_i}{\partial t} \frac{\partial \psi(x, t)}{\partial x_i} dt + \int_0^T p_i \frac{\partial}{\partial x_i} \left(\frac{\partial \psi}{\partial t} \right) dt \right] dx \\
&+ \int_\Omega \int_0^T \varepsilon h Q_\varepsilon dt dx.
\end{aligned}
\tag{23}
$$

Proof. The quadratic cost $J_\varepsilon(Q_\varepsilon)$ defined by (3), can be written in the following form:

$$
J_\varepsilon(Q_\varepsilon) = \frac{1}{2} \sum_{i=1}^{n} \int_\omega \left(\widetilde{\chi}_\omega \frac{\partial z}{\partial x_i} - z_i^d \right)^2 dx + \frac{\varepsilon}{2} \int_\Omega \int_0^T Q_\varepsilon^2(t) dt dx. \tag{24}
$$

Let $z_\beta = z(Q_\varepsilon + \beta h)$ and $z = z(Q_\varepsilon)$, using (24), we have

$$
\begin{aligned}
\lim_{\beta \longrightarrow 0} \frac{J_\varepsilon(Q_\varepsilon + \beta h) - J_\varepsilon(Q_\varepsilon)}{\beta} &= \lim_{\beta \longrightarrow 0} \sum_{i=1}^{n} \frac{1}{2} \int_\omega \frac{\left(\widetilde{\chi}_\omega \frac{\partial z_\beta}{\partial x_i} - z_i^d \right)^2 - \left(\widetilde{\chi}_\omega \frac{\partial z}{\partial x_i} - z_i^d \right)^2}{\beta} dx \\
&+ \lim_{\beta \longrightarrow 0} \frac{\varepsilon}{2} \int_\Omega \int_0^T \frac{(Q_\varepsilon + \beta h)^2 - Q_\varepsilon^2}{\beta} dt dx.
\end{aligned}
\tag{25}
$$

Consequently,

$$
\lim_{\beta \longrightarrow 0} \frac{J_\varepsilon(Q_\varepsilon + \beta h) - J_\varepsilon(Q_\varepsilon)}{\beta}
$$

$$
= \lim_{\beta \longrightarrow 0} \sum_{i=1}^{n} \frac{1}{2} \int_\omega \widetilde{\chi}_\omega \frac{(\frac{\partial z_\beta}{\partial x_i} - \frac{\partial z}{\partial x_i})}{\beta} (\widetilde{\chi}_\omega \frac{\partial z_\beta}{\partial x_i} + \widetilde{\chi}_\omega \frac{\partial z}{\partial x_i} - 2z_i^d) dx
$$

$$
+ \frac{1}{2} \int_\Omega \int_0^T (2\varepsilon h Q_\varepsilon + \beta \varepsilon h^2) dt dx \tag{26}
$$

$$
= \sum_{i=1}^{n} \int_\omega \widetilde{\chi}_\omega \frac{\partial \psi(x,T)}{\partial x_i} \widetilde{\chi}_\omega (\frac{\partial z(x,T)}{\partial x_i} - \widetilde{\chi}_\omega^* z_i^d) dx + \int_\Omega \int_0^T \varepsilon h Q_\varepsilon dt dx
$$

$$
= \sum_{i=1}^{n} \int_\omega \widetilde{\chi}_\omega \frac{\partial \psi(x,T)}{\partial x_i} \widetilde{\chi}_\omega p_i(x,T) dx + \varepsilon \int_\Omega \int_0^T h Q_\varepsilon dt dx.
$$

From (10) and (26), we deduce that

$$
\lim_{\beta \longrightarrow 0} \frac{J_\varepsilon(Q_\varepsilon + \beta h) - J_\varepsilon(Q_\varepsilon)}{\beta}
$$

$$
= \sum_{i=1}^{n} \int_\Omega \widetilde{\chi}_\omega^* \widetilde{\chi}_\omega \left[\int_0^T \frac{\partial p_i}{\partial t} \frac{\partial \psi(x,t)}{\partial x_i} dt + \int_0^T p_i \frac{\partial}{\partial x_i} (\frac{\partial \psi}{\partial t}) dt \right] dx \tag{27}
$$

$$
+ \int_\Omega \int_0^T \varepsilon h Q_\varepsilon dt dx.
$$

Theorem 4.1 *Let $Q_\varepsilon \in L^2(0,T;L^2(\Omega))$ and $z_\varepsilon = z(Q_\varepsilon)$ be the associated state solution of (1), we have*

$$
Q_\varepsilon(t) = \frac{-1}{\varepsilon} \sum_{i=1}^{n} \widetilde{\chi}_\omega \frac{\partial z(x,t)}{\partial x_i} \widetilde{\chi}_\omega p_i(t) \tag{28}
$$

is a solution of the problem (20).

Proof. Choose $h \in L^\infty(0,T,L^2(\Omega))$ with $Q_\varepsilon + \beta h \in L^2(0,T;L^2(\Omega))$ for $\beta > 0$. The critical point of J_ε is Q_ε, we have

$$
0 \leq \lim_{\beta \longrightarrow 0} \frac{J_\varepsilon(Q_\varepsilon + \beta h) - J_\varepsilon(Q_\varepsilon)}{\beta}. \tag{29}
$$

Using Lemma (4.1) and replacing $\dfrac{\partial \psi}{\partial t}$ in the system (7), we have

$$
\begin{aligned}
0 \;\le\; & \lim_{\beta \longrightarrow 0} \frac{Q_\varepsilon(z_\varepsilon + \beta h) - Q_\varepsilon(z_\varepsilon)}{\beta} \\
= \;& \sum_{i=1}^{n} \int_\Omega \widetilde{\chi}_\omega^* \widetilde{\chi}_\omega \left[\int_0^T \frac{\partial \psi}{\partial x_i}\frac{\partial p_i}{\partial t} dt \right] dx \\
+ \;& \sum_{i=1}^{n} \int_\Omega \widetilde{\chi}_\omega^* \widetilde{\chi}_\omega \left[\int_0^T \left(-\Delta^2 \frac{\partial \psi}{\partial x_i} + Q_\varepsilon(t)\nabla \frac{\partial \psi}{\partial x_i} + \frac{\partial}{\partial x_i}(h(t)\nabla z))p_i dt \right] dx \\
+ \;& \int_\Omega \int_0^T \varepsilon h Q_\varepsilon dt dx.
\end{aligned}
\tag{30}
$$

Using (22), we obtain

$$
\begin{aligned}
0 \;\le\; & \sum_{i=1}^{n} \int_\Omega \widetilde{\chi}_\omega^* \widetilde{\chi}_\omega \left[\int_0^T \frac{\partial \psi}{\partial x_i}(\frac{\partial p_i}{\partial t} - \Delta^2 p_i - Q(t)\nabla p_i)dt + \frac{\partial}{\partial x_i}(h(t)\nabla z)p_i dt \right] dx \\
+ \;& \int_\Omega \int_0^T \varepsilon h Q_\varepsilon dt dx. \\
= \;& \sum_{i=1}^{n} \int_\Omega \widetilde{\chi}_\omega^* \widetilde{\chi}_\omega \int_0^T (h(t)\nabla z)\frac{\partial p_i}{\partial x_i} dt dt + \int_\Omega \int_0^T \varepsilon h Q_\varepsilon dt dx \\
= \;& \int_\Omega \int_0^T h(t) \left[\nabla z \widetilde{\chi}_\omega^* \widetilde{\chi}_\omega \sum_{i=1}^{n} \frac{\partial p_i}{\partial x_i} + \varepsilon h Q_\varepsilon \right] dt dx.
\end{aligned}
\tag{31}
$$

We deduce the characterization

$$
Q_\varepsilon(t) = \frac{-1}{\varepsilon}(\widetilde{\chi}_\omega \nabla z)(\widetilde{\chi}_\omega Div(p)).
\tag{32}
$$

5 Numerical Approach

We choose the following one dimensional equation:

$$
\begin{cases}
\dfrac{\partial z}{\partial t} + \dfrac{\partial^2 z}{\partial x^2} = Q(t)\dfrac{\partial z}{\partial x}, & [0,1], \\
z(x,0) = z_0(x), & [0,1], \\
z = 0, & \text{at } x = 0,1.
\end{cases}
\tag{33}
$$

Such transport equation may describe the concentration of a contaminant in a convective-diffusive problem, see [6]. The optimal control Q_n is calculated by choosing $\varepsilon = \dfrac{1}{n}$ and

$$
\begin{cases}
Q_{n+1}(t) = -n(\widetilde{\chi}_\omega \nabla z_n)(\widetilde{\chi}_\omega Div(p_n)), \\
Q_0 = 0,
\end{cases}
\tag{34}
$$

where p_n is the output of

$$\begin{cases} \dfrac{\partial p_n(x,t)}{\partial t} = \dfrac{\partial^2 p_n(x,t)}{\partial x^2} + Q_n(t)\dfrac{\partial p_n}{\partial x}(x,t), & [0,1], \\ p_n(x,T) = (\dfrac{\partial z_Q(T)}{\partial x} - \widetilde{\chi}_\omega^* z^d(x)), & [0,1], \\ p = 0, \text{ at } x = 0,1. \end{cases} \tag{35}$$

The optimal control (34) is a bounded sequence deduced from Theorem 4.1, which allows us to establish the following algorithm:

Step 1 : Initializing of the considered problem

　Time T.
　Desired function z^d.
　Error ε.
　Subregion ω.

Step 2 : While $\parallel Q_{n+1} - Q_n \parallel \leq \varepsilon$

　Find z_n and $\dfrac{\partial z_n}{\partial x}(T)$ solution of (33).
　Find $p_n(t)$ solution of (35).
　Find the control Q_{n+1} by (34).

Step 3 : The solution of the problem (20) is Q_n verifying $\parallel Q_{n+1} - Q_n \parallel \leq \varepsilon$.

6　Open Problems

The coupled systems are a very important class of bilinear systems. One of the important applications of such systems are the predator-prey models, which are a couple of nonlinear differential equations used to describe the interaction between two species, one as a predator and the other as a prey. Consider the following important regional control problem of the predator-prey system:

$$\min_{Q \in L^2(0,T;L^2(\Omega))} J_\varepsilon(Q). \tag{36}$$

The cost J_ε is defined for $\varepsilon > 0$ by

$$J_\varepsilon(Q) \;=\; \frac{1}{2}\left\|\widetilde{\chi}_\omega y(T) - \widetilde{\chi}_\omega z(T)\right\|^2_{L^2(\omega)} + \frac{\varepsilon}{2}\left\|Q(x,t)\right\|^2_{L^2(0,T;L^2(\Omega))} \tag{37}$$

and constrained by the model

$$\begin{cases} \dfrac{\partial y}{\partial t} = \Delta^2 y - Q(x,t)\dfrac{\partial z}{\partial x}, & \Theta, \\ \dfrac{\partial z}{\partial t} = \Delta^2 z - Q(x,t)\dfrac{\partial y}{\partial x}, & \Theta, \\ y(x,0) = y_0(x), z(x,0) = z_0(x), & \Omega. \\ y = z = 0, & \Sigma. \end{cases} \tag{38}$$

This important problem of regional optimal control is still under consideration.

7 Conclusion

This work proposes a solution for the gradient optimal control problem governed by an infinite dimensional bilinear system. The approach gives a respond to many open nonlinear problems, for example, the control problems governed by bilinear coupled systems.

References

[1] S. A. Alharbi, A. S. Rambely and A. O. Almatroud. Dynamic Modelling of Boosting the Immune System and Its Functions by Vitamins intervention. *Nonlinear Dynamics and Systems Theory* **19** (2) (2019) 263–273.

[2] J. Ball, J.E. Marsden, and M. Slemrod. Controllability for Distributed Bilinear systems. *SIAM J. on Control and Opt.* **40** (1982) 575–597.

[3] S. Bichiou, M.K. Bouafoura and N. B. Braiek. A Piecewise Orthogonal Functions-Based Approach for Minimum Time Control of Dynamical Systems. *Nonlinear Dynamics and Systems Theory* **19** (2019) 274–288.

[4] M. E. Bradly, S. Lenhart and J. Yong. Bilinear Optimal control of the Velocity term in a Kirchhoff plate equation *J. of Mathematical Analysis and Applications* **238** (1999) 451–467.

[5] A. El Jai, A.J. Pritchard, M. C. Simon and E. Zerrik. Regional controllability of distributed systems. *International Journal of Control* **62** (1995) 1351–1365.

[6] S. Lenhart. Optimal control of a convective-diffusive fluid problem. *Math. Models Method Appl. Sci.* **5** (1995) 225–237.

[7] S.A. Ould Beinane, A. Kamal and A. Boutoulout. Regional Gradient controllability of semilinear parabolic systems. *International Review of Automatic Control (I.RE.A.CO)* **6** (2013) 641–653.

[8] M. Ould Sidi. Variational necessary conditions for optimal control problems. *Journal of Mathematics and Computer Science* **21**(3) (2020) 186–191.

[9] A. Pazy. *Semigroups of Linear Operators and Applications to Partial Differential Equations.* Springer-Verlag, New-York, 1983.

[10] E. Zerrik and M. Ould Sidi. Regional controllability of linear and semi linear hyperbolic systems. *Int. Journal of Math. Analysis* **4** (2010) 2167–2198.

[11] E. Zerrik and M. Ould Sidi. An output controllability of bilinear distributed system. *International Review of Automatic Control* **3** (2010) 466–473.

[12] E. Zerrik and M. Ould Sidi. Regional Controllability for Infinite Dimensional Distributed Bilinear Systems. *Int. Journal of control* **84** (2011) 2108–2116.

[13] E. Zerrik and M. Ould Sidi. Constrained regional control problem for distributed bilinear systems. *IET Cont. Theory. Appl.* **7** (2013) 1914–1921.

[14] R. Zine and M. Ould Sidi. Regional optimal control problem with minimum energy for a class of bilinear distributed systems. *IMA J. Math. Control Info.* **35** (2018) 1187–1199.

[15] R. Zine and M. Ould Sidi. Regional optimal control problem governed by distributed bilinear hyperbolic systems. *International Journal of Control, Automation and Systems* **16** (2018) 1060–1069.

[16] R. Zine. Optimal control for a class of bilinear hyperbolic distributed systems. *Far East Journal of Mathematical Sciences* **102** (2017) 1761–1775.

Absolutely Unstable Differential Equations with Aftereffect

V.Yu. Slyusarchuk[*]

Department of Mathematics, National University of Water and Environmental Engineering, 11, Soborna Str., Rivne, 33028, Ukraine

Abstract: For differential equations with a finite number of delays in a finite-dimensional Banach space, the conditions for the instability of the zero solution are obtained at arbitrary constant delays.

Keywords: *differential-difference equations; absolutely unstable solutions; estimates of the spectra of operator functions.*

Mathematics Subject Classification (2010): 34K06, 34K20, 34K40, 47A10.

1 Introduction

A significant part of publications on the theory of oscillations deal with the stability of solutions of evolution equations (see [1]– [5]) and, in particular, the absolute stability of solutions of differential-difference equations (see [6], [7]– [11]). However, for such equations the instability of solutions is no less important. For example, stable evolutionary processes occurring in complex dynamic systems are possible due to the instability of some components of these systems [12]. The coexistence of stability and instability in nonlinear dynamical systems is their characteristic property.

It is natural to pay attention to the study of the absolute instability of solutions of differential equations with aftereffect. For the study of such equations see [10], [13]– [15].

In [13], sufficient conditions are obtained for the absolute instability of the zero solution of a nonlinear differential-difference equation

$$\frac{dx(t)}{dt} = Ax(t) + G(t, x(t - \Delta))$$

---

[*] Corresponding author: `mailto:V.E.Slyusarchuk@gmail.com`

in a Banach space using the essentially approximative spectrum of the operator A. In [10] and [14], necessary and sufficient conditions for the absolute instability of zero solutions to linear scalar differential-difference equations of delay and neutral types and sufficient conditions for absolute instability of solutions to systems of linear differential-difference equations of delay type are obtained. In [15], necessary and sufficient conditions are established for the absolute instability of zero solutions of linear differential-difference equations with self-adjoint operator coefficients and an infinite number of deviations of the argument.

Examples of absolutely stable and absolutely unstable systems are given in [8] and [10].

Let E be a finite-dimensional Banach space over a field $\mathbb{C}$ with a norm $\| \cdot \|_E$ and $L(E, E)$ be a Banach algebra of linear continuous operators $A : E \to E$ with a unit operator I and a norm $\|A\|_{L(E,E)} = \sup_{\|x\|_E=1} \|Ax\|_E$.

Consider the equations

$$\frac{dx(t)}{dt} = A_0 x(t) + \sum_{k=1}^{n} A_k x(t - \Delta_k), \quad t \geq 0, \tag{1}$$

and

$$\frac{dx(t)}{dt} = A_0 x(t) + \sum_{k=1}^{n} A_k x(t - \Delta_k) + F(t, x(t), x(t - \Delta_1), \ldots, x(t - \Delta_n)), \quad t \geq 0, \tag{2}$$

where $n \in \mathbb{N}$, $A_0, A_1, \ldots A_n$ are the elements of the algebra $L(E, E)$, $\Delta_1, \ldots, \Delta_n$ are non-negative numbers, and $F : [0, +\infty) \times E^{n+1} \to E$ is a continuous mapping for which $F(t, 0, 0, \ldots, 0) = 0$ for all $t \geq 0$.

The purpose of this paper is to find the conditions for the instability of zero solutions of equations (1) and (2) for arbitrary $\Delta_1 \geq 0, \ldots, \Delta_n \geq 0$. In this case, the zero solutions of equations (1) and (2) will be called absolutely unstable.

2 Preliminaries

We will use the following sets:

$$\mathbb{C}_+ = \{z \in \mathbb{C} : \operatorname{Re} z > 0\},$$

$$\mathbb{C}_- = \{z \in \mathbb{C} : \operatorname{Re} z < 0\},$$

$$\mathbb{C}_0 = \{z \in \mathbb{C} : \operatorname{Re} z = 0\},$$

$$\mathbb{C}_\gamma = \{z \in \mathbb{C} : \operatorname{Re} z = \gamma\},$$

$$\mathbb{C}_{(\gamma_1, \gamma_2)} = \{z \in \mathbb{C} : \operatorname{Re} z \in (\gamma_1, \gamma_2)\},$$

$$\mathbb{C}_{[\gamma_1, \gamma_2]} = \{z \in \mathbb{C} : \operatorname{Re} z \in [\gamma_1, \gamma_2]\},$$

$$i\mathbb{C}_+ = \{iz : z \in \mathbb{C}_+\},$$

$$-i\mathbb{C}_+ = \{-iz : z \in \mathbb{C}_+\},$$

$$K^n = \{z = (z_1, \ldots, z_n) \in \mathbb{C}^n : |z_l| \leq 1, l = \overline{1, n}\}$$

and

$$T^n = \{z = (z_1, \ldots, z_n) \in \mathbb{C}^n : |z_l| = 1, l = \overline{1, n}\}.$$

where $\operatorname{Re} z$ is the real part of the number $z \in \mathbb{C}$, i is the imaginary unit, $\gamma, \gamma_1, \gamma_2 \in \mathbb{R}$ and $\gamma_1 < \gamma_2$.

We denote by $\sigma(A)$ the spectrum of the operator $A \in L(E, E)$, and by $\operatorname{co} G$, $\operatorname{int} G$ and $\partial\, G$ the convex hull, the interior, and the boundary of the set G, respectively.

In the sequel the following two theorems on the properties of the spectrum of values of operator functions are of importance as well as the theorem on the instability of the zero solution of equation (2) in the first approximation.

Theorem 2.1 *Let a function $X(z) = X(z_1, \ldots, z_n)$ with values in $L(E, E)$ be continuous with respect to $z = (z_1, \ldots, z_n)$ on $\Omega = \Omega_1 \times, \ldots, \times \Omega_n$, where $\Omega_1, \ldots, \Omega_n$ are bounded closed subsets of the set $\mathbb{C}$, and holomorphic for each variable z_k on $\operatorname{int} \Omega_k$, $i = \overline{1, n}$, for arbitrary $z_l \in \Omega_l$, $l \in \{1, \ldots, n\} \setminus \{k\}$.*
Then, $\operatorname{co} \bigcup_{z \in \Omega} \sigma(X(z)) = \operatorname{co} \bigcup_{z \in Q} \sigma(X(z))$, where $Q = \partial\, \Omega_1 \times, \ldots, \times \partial\, \Omega_n$.

Note that the statement of Theorem 2.1 is correct if the Banach algebra $L(E, E)$ is replaced by an arbitrary Banach algebra with unit [16]. This statement is a generalization of the maximum principle of module [17].

Theorem 2.2 *Let the following conditions be satisfied:*
(1) $Y(z)$ is a continuous function on $\mathbb{C}_{[\gamma_1, \gamma_2]}$ with values in $L(E, E)$;
(2) $\sigma(Y(z)) \subset \mathbb{C}_+$ for all $z \in \mathbb{C}_{\gamma_1}$;
(3) $\sigma(Y(z)) \subset \mathbb{C}_-$ for all $z \in \mathbb{C}_{\gamma_2}$;
(4) for the set

$$N(y) = \{x + yi : x \in (\gamma_1, \gamma_2),\ \sigma(Y(x + yi)) \cap \mathbb{C}_0 \neq \emptyset\}, \quad y \in \mathbb{R}, \tag{3}$$

the relations

$$N(y_1) \subset i\mathbb{C}_+ \tag{4}$$

and

$$N(y_2) \subset -i\mathbb{C}_+ \tag{5}$$

are satisfied for some numbers $y_1 > 0$ and $y_2 < 0$.
Then there is a point $z_0 \in \mathbb{C}_{(\gamma_1, \gamma_2)}$ for which $0 \in \sigma(Y(z_0))$.

Proof. The spectrum $\sigma(Y(z))$ will be considered as a function defined on the set $\mathbb{C}_{[\gamma_1, \gamma_2]}$ with values in the set of non-empty compact subsets of the set $\mathbb{C}_{[\gamma_1, \gamma_2]}$ using the Hausdorff distance between two sets [18]. By virtue of the first condition of the theorem and the finite dimension of the space E, this function is continuous on the set $\mathbb{C}_{[\gamma_1, \gamma_2]}$ [19]. Also, this function is bounded and uniformly continuous on each compact subset of $\mathbb{C}_{[\gamma_1, \gamma_2]}$. Therefore, by the second and third conditions of the theorem, the set $N(y)$ is a non-empty and compact set for each $y \in \mathbb{R}$.

According to (3), each point $x + yi \in N(y)$ corresponds to a set

$$M(x + yi) \subset \sigma(Y(x + yi)) \cap \mathbb{C}_0$$

containing at least one element. Consider the set

$$N_*(y) = \bigcup_{x + yi \in N(y)} M(x + yi).$$

Due to the uniform continuity of $\sigma(Y(x + yi))$ on

$$\mathbb{C}_{[\gamma_1, \gamma_2]} \cap \{z \in \mathbb{C} : |\operatorname{Im} z| \leq \max\{y_1, |y_2|\}\},$$

the set $N_*(y)$ continuously depends on y on $[y_2, y_1]$. Considering that by virtue of (4) and (5)

$$N_*(y_1) \subset i\mathbb{C}_+$$

and

$$N_*(y_2) \subset -i\mathbb{C}_+,$$

we conclude that $0 \in N_*(y_0)$ for some $y_0 \in (y_2, y_1)$. Then $0 \in \sigma(Y(x_0 + y_0 i))$ for some $x_0 \in (\gamma_1, \gamma_2)$.

Theorem 2.2 is proven. $\square$

It is obvious that Theorem 2.2 is a generalization of the first Bolzano-Cauchy theorem.

Denote by $B[0, r]$ the closed ball $\{x \in E : \|x\|_E \leq r\}$.

Theorem 2.3 *Suppose that*

(1) $\left\{ p \in \mathbb{C}_+ : 0 \in \sigma\left(-pI + A_0 + \sum_{k=1}^{n} e^{-p\Delta_k} A_k \right) \right\} \neq \emptyset$;

(2) there are numbers $r > 0$ and $N > 0$ such that the relation

$$\sup_{t \geq 0} \|F(t, x_1, x_2, \ldots, x_{n+1}) - F(t, y_1, y_2, \ldots, y_{n+1})\|_E \leq N \max_{l=\overline{1,n+1}} \|x_l - y_l\|_E$$

for all $x_l, y_l \in B[0, r]$, $l = \overline{1, n+1}$, is satisfied;

(3) there are numbers $r > 0$, $b > 0$ and $\mu > 0$ such that the relation

$$\sup_{t \geq 0} \|F(t, x_1, x_2, \ldots, x_{n+1})\|_E \leq b \max_{l=\overline{1,n+1}} \|x_l\|_E^{1+\mu},$$

for all $x_l \in B[0, r]$, $l = \overline{1, n+1}$, is satisfied.

Then the zero solution of equation (2) is unstable.

Note that the substantiation of Theorems 2.1 and 2.3 is given in papers [16] and [6], respectively.

3   Main Results

Theorem 3.1 *Suppose that*

$$\bigcup_{z \in T^n} \sigma\left(A_0 + \sum_{l=1}^{n} z_l A_l \right) \subset \mathbb{C}_+. \tag{6}$$

Then the zero solution of equation (1) is absolutely unstable.

Proof. We fix arbitrary $\Delta_1 \geq 0, \ldots, \Delta_n \geq 0$. Consider the characteristic function $\chi : \mathbb{C} \to L(E, E)$, which corresponds to equation (1) and is determined by the equality

$$\chi(p) = -pI + A_0 + \sum_{k=1}^{n} e^{-p\Delta_k} A_k.$$

Theorem 2.2 is applicable to this function in the case of $\gamma_1 = 0$ and $\gamma_2 = 2 \sum_{l=0}^{n} \|A_l\|_{L(E,E)}$. Indeed, the function $\chi(p)$, as defined, is continuous in $\mathbb{C}_{[0,\gamma_2]}$. Because of (6) and Theorem 2.1

$$\bigcup_{z \in K^n} \sigma\Big(A_0 + \sum_{l=1}^{n} z_l A_l\Big) \subset \mathbb{C}_+.$$

Therefore, for all $p \in \mathbb{C}_{[0,\gamma_2]}$

$$\sigma\Big(A_0 + \sum_{k=1}^{n} e^{-p\Delta_k} A_k\Big) \subset \mathbb{C}_+.$$

Consequently, according to the Dunford theorem on the spectrum mapping of the operator, [20] $\sigma(\chi(p)) \subset \mathbb{C}_+$ for all $p \in \mathbb{C}_0$ and $\sigma(\chi(p)) \subset \mathbb{C}_-$ for all $p \in \mathbb{C}_{\gamma_2}$. Also, according to the Dunford theorem, the set $N(y) = \{x + yi : x \in (0, \gamma_2), \ \sigma(\chi(x+yi)) \cap \mathbb{C}_0 \neq \emptyset\}$ for $y_1 = \gamma_2$ and $y_2 = -\gamma_2$ satisfies relations (4) and (5).

Thus, for the function $\chi(p)$, the conditions of Theorem 2.2 are satisfied.

Consequently, by Theorem 2.2, there is a $p_0 \in \mathbb{C}_{(0,\gamma_2)}$ for which $0 \in \sigma(\chi(p_0))$. This means that for some normalized vector $a \in E$, the vector function $x(t) = e^{p_0 t} a$ is a solution of equation (1). By virtue of the linearity of equation (1) for each $\varepsilon > 0$, the function $\varepsilon x(t)$ is also a solution of this equation. Since $\mathrm{Re}\, p_0 > 0$, we have $\lim_{t \to +\infty} \|x(t)\|_E = +\infty$. Therefore, the zero solution of equation (1) is unstable. From the arbitrariness of the choice of $\Delta_1 \geq 0, \ldots, \Delta_n \geq 0$, it follows that the zero solution of equation (1) is absolutely unstable.

Theorem 3.1 is proven. $\square$

Theorem 3.2 *Suppose that*
(1) the relation (6) is satisfied;
(2) the second and third conditions of Theorem 2.3 are satisfied.
Then the zero solution of equation (2) is absolutely unstable.

Proof. Fix arbitrary $\Delta_1 \geq 0, \ldots, \Delta_n \geq 0$. By virtue of the first condition of the theorem and the proof of Theorem 3.1, the first condition of the Theorem 2.3 is satisfied. Therefore, because of Theorem 2.3 and the second condition of Theorem 3.2, the zero solution of equation (2) is unstable. Due to the arbitrariness of the choice of $\Delta_1 \geq 0, \ldots, \Delta_n \geq 0$, this solution is absolutely unstable.

Theorem 3.2 is proven. $\square$

Corollary 3.1 *If $\sigma(A_0) \subset \mathbb{C}_+$ and the value of $\sum_{l=1}^{n} \|A_l\|_{L(E,E)}$ is sufficiently small, then the zero solutions of equations (1) and (2) are absolutely unstable.*

References

[1] Yu. L. Daletsky and M. G. Krein. *Stability of Solutions of Differential Equations in a Banach Space.* Nauka, Moscow, 1970. [Russian]

[2] D. Henry. *Geometric Theory of Semilinear Parabolic Equations.* Springer-Verlag, Berlin-Heidelberg-New York, 1981.

[3] V. Lakshmikantham, S. Leela, and A. A. Martynyuk. *Motion Stability: The Comparison Method.* Naukova dumka, Kiev, 1991. [Russian]

[4] T. A. Lukyanova and A. A. Martynyuk. Stability Analysis of Impulsive Hopfield-Type Neu-
ron System on Time Scale. *Nonlinear Dynamics and Systems Theory* **17** (3) (2017) 315–326.

[5] A. Yu. Aleksandrov, E. B. Aleksandrova, A. V. Platonov, and M. V. Voloshin. On the Global
Asymptotic Stability of a Class of Nonlinear Switched Systems. *Nonlinear Dynamics and
Systems Theory* **17** (2) (2017) 107–120.

[6] V. Yu. Slyusarchuk. *Instability of Solutions to Evolution Equations*. Publishing House of the
National University of Water Management and Environmental Management, Rivne, 2004.
[Ukrainian]

[7] Yu. M. Repin. On stability conditions for systems of linear differential equations for any
delays. *Scientific notes of the Ural University*, Sverdlovsk **23** (1960) 34-41. [Russian]

[8] V. S. Gozdek. On the galloping of landing gear carriages when the aircraft is moving along
an unpaved aerodrome. *Engineering Journal* **4** (1965) 743-745. [Russian]

[9] L. A. Zhivotovsky. Absolute stability of solutions of differential equations with several de-
lays. In: *Proceedings of a seminar on the theory of differential equations with deviating
argument* **23** (1969) 919–928. [Russian]

[10] V. Yu. Slyusarchuk. *Absolute Stability of Dynamical Systems from Aftereffect*. Publishing
House of the Ukrainian State University of Water Management and Environmental Man-
agement, Rivne, 2003. [Ukrainian]

[11] A. M. Kovalev, A. A. Martynyuk, O. A. Boichuk, A. G. Mazko, R. I. Petryshyn, V. Ye.
Slyusarchuk, A. L. Zuyev, and V. I. Slyn'ko. Novel Qualitative Methods of Nonlinear Me-
chanics and their Application to the Analisis of Multifrequency Oscillations, Stability and
Control Problems. *Nonlinear Dynamics and Systems Theory* **9** (2) (2009) 117–145.

[12] D. Ruelle and F. Takens. On the Nature of Turbulence. *Commun. Math. Phys.*, Springer-
Verlag **20** (1971) 167–192.

[13] V. Yu. Slyusarchuk. Sufficient conditions for the absolute instability of solutions of
differential-difference equations in a Banach space. *Investigation of mathematical models*,
Akad. Nauk Ukrainy, Inst. Mat., Kiev, 1997, 216-220. [Ukrainian]

[14] V. Yu. Slyusarchuk. Conditions for the absolute instability of solutions of differential-
difference equations. *Nonlinear Oscil.* **7** (3) (2004) 430–436. [Ukrainian]

[15] V. Yu. Slyusarchuk. Necessary and Sufficient Conditions for the Absolute Instability of So-
lutions of Linear Differential-Difference Equations with Self-Adjoint Operator Coefficients.
Ukrain. Mat. Zh. **70** (5) (2018) 715–724. [Ukrainian]

[16] V. E. Slyusarchuk. Estimates of the spectra and the invertibility of functional operators.
Mat. Sb. **105** (2) (1978) 269–285. [Russian]

[17] A. I. Markushevich. *Short Course of the Theory of Analytic Functions*. Nauka, Moskov,
1966. [Russian]

[18] K. Kuratowski. *Topology*, Vol. I. Mir, Moskov, 1966. [Russian]

[19] T. Kato. *Perturbation Theory for Linear Operators*. Springer-Verlag, Heidelberg-New York,
1966.

[20] N. Danford. Spectral theory I, Convergence to hrojections. *Trans. Amer. Math. Soc.* **54**
(1943) 185–217.

Stability of the Artificial Equilibrium Points in the Low-Thrust Restricted Three-Body Problem when the Bigger Primary is a Source of Radiation

Md. Sanam Suraj [1], Amit Mittal [2] and Krishan Pal [3*]

[1] *Department of Mathematics, Sri Aurobindo College, University of Delhi, New Delhi, India*
[2] *Department of Mathematics, A.R.S.D. College, University of Delhi, New Delhi, India*
[3] *Department of Mathematics, Maharaja Agrasen College, University of Delhi, New Delhi, India*

Abstract: This paper investigates the existence and the stability of artificial equilibrium points (AEPs) in the low-thrust restricted three-body problem when the bigger primary is a source of radiation and the smaller one is a point mass. The linear stability of the AEPs has been studied. Firstly, we have derived the equations of motion of the spacecraft in the synodic coordinate system. The AEPs are obtained by cancelling the gravitational and centrifugal forces with continuous control acceleration at the non-equilibrium points. The positions of these AEPs will depend on the magnitude and directions of low-thrust acceleration. Secondly, we have calculated the numerical values of the AEPs and their movement shown graphically for given thrust parameters. We have found the stability regions in the $x - y$, $x - z$, $y - z$-planes and studied the effect of the radiation pressure on the motion of the spacecraft. Further, we have drawn the zero velocity curves (ZVCs) to determine the possible regions of motion in which the spacecraft is free to move.

Keywords: *restricted three-body problem, artificial equilibrium points, low-thrust, stability, radiation pressure, zero velocity curves.*

Mathematics Subject Classification (2010): 70F07, 70F10, 70F15.

* Corresponding author: mailto:kpal1987@gmail.com

1   Introduction

The restricted three-body problem with many perturbing forces, like oblateness, radiation forces of the primaries, Coriolis and centrifugal forces have been studied by many scientists and researchers. There are five Lagrangian points in the classical restricted three-body problem (R3BP), three of them are on the straight line joining the primaries, called collinear libration points, and two of them set up equilateral triangle with the primaries. Szebehely [1] has investigated the five libration points. The collinear libration points $L_{1,2,3}$ are always unstable in the linear sense for any value of the mass parameter μ, whereas the triangular libration points $L_{4,5}$ are stable if $\mu < \mu_c = 0.03852$. Kunitsyn and Perezhogin [2], Kumar and Choudhry [3], Abouelmagd [4], and Singh and Emmanuel [5] have studied the stability properties of the equilibrium points in the photogravitational R3BP. Zotos [6] has studied numerically the case of the planar circular photogravitational R3BP where the more massive primary is an emitter of radiation. He has found that the radiation pressure factor has a huge impact on the character of orbits. Srivastava et al. [7] have introduced the Kustaanheimo-Stiefel (KS)-transformation to reduce the order of singularities arising due to the motion of an infinitesimal body in the vicinity of the smaller primary in the R3BP when the bigger primary is a source of radiation and the smaller one is an oblate spheroid. They have found that the KS-regularization reduces the order of the pole from five to three at the point of singularity of the governing equations of motion. Correa et al. [8] introduced two models of the restricted three-body and four-body problems. They have investigated the transfer orbits from a parking orbit around the Earth to the halo orbit in both the dynamical models. Also, they have compared the total velocity increment to both the models. Prado [9] has worked on the space trajectories in the circular restricted three-body problem. Further, he assumed that the spacecraft moves under the gravitational forces of two massive bodies which are in circular orbits. He also investigated the orbits which can be used to transfer a spacecraft from one body back to the same body or to transfer a spacecraft from one body to the respective Lagrangian points L_4 and L_5.

The Lagrangian points are only five positions in space where the small object if placed there, would maintain its position relative to the two massive bodied. If, however, the object is equipped with a suitable propulsion system, capable of balancing the gravitational pull of the two massive bodies, other equilibrium points can be generated allowing the third body to be stationary with respect to the first two bodies. According to Dusek [10] these new points are usually known as the Artificial Equilibrium Points(AEPs). Recently, low-thrust propulsion systems such as the solar sail and the electric propulsion systems are being developed not only for controlling satellite orbit, but also as main engines for interplanetary transfer orbits. These low-thrust propulsion systems are able to provide continuous control acceleration to the spacecraft and thus increase mission design flexibility. Describing the locations and investigating the stability conditions of the AEPs have been made by many authors. In particular, Farquhar [11] has studied the concept of telecommunication systems using the Lagrange points and investigated ballistic periodic orbits about these points in the Earth-Moon system. Simmons et al. [12] and Broschart and Scheeres [13] have studied the stability of equilibrium points with continuous control acceleration. Scheeres et al. [14] have analyzed a control law which stabilizes unstable periodic halo orbits about an Earth-Sun libration point with continuous acceleration taking hills problem and discussed applications to the spacecraft formation flight. Thereafter, many authors have been worked on the solar sails, see Morimoto et al. [15, 16], Baig and

McInnes [17], Bombardelli and Pelaez [18]. They have studied the stability of the artificial equilibrium points in the circular restricted three-body problem. Also, they have investigated the equilibrium points for hybrid low-thrust propulsion system. Bu et al. [19] have investigated the positions and dynamical characteristic of the AEPs in a binary asteroid system with continuous low-thrust. They have found the stable regions of the AEPs by a parametric analysis and studied the effect of the mass ratio and ellipsoid parameters on the stable region. Further, they have analyzed the effect of the continuous low-thrust on the feasible region of motion by ZVCs. More recently, Sushil et al. [20] have been studied the existence and stability of equilibrium points in the restricted three-body problem with a geo-centric satellite including the Earth's equatorial ellipticity.

In the present paper, we have studied the effect of radiation pressure of the bigger primary on the motion of the spacecraft. This paper is an extension of the work of Morimoto et al. [15]. This paper is organized as follows. In Section 2, we have derived the equations of motion of the spacecraft. In Section 3, we have found the locations of the AEPs. In Section 4, we have found the stability conditions and stable regions. In Section 5, we have drawn the zero velocity curves. Finally, in Section 6, we have concluded the results obtained.
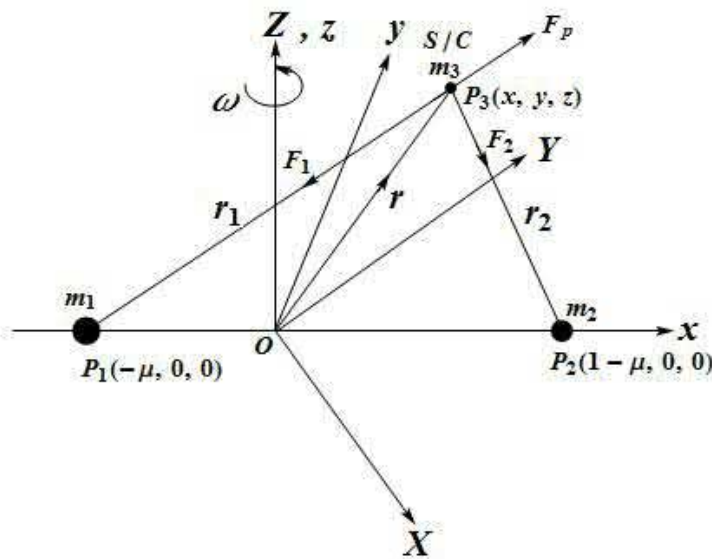
Figure 1: Configuration of the problem.

2   Equation of Motion

Let two celestial bodies of masses m_1 and m_2 $(m_1 > m_2)$ be the primaries moving with angular velocity ω in circular orbits about their center of mass O taken as the origin, and let the infinitesimal body (a spacecraft) of mass m_3 is moving in the plane of motion of m_1 and m_2. The motion of the spacecraft is affected by the motion of m_1 and m_2 but without affecting their motion. In this problem, we assume that the bigger primary is a source of radiation and the smaller one is a point mass. The line joining the primaries

m_1 and m_2 is taken as the X-axis, the line which passes through O and is perpendicular to the X-axis and lying in the plane of motion of m_1 and m_2 is considered as the Y-axis, and the line which passes through the origin and is perpendicular to the plane of motion of the primaries is taken as the Z-axis. We have taken the synodic system of coordinates $O\,(xyz)$, initially coincident with the inertial system of coordinates $O\,(XYZ)$, rotating with the angular velocity ω about the z-axis (the z-axis is coincident with the Z-axis). A complete diagram of the formulated problem is shown in Figure 1. Let the primaries of masses m_1 and m_2 be located at $P_1\,(-\mu,\,0,\,0)$ and $P_2\,(1-\mu,\,0,\,0)$, respectively, and the spacecraft is located at the point $P_3\,(x,\,y,\,z)$ (see Fig. 1). The angular velocity of the primaries is given by the relation $\omega = \sqrt{\frac{G(m_1+m_2)}{l^3}}$, where l is the distance between the primaries, and G is the gravitational constant. We scale the units by taking the sum of the masses and the distance between the primaries both equal to unity. Therefore, $m_1 = 1 - \mu$, $m_2 = \mu$, $\mu = \frac{m_2}{m_1+m_2}$ and $\mu \in (0,\,0.5]$ with $m_1 + m_2 = 1$. The scale of time is chosen so that the gravitational constant is unity and thus, the angular velocity of the primaries is one. The equation of motion of the spacecraft in vector form is expressed as

$$\frac{d^2\mathbf{r}}{dt^2} + 2\boldsymbol{\omega} \times \frac{d\mathbf{r}}{dt} = \boldsymbol{a} - \nabla\Omega = \mathbf{F}, \tag{1}$$

where Ω is the effective potential of the system that combines the gravitational potential and the potential from the centripetal acceleration, and which is given by

$$\Omega = -\frac{n^2}{2}(x^2 + y^2) - \frac{q\,(1-\mu)}{r_1} - \frac{\mu}{r_2},$$

and

$$
\begin{aligned}
\mathbf{F} &= \text{the total force acting on } \quad m_3 \\
&= \mathbf{F_1} + \mathbf{F_2}, \\
\mathbf{F_1} &= \text{the gravitational force exerted on } \quad m_3 \quad \text{due} \\
&\quad \text{to } \quad m_1 \quad \text{along} \quad \mathbf{P_3P_1}, \\
\mathbf{F_2} &= \text{the gravitational force exerted on } \quad m_3 \quad \text{due} \\
&\quad \text{to } \quad m_2 \quad \text{along} \quad \mathbf{P_3P_2}.
\end{aligned}
$$

The vector $\boldsymbol{a} = (a_x,\,a_y,\,a_z)$ is the low-thrust acceleration and $\mathbf{r} = (x,\,y,\,z)^T$ is the position vector of the spacecraft. Thus, the equations of motion of the spacecraft with continuous low-thrust in the dimensionless co-ordinate system can be written as

$$\left.\begin{aligned}
\ddot{x} - 2n\dot{y} &= -\Omega_x + a_x = -\Omega_x^*, \\
\ddot{y} + 2n\dot{x} &= -\Omega_y + a_y = -\Omega_y^*, \\
\ddot{z} &= -\Omega_z + a_z = -\Omega_z^*,
\end{aligned}\right\} \tag{2}$$

where
Ω^* is the potential of the system with continuous low-thrust that can be written as
$\Omega^* = \Omega - \boldsymbol{a}.\mathbf{r} = \Omega - a_x x - a_y y - a_z z,$

$$= -\frac{n^2}{2}(x^2 + y^2) - \frac{q\,(1-\mu)}{r_1} - \frac{\mu}{r_2} - a_x x - a_y y - a_z z,$$

where

$$r_1 = \sqrt{(x+\mu)^2 + y^2 + z^2}, \quad r_2 = \sqrt{(x+\mu-1)^2 + y^2 + z^2},$$

and

$q = 1 - \frac{F_p}{F_g} = 1 - p,$

q=the radiation parameter,

p=the radiation pressure,

F_g= the gravitational attraction force due to the bigger primary m_1,

F_p= the radiation pressure due to bigger primary m_1,

n is the mean motion of the primaries whose value is one in this problem. The magnitude of control acceleration is given by

$a = \sqrt{a_x{}^2 + a_y{}^2 + a_z{}^2}.$

3 The Locations of Artificial Equilibrium Points

The AEPs are the solutions of the equations $\Omega_x^* = 0$, $\Omega_y^* = 0$, $\Omega_z^* = 0$. In order to find the AEPs of the system, take the velocity and acceleration of the system equal to 0, i.e., $\dot{x} = \dot{y} = \dot{z} = 0$, $\ddot{x} = \ddot{y} = \ddot{z} = 0$. The AEPs denoted by (x_0, y_0, z_0) are the solution of the equations given by

$$\left.\begin{aligned}
-x_0 + \frac{q(1-\mu)}{r_1^3}(x_0+\mu) + \frac{\mu}{r_2^3}(x_0 - \mu_1 - 1) - a_x &= 0, \\
-y_0 + \frac{q(1-\mu)}{r_1^3}y_0 + \frac{\mu}{r_2^3}y_0 - a_y &= 0, \\
\frac{q(1-\mu)}{r_1^3}z_0 + \frac{\mu}{r_2^3}z_0 - a_z &= 0.
\end{aligned}\right\} \tag{3}$$

The AEPs which lie on the x-axis are called collinear and are obtained from Eqs. (3) by taking $y = z = 0$. The AEPs which lie in the xy-plane but not on the x-axis are called non-collinear. We have obtained five AEPs denoted by L_1, L_2, L_3, L_4 and L_5 for given parameters. In Tables 1 and 2, we have presented the numerical values of a few AEPs for the fixed values of $\mu = 0.1$, $q = 0.99$ and varying $\boldsymbol{a}$ in the x-direction. From Tables 1 and 2, we have observed that there exist three collinear and two non-collinear AEPs.

The locations of the collinear and non-collinear AEPs are shown in Fig. 2 for the different values of the radiation parameter $q(0 < q < 1)$ and low-thrust acceleration $\boldsymbol{a} = (a_x, 0, 0)$. From Fig. 2 (a), we have observed that when $\boldsymbol{a} = (a_x, 0, 0)$ is increasing, the AEPs L_1, L_2 and L_3 have almost negligible movement, the AEPs L_4 and L_5 move towards the y-axis, and we have noticed that the non-collinear AEPs L_4 and L_5 are symmetric about the x-axis. From Fig. 2 (b), we have observed that when q is increasing, all the AEPs are going away from the primary m_1 and the AEPs L_4 and L_5 are symmetric about the x-axis. We have also observed that the AEPs are the new positions of the equilibrium points with the effect of the continuous low-thrust $\boldsymbol{a}$ and radiation parameter q, these points are different from the natural libration points.

(a)   (b)
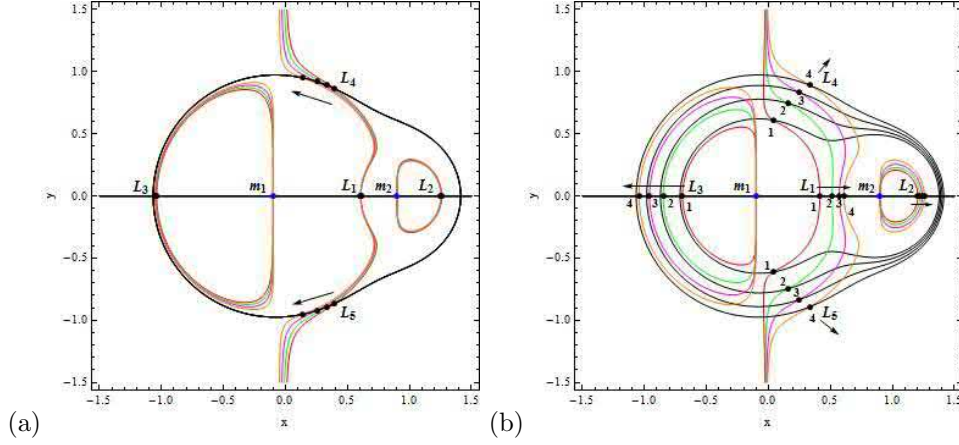
Figure 2: The locations of the five AEPs in the low-thrust R3BP with the effect of radiation pressure for $\mu = 0.1$. (a) For $q = 0.99$ and for $\boldsymbol{a} = (0.0001, 0, 0)\,(black, red)$, $(0.015, 0, 0)\,(black, green)$, $(0.03, 0, 0)\,(black, magenta)$, $(0.045, 0, 0)\,(black, orange)$. (b) For $\boldsymbol{a} = (0.015, 0, 0)$ and for $q = 0.25\,(black, red)$, $0.50\,(black, green)$, $0.75\,(black, magenta)$, $0.99\,(black, orange)$.

$\mu = 0.1$				
$q = 0.99$				
$\boldsymbol{a}$	L_1	L_2	L_3	$L_{4,5}$
$\boldsymbol{a} = 0.0001$	(0.607756, 0)	(1.25887, 0)	(-1.03844, 0)	(0.396291, $\pm$ 0.864259)
$\boldsymbol{a} = 0.0150$	(0.606693, 0)	(1.25643, 0)	(-1.04315, 0)	(0.334002, $\pm$0.891111)
$\boldsymbol{a} = 0.0300$	(0.605617, 0)	(1.25400, 0)	(-1.04793, 0)	(0.251705, $\pm$0.920949)
$\boldsymbol{a} = 0.0450$	(0.604536, 0)	(1.25161, 0)	(-1.05276, 0)	(0.135929, $\pm$0.951772)

Table 1: The AEPs in the xy-plane when $\boldsymbol{a}$ is varying in the x-direction.

$\mu = 0.1$				
$\boldsymbol{a} = 0.015$				
q	L_1	L_2	L_3	$L_{4,5}$
$q = 0.25$	(0.413878, 0)	(1.20345, 0)	(-0.693390, 0)	(0.039034, $\pm$0.610877)
$q = 0.50$	(0.513221, 0)	(1.21998, 0)	(-0.849261, 0)	(0.154312, $\pm$0.747250)
$q = 0.75$	(0.570035, 0)	(1.23791, 0)	(-0.958911, 0)	(0.251001, $\pm$0.832607)
$q = 0.99$	(0.606693, 0)	(1.25643, 0)	(-1.043150, 0)	(0.334002, $\pm$0.891111)

Table 2: The AEPs in the xy-plane when q is varying and $\boldsymbol{a} = (0.015, 0, 0)$.

4   Stability Analysis and Stable Regions

To establish the spacecraft at a non-equilibrium point, a continuous low-thrust is provided to the spacecraft. Now, give the small displacement to (x_0, y_0, z_0) as $x = x_0 + \delta_x$, $y =$

$y_0 + \delta_y$, $z = z_0 + \delta_z$, $(\delta_x, \delta_y, \delta_z << 1)$. Using the above displacements, the linearized equations of motion (according to Morimoto et al. [16]) corresponding to Eqs. (2) are given by

$$
\left.
\begin{aligned}
\ddot{\delta}_x - 2n\dot{\delta}_y &= \Omega^0_{xx}\delta_x + \Omega^0_{xy}\delta_y + \Omega^0_{xz}\delta_z, \\
\ddot{\delta}_y + 2n\dot{\delta}_x &= \Omega^0_{yx}\delta_x + \Omega^0_{yy}\delta_y + \Omega^0_{yz}\delta_z, \\
\ddot{\delta}_z &= \Omega^0_{zx}\delta_x + \Omega^0_{zy}\delta_y + \Omega^0_{zz}\delta_z,
\end{aligned}
\right\}
\tag{4}
$$

where the superscript "0" overhead in Eqs. (4) indicates that the values are to be calculated at the AEP (x_0, y_0, z_0) under consideration. The characteristic root λ satisfies the given characteristic equation

$$
\left.
\begin{aligned}
&\lambda^6 + (\Omega^0_{xx} + \Omega^0_{yy} + \Omega^0_{zz} + 4)\,\lambda^4 + (\Omega^0_{xx}\Omega^0_{yy} + \Omega^0_{xx}\Omega^0_{zz} + \Omega^0_{yy}\Omega^0_{zz} - (\Omega^0_{xy})^2 \\
&-(\Omega^0_{xz})^2 - (\Omega^0_{yz})^2 + 4\Omega^0_{zz})\,\lambda^2 + \Omega^0_{xx}\Omega^0_{yy}\Omega^0_{zz} + 2\,\Omega^0_{xy}\Omega^0_{xz}\Omega^0_{yz} - (\Omega^0_{xy})^2\Omega^0_{zz} \\
&\hspace{6cm} -(\Omega^0_{xz})^2\Omega^0_{yy} - (\Omega^0_{yz})^2\Omega^0_{xx} = 0.
\end{aligned}
\right\}
\tag{5}
$$

If $k = \lambda^2$, we obtain

$$
\left.
\begin{aligned}
&k^3 + (\Omega^0_{xx} + \Omega^0_{yy} + \Omega^0_{zz} + 4)\,k^2 + (\Omega^0_{xx}\Omega^0_{yy} + \Omega^0_{xx}\Omega^0_{zz} + \Omega^0_{yy}\Omega^0_{zz} - (\Omega^0_{xy})^2 \\
&-(\Omega^0_{xz})^2 - (\Omega^0_{yz})^2 + 4\Omega^0_{zz})\,k + \Omega^0_{xx}\Omega^0_{yy}\Omega^0_{zz} + 2\,\Omega^0_{xy}\Omega^0_{xz}\Omega^0_{yz} - (\Omega^0_{xy})^2\Omega^0_{zz} \\
&\hspace{6cm} -(\Omega^0_{xz})^2\Omega^0_{yy} - (\Omega^0_{yz})^2\Omega^0_{xx} = 0.
\end{aligned}
\right\}
\tag{6}
$$

The Eqn. (6) is a cubic equation in k that can be written as

$$
k^3 + d_1 k^2 + d_2 k + d_3 = 0,
\tag{7}
$$

where

$$
\begin{aligned}
d_1 &= \Omega^0_{xx} + \Omega^0_{yy} + \Omega^0_{zz} + 4 = 1, \\
d_2 &= \Omega^0_{xx}\Omega^0_{yy} + \Omega^0_{xx}\Omega^0_{zz} + \Omega^0_{yy}\Omega^0_{zz} - (\Omega^0_{xy})^2 - (\Omega^0_{xz})^2 - (\Omega^0_{yz})^2 + 4\Omega^0_{zz}, \\
d_3 &= \Omega^0_{xx}\Omega^0_{yy}\Omega^0_{zz} + 2\,\Omega^0_{xy}\Omega^0_{xz}\Omega^0_{yz} - (\Omega^0_{xy})^2\Omega^0_{zz} - (\Omega^0_{xz})^2\Omega^0_{yy} - (\Omega^0_{yz})^2\Omega^0_{xx}.
\end{aligned}
$$

Now, we determine the linear stability of the AEPs by finding the characteristic roots of Eqn. (7). We know that all the characteristic roots of a cubic equation are either real numbers or one of them is a real number and the other characteristic roots are imaginary numbers. According to the stability theory, a necessary and sufficient condition for an AEP to be linearly stable is that all the characteristic roots of Eqn. (5) lie in the left-hand side of the λ-plane (i.e., $\lambda \le 0$). If one or more characteristic roots of Eqn. (5) lie in the right-hand side of the λ-plane, then the AEP is always unstable. If all the characteristic roots of Eqn. (5) lie to the left-hand side of the λ-plane, then Eqn. (7) must have three real and negative roots. The resulting linear stability conditions according to Morimoto et al. [16] and Descarte's sign rule often are $D \ge 0$, $d_2 > 0$ and $d_3 > 0$, where D is the discriminant of the cubic Eqn. (7) and is given by

$$
D = \frac{1}{4}\left(d_3 + \frac{16 - 18\,d_2}{27}\right)^2 + \frac{1}{27}\left(d_2 - \frac{4}{3}\right)^3.
\tag{8}
$$

Finally, it is concluded that the system of AEPs is linearly stable when $D \geq 0$, $d_2 > 0$ and $d_3 > 0$.

Further, we have plotted the stability regions in the $x - y$, $x - z$ and $y - z$-planes as shown in Fig. 3. The gray areas in Figs. 3 indicate the stability regions of the AEPs satisfying the stability conditions $D \geq 0$, $d_2 > 0$ and $d_3 > 0$. From Fig. 3 (a, b), we have observed that the stability regions reduce around m_2 and expand around m_1 for the increasing values of radiation parameter q $(0 < q < 1)$. Further, from Fig. 3 (c, d, e, f), we have observed that the stability regions increase around both the primaries m_1 and m_2 for the increasing values of radiation parameter q $(0 < q < 1)$.

5   Zero Velocity Curves

The Jacobian integral of the equations of motion in the classical system is defined as

$$C = 2\Omega + (\dot{x}^2 + \dot{y}^2 + \dot{z}^2). \tag{9}$$

The Jacobian integral of the equations of motion with the continuous low-thrust is defined as

$$C' = 2\Omega^* + (\dot{x}^2 + \dot{y}^2 + \dot{z}^2). \tag{10}$$

We have plotted the ZVCs by taking $\dot{x} = \dot{y} = \dot{z} = 0$. The white domains correspond to the Hills region, and the cyan color indicates the forbidden regions, while the thick black lines show the ZVCs. In these ZVCs, the black dots indicate the positions of the AEPs, while the blue dots indicate the positions of two primaries.

In Figs. 4, we have plotted the ZVCs for the fixed values of $\mu = 0.1$, $q = 0.99$, $C' = -3.57174$ and for different values of low-thrust acceleration $\boldsymbol{a}$. Fig. 4 (a) indicates the ZVC for the low-thrust acceleration $\boldsymbol{a} = (0.0001, 0, 0)$ and shows that there exists a circular land (white domains) around both the primaries and the spacecraft is trapped in these regions, where the motion is possible, and the circular strip (the cyan color) shows the forbidden region where the motion is not possible. Thus, the spacecraft can move around both the primaries and can not move from one primary to the other primary.

In Fig. 4 (b), as we have increased the value of the low-thrust acceleration $\boldsymbol{a} = (0.15, 0, 0)$, it is observed that the spacecraft can freely move in the entire white domain. In Fig. 4 (c), there exist a limiting situation for $\boldsymbol{a} = (0.245, 0, 0)$ and a cusp at L_3, it is observed that the spacecraft can freely move in the entire white domain. In Fig. 4 (d), the curves of zero velocity constitute two branches for $\boldsymbol{a} = (0.335, 0, 0)$. The first branch contains L_4 and the other branch contains L_5. Also, the curves split into two parts at L_3 and shrink to the tadpole shaped curves around L_4 and L_5. Hence, there is only forbidden region around L_4 and L_5 in the tadpole shaped region and the spacecraft is free to move everywhere in the plane.

6   Conclusion

In this paper, we have studied the existence and stability of the AEPs in the low-thrust R3BP when the bigger primary is a source of radiation and the smaller one is a point mass. The AEPs are obtained by introducing the continuous low-thrust at the non-equilibrium points. The positions of these AEPs will depend on the magnitude and directions of the low-thrust acceleration. We have calculated a few AEPs numerically as shown in
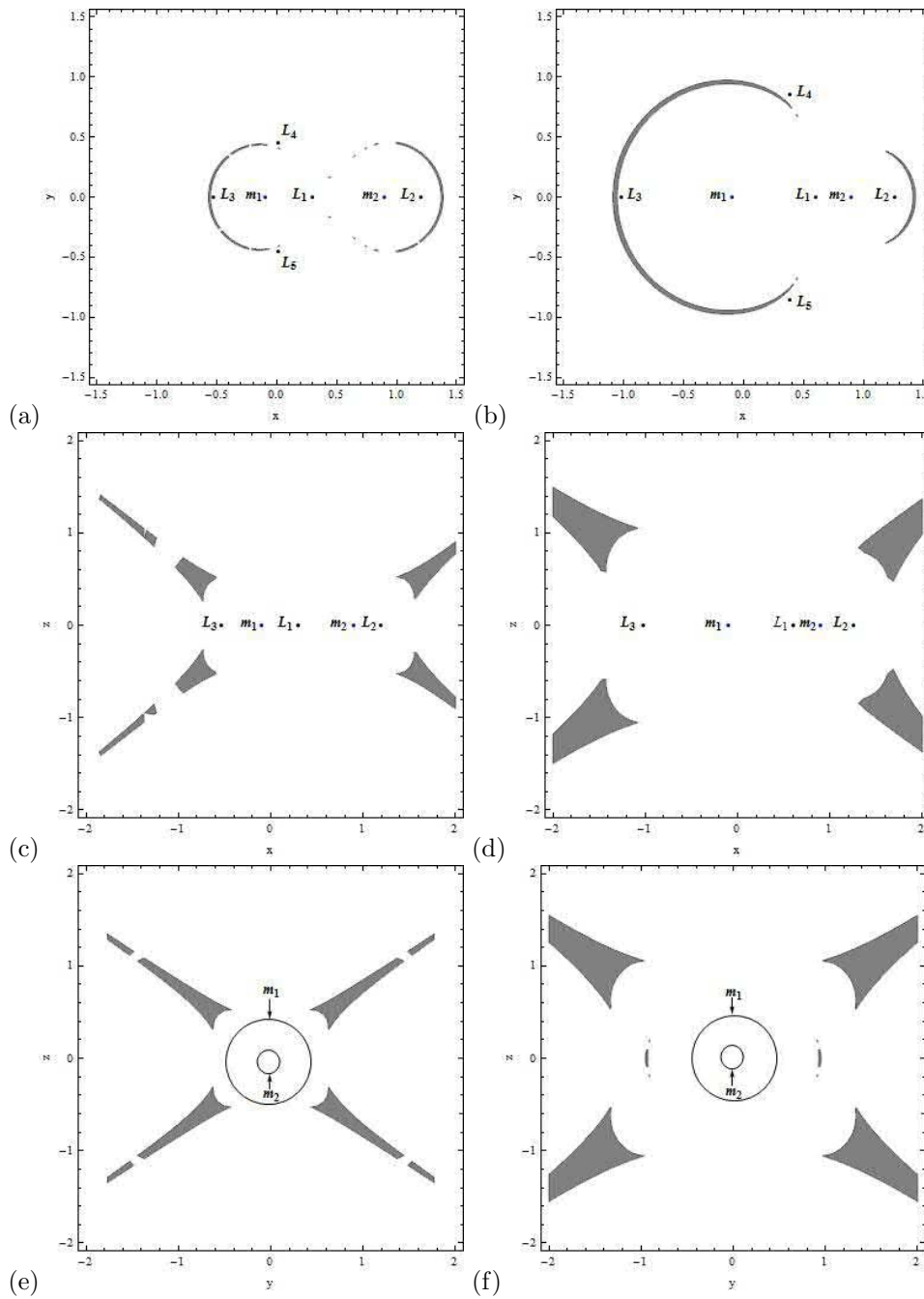
Figure 3: The stable regions (gray area) in the low-thrust R3BP with the effect of the radiation pressure q $(0 < q < 1)$ for fixed value of the mass parameter $\mu = 0.1$. (a, b) In the $x - y$-plane for $q = 0.1$, 0.95, respectively; (c, d) In the $x - z$-plane for $q = 0.1$, 0.95, respectively; (e, f) In the $y - z$-plane for $q = 0.1$, 0.95, respectively.
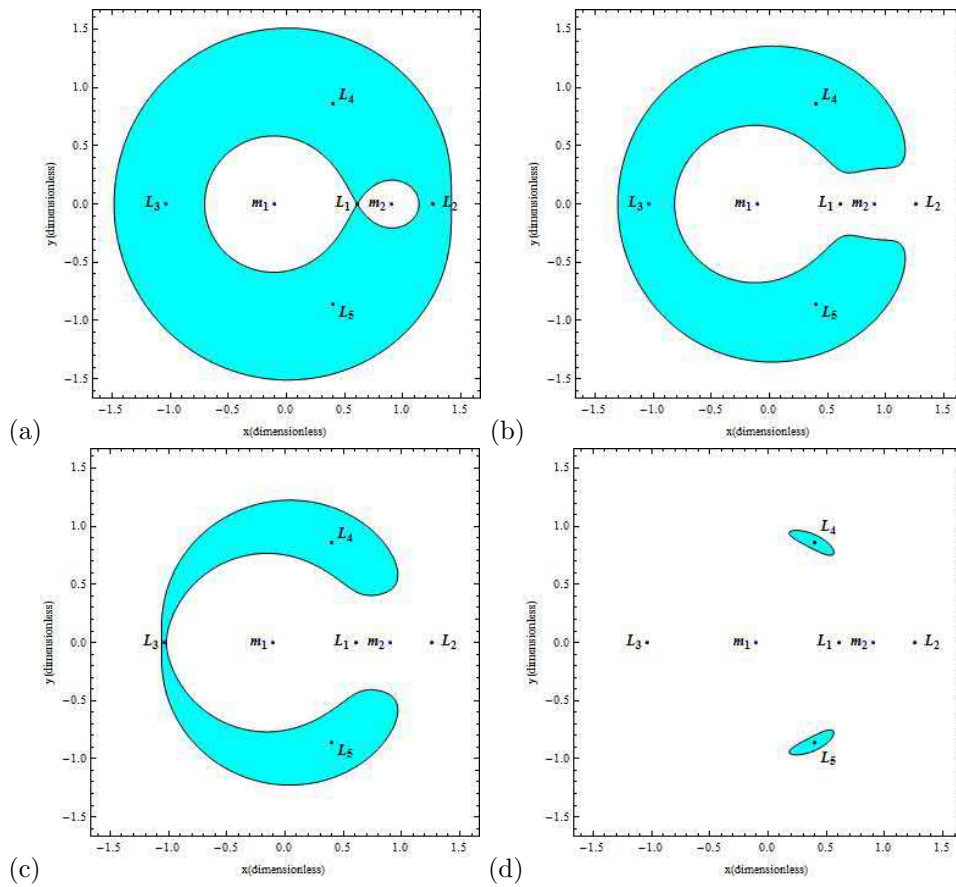
Figure 4: The ZVCs in the low-thrust R3BP for the fixed values of $\mu = 0.1$, $q = 0.99$ and for different values of the low-thrust acceleration a.

Tables 1 and 2. From Tables 1 and 2, we have observed that there exist three collinear and two non-collinear AEPs. It is noticed that the non-collinear AEPs L_4 and L_5 are symmetric about the x-axis for the varying low-thrust acceleration in the x-direction. The movement of the AEPs is shown graphically and displayed in Figs. 2 with the effect of the radiation and low-thrust parameters. It is found that the radiation parameter has more impact on the positions of the AEPs. In our case, the positions of the AEPs are different from those in Morimoto et al. [16], Baig and McInnes [17] and Bu et al. [19] due to the presence of the radiation parameter $q\,(0 < q < 1)$ of the bigger primary. But the positions of these AEPs can be similar to those in the works of Morimoto et al. [16], Baig and McInnes [17], and Bu et al. [19] when $q = 1$ and $\boldsymbol{a} \neq (0,\,0,\,0)$.

Next, the effect of the radiation parameter $q\,(0 < q < 1)$ is studied on stable regions of the spacecraft. From Figs. 3 (a, b), we have observed that the stable regions reduce around the second primary m_2 and expand around the first primary m_1 for the increasing values of the radiation parameter $q\,(0 < q < 1)$ and for a fixed value of the mass parameter $\mu = 0.1$. Further, from Figs. 3 (c, d, e f), we have observed that the stable regions in the $x - z$ and $y - z$-planes increase for the increasing values of the radiation parameter $q\,(0 < q < 1)$ and for a fixed value of the mass parameter $\mu = 0.1$. We have observed that the stability regions are different from those in Morimoto et al. [16] and Bu et al. [19] when $q\,(0 < q < 1)$ is effective. When $\boldsymbol{a} = (0,\,0,\,0)$ and $q = 1$, the obtained results are in agreement with those by Szebehely [1]. Furthermore, from Figs. 3, it is also observed that the AEPs which lie in the stable regions (gray areas) will be linearly stable and otherwise unstable.

Finally, in Figs. 4, we have drawn the ZVCs. It is concluded that for different values of the low-thrust acceleration $\boldsymbol{a}$ and for a fixed value of the mass parameter $\mu = 0.1$, we have different trapped areas in which the spacecraft can freely move. It is clear that the low-thrust acceleration $\boldsymbol{a}$ has subsequent impact on the regions where the spacecraft can move.

Acknowledgment

References

[1] V. Szebehely. Theory of orbits, the restricted problem of three-bodies. *Academic press.* New York, 1967.

[2] A. L. Kunitsyn and A. A. Perezhogin. On the stability of triangular libration points of the photogravitational restricted circular three-body problem. *Celest. Mech. Dyn. Astron.* **18**(4) (1978) 395–408.

[3] V. Kumar and R. K. Choudhry. Nonlinear stability of the triangular libration points for the photo gravitational elliptic restricted problem of three bodies. *Celest. Mech. Dyn. Astron.* **48**(4) (1990) 299–317.

[4] E. I. Abouelmagd. The effect of photogravitational force and oblateness in the perturbed restricted three-body problem. *Astrophys. Space Sci.* **346**(1) (2013) 51–69.

[5] J. Singh and A. B. Emmanuel. Stability of triangular points in the photogravitational CR3BP with Poynting-Robertson drag and a smaller triaxial primary. *Astrophys. Space Sci.* **353** (1) (2014) 97–103.

[6] E. E. Zotos. Unveiling the influence of the radiation pressure in nature of orbits in the photogravitational restricted three-body problem. *Astrophys. Space Sci.* **360** (1) (2015). Doi.10.1007/s10509-015-2513-2.

[7] V. K. Srivastava, J. Kumar and B. S. Kushvah. Regularization of circular restricted three-body problem accounting radiation pressure and oblateness. *Astrophys. Space Sci.* **362** (49) (2017). Doi.10.1007/s10509-017-3021-3.

[8] A. A. Correa, A. Prado, T. J. Stuchi and C. Beauge. Comparison of transfer orbits in the restricted three and four-body problems. *Nonlinear Dynamics and Systems Theory* **7** (3) (2007) 267–277.

[9] A. F. B. A. Prado. A survey on space trajectories in the model of three-bodies. *Nonlinear Dynamics and Systems Theory* **6** (4) (2006) 389–400.

[10] H. M. Dusek. Motion in the vicinity of libration points of a generalized restricted three-body model. *Prog. Astronaut. Rocket.* **17** (1966) 37–54.

[11] R. W. Farquhar Lunar communications with libration point satellites. *Spacecraft and Rockets.* **4** (10) (1967) 1383–1384.

[12] J. F. L. Simmons, A. J. C. McDonald and J. C. Brown. The restricted three-body problem with radiation pressure. *Celest. Mech. Dyn. Astron.* **35** (1985) 145–187.

[13] S. B. Broschart and D. J. Scheeres. Control of hovering spacecraft near small bodies: Application to Asteroid 25143 Itokwa. *J. Guid. Control Dyn.* **28** (2) (2005) 343–354.

[14] D. J. Scheeres, F. Y. Hsiao and N. X. Vinh. Stabilizing motion relative to an unstable orbit: Application to spacecraft formation flight. *J. Guid. Control Dyn.* **26** (1) (2003) 62–73.

[15] M. Y. Morimoto, H. Yamakawa and K. Uesugi. Periodic Orbits with low-thrust restricted three-body problem. *J. Guid. Control Dyn.* **29** (5) (2006) 1131–1139.

[16] M. Y. Morimoto, H. Yamakawa and K. Uesugi. Artificial equilibrium points in the low-thrust restricted three-body problem. *J. Guid. Control Dyn.* **30** (5) (2007) 1563–1567.

[17] S. Baig and C. R. McInnes. Artificial three-body equilibria for hybrid low-thrust propulsion. *J. Guid. Control Dyn.* **31** (6) (2008) 1644–1655.

[18] C. Bombardelli and J. Pelaez. On the stability of artificial equilibrium points in the circular restricted three-body problem. *Celest. Mech. Dyn. Astron.* **109** (1) (2011) 13–26. Doi.10.1007/s10569-010-9317.

[19] Shichao. Bu, Li. Shuang and Yang. Hongwei. Artificial equilibrium points in binary asteroid systems with continuous low-thrust. *Astrophys. Space Sci.* **362** (137) (2017). Doi.10.1007/s10509-017-31197-7.

[20] S. Yadav, V. Kumar and R. Aggarwal. Existence and stability of equilibrium points in the restricted three-body problem with a Geo-Centric satellite including the Earth's equatorial ellipticity. *Nonlinear Dynamics and Systems Theory* **19** (4) (2019) 537–550.

Obituary for Nelly Nikitina (1939 – 2020)

On June 27, 2020, a renowned scientist in the field of theoretical mechanics and chaotic dynamics, doctor of physical and mathematical sciences Nikitina Nelly Vladimirovna died of chronic heart failure at the age of 81.

She was born on March 5, 1939, in the city of Tambov in the family of a career military man. In 1962, she graduated from the Saratov Polytechnic Institute, and for a few years she worked at several engineering enterprises of the former USSR. During 1973 – 1976, she was doing postgraduate studies at the Institute of Mechanics of the Academy of Sciences of the Ukrainian SSR (currently the S.P. Timoshenko Institute of Mechanics of the National Academy of Sciences of Ukraine), and in 1977, she defended a PhD thesis in Physical and Mathematical Sciences (under the supervision of academician of the Academy of Sciences of the Ukrainian SSR N.A. Kilchevsky).

Since 1983, Nikitina hold an appointment as a senior researcher at the Stability of Processes Department of the Institute of Mechanics of the NAS of Ukraine. In 2000, Nikitina defended her habilitational thesis for the degree of Doctor of Science in Physics and Mathematics (dissertation adviser academician of the NAS of Ukraine A.A. Martynyuk). From 2001 until the last days of her life, Nikitina worked as a leading researcher at the Stability of Processes Department of the Institute of Mechanics of the NAS of Ukraine.

The main scientific areas of her investigations were:
– stability of motion of nonlinear mechanical systems;
– analysis of motion of wheeled transport vehicles;
– analysis of complex vibrations of electromechanical systems under periodic effects;
– dynamic analysis of systems with chaotic behavior of trajectories.

For the time of her scientific activities, Nikitina published over 100 scientific papers in national and international journals. Some of her scientific results are summarized in

the monograph: N.V. Nikitina. *Nonlinear Systems with Complex and Chaotic Behavior of Trajectories.* Kiev: Phoenix, 2012, 236 p.

Along with the research activities, Nikitina took a great interest in working with postgraduate students of the Stability of Processes Department, being in the same breath a strict teacher and a friendly person.

In her free time, among other interests, Nikitina went in for tourism and oriental practices. Also, Dr. Nikitina was keenly interested in the issues of the world history and literature.

The bright memory of a renowned scientist and a pleasant conversationalist, Nelly Vladimirovna Nikitina, will be cherished by everyone who knew her and worked with her.

A.A. Martynyuk